Exelon Generation

4300 Winfield Road
Warrenville, IL 60555
630 657 2000 Office

RS-14-310

10 CFR 50.90

December 30, 2014

U. S. Nuclear Regulatory Commission
ATTN: Document Control Desk
Washington, DC 20555-0001

Dresden Nuclear Power Station, Units 2 and 3
Renewed Facility Operating License Nos. DPR-19 and DPR-25
NRC Docket Nos. 50-237 and 50-249

Subject: License Amendment Request Regarding Spent Fuel Storage Pool Criticality Methodology and Proposed Change to Technical Specification 4.3.1, "Criticality"

References:

1. Letter from Brenda L. Mozafari (U. S. NRC) to Exelon Generation Company, LLC, "Summary of August 23, 2013, Meeting with Exelon Generation Company, LLC Regarding AREVA XM Fuel Transition Request for Dresden and Quad Cities Nuclear Stations (TAC Nos. MF2422, MF2423, MF2424, and MF2425)," dated September 11, 2014 (ADAMS Accession No. ML14241A633)

2. Letter from Brenda L. Mozafari (U. S. NRC) to Exelon Generation Company, LLC, "Summary of May 19, 2014, Meeting with Exelon Generation Company, LLC Regarding AREVA XM Fuel Transition for Dresden and Quad Cities Nuclear Stations (TAC Nos. MF2422, MF2423, MF2424, and MF2425)," dated September 11, 2014 (ADAMS Accession No. ML14226B012)

3. Letter from Brenda L. Mozafari (U. S. NRC) to Exelon Generation Company, LLC, "Summary of August 19, 2014, Closed Meeting with Exelon Generation Company, LLC (Exelon) Regarding AREVA XM Fuel Transition for Dresden and Quad Cities Nuclear Stations (TAC Nos. MF2422, MF2423, MF2424, and MF2425)," dated September 22, 2014 (ADAMS Accession No. ML14254A153)

In accordance with 10 CFR 50.90, "Application for amendment of license, construction permit, or early site permit," Exelon Generation Company, LLC (EGC) requests an amendment to Renewed Facility Operating License Nos. DPR-19 and DPR-25 for Dresden Nuclear Power Station (DNPS), Units 2 and 3, respectively. Specifically, EGC is utilizing a new Criticality Safety Analysis (CSA) methodology for performing the criticality safety evaluation for legacy fuel types in addition to the new ATRIUM 10XM fuel design in the spent fuel pool (SFP). In addition, EGC is proposing a change to the DNPS Technical Specification (TS) 4.3.1, "Criticality," in support of the new CSA. EGC proposes to add a new TS 4.3.1.1.c that will require an in-rack k-

infinity limit for the fuel assemblies that are allowed to be stored in the DNPS Units 2 and 3 SFPs storage racks.

EGC participated in several meetings with the NRC Staff regarding the planned transition from Westinghouse Optima2 fuel to the new AREVA ATRIUM 10XM fuel design at DNPS and Quad Cities Nuclear Power Station (QCNPS). During these meetings, EGC's plan to submit this amendment request supporting the use of a new CSA methodology for performing the criticality safety evaluation in the spent fuel pool was discussed. A separate amendment request will be submitted to support the transition to ATRIUM 10XM fuel at DNPS and QCNPS. The attached evaluation addresses all the CSA methodology issues discussed at these meetings as summarized in References 1, 2, and 3.

The following attachments are included in support of this proposed change:

Attachment 1: Evaluation of Proposed Changes

Attachment 2: Mark-up of Technical Specifications Page (Note that there are no TS Bases associated with the Design Features section of the TS)

Attachment 3: Holtec International Report No. HI-2146153, Revision 1, "Licensing Report for the Criticality Analysis of the Dresden Unit 2 and 3 SFP for ATRIUM 10XM Fuel Design" (Proprietary)

Attachment 4: Holtec International Report No. HI-2104790, Revision 1, "Nuclear Group Computer Code Benchmark Calculations" (Proprietary)

Attachment 5: Holtec International Affidavit Requesting Proprietary Report be Withheld from Public Disclosure

Attachment 6: Holtec International Report No. HI-2146153, Revision 1, "Licensing Report for the Criticality Analysis of the Dresden Unit 2 and 3 SFP for ATRIUM 10XM Fuel Design" (Non-Proprietary)

Attachment 7: Holtec International Report No. HI-2104790, Revision 1, "Nuclear Group Computer Code Benchmark Calculations" (Non-Proprietary)

Attachments 3 and 4 contain information proprietary to Holtec International. As Attachments 3 and 4 contain information proprietary to Holtec International, these documents are supported by an affidavit (i.e., Attachment 5) signed by Holtec International, the owner of the information. The affidavit sets forth the basis on which the information may be withheld from public disclosure by the NRC and addresses with specificity the considerations listed in paragraph (b)(4) of 10 CFR 2.390, "Public inspections, exemptions, requests for withholding." Accordingly, it is respectfully requested that the information which is proprietary to Holtec International be withheld from public disclosure. A non-proprietary version of Attachments 3 and 4 are provided in Attachments 6 and 7, respectively.

The proposed change has been reviewed by the DNPS Plant Operations Review Committee and approved by the Nuclear Safety Review Board in accordance with the requirements of the EGC Quality Assurance Program.

EGC requests approval of the proposed change by December 31, 2015. Once approved, the amendment will be implemented within 30 days. This implementation period will provide adequate time for the affected station documents to be revised using the appropriate change control mechanisms.

In accordance with 10 CFR 50.91, "Notice for public comment; State consultation," paragraph (b), EGC is notifying the State of Illinois of this application for license amendment by transmitting a copy of this letter and its attachments to the designated State Official.

There are no regulatory commitments contained in this letter. Should you have any questions concerning this letter, please contact Mr. Timothy A Byam at (630) 657-2818.

I declare under penalty of perjury that the foregoing is true and correct. Executed on the 30th day of December 2014.

Respectfully,

Patrick R. Simpson
Manager – Licensing

Attachments:

1. Evaluation of Proposed Changes
2. Mark-up of Technical Specifications Page
3. Holtec International Report No. HI-2146153, Revision 1, "Licensing Report for the Criticality Analysis of the Dresden Unit 2 and 3 SFP for ATRIUM 10XM Fuel Design" (Proprietary Version)
4. Holtec International Report No. HI-2104790, Revision 1, "Nuclear Group Computer Code Benchmark Calculations" (Proprietary Version)
5. Holtec International Affidavit Requesting Proprietary Report be Withheld from Public Disclosure
6. Holtec International Report No. HI-2146153, Revision 1, "Licensing Report for the Criticality Analysis of the Dresden Unit 2 and 3 SFP for ATRIUM 10XM Fuel Design" (Non-Proprietary Version)
7. Holtec International Report No. HI-2104790, Revision 1, "Nuclear Group Computer Code Benchmark Calculations" (Non-Proprietary Version)

cc: USNRC Region III, Regional Administrator
USNRC Senior Resident Inspector, Dresden Nuclear Power Station
Illinois Emergency Management Agency – Division of Nuclear Safety

ATTACHMENT 1
Evaluation of Proposed Changes

Subject: License Amendment Request Regarding Spent Fuel Storage Pool Criticality Methodology and Proposed Change to Technical Specification 4.3.1, "Criticality"

1.0 SUMMARY DESCRIPTION

In accordance with 10 CFR 50.90, "Application for amendment of license, construction permit, or early site permit," Exelon Generation Company, LLC (EGC) requests an amendment to Renewed Facility Operating License Nos. DPR-19 and DPR-25 for Dresden Nuclear Power Station (DNPS), Units 2 and 3, respectively. Specifically, EGC is utilizing a new Criticality Safety Analysis (CSA) methodology for performing the criticality safety evaluation for legacy fuel types in addition to the new ATRIUM 10XM fuel design in the spent fuel pool (SFP). In addition, EGC is proposing a change to the DNPS Technical Specification (TS) 4.3.1, "Criticality," in support of the new CSA. EGC proposes to add a new TS 4.3.1.1.c that will require an in-rack k-infinity limit for the fuel assemblies that are allowed to be stored in the DNPS Units 2 and 3 SFPs storage racks.

2.0 DETAILED DESCRIPTION

Spent Fuel Pool Criticality Safety Analysis

EGC is planning to transition from Westinghouse Optima2 fuel to the new AREVA ATRIUM 10XM fuel design at DNPS in third quarter 2016. Based on the EGC plans to transition to a new fuel design, the SFP criticality analysis is being revised by Holtec International to account for the new ATRIUM 10XM fuel in addition to the legacy fuel designs. While this revised SFP CSA supports the planned transition to ATRIUM 10XM fuel, this new analysis is not required to support the NRC review and approval of the separate fuel transition amendment request to be submitted in early 2015.

This proposed change requests NRC approval of the new methodology for the CSA in support of storage of Boiling Water Reactor (BWR) spent fuel in the DNPS Unit 2 and Unit 3 SFPs. The DNPS Unit 2 and 3 SFP racks are identical and are designed to accommodate BWR fuel. Currently, the SFP racks credit BORAL for reactivity control. This new analysis will also credit the BORAL and will include a new fuel design, ATRIUM 10XM, in addition to the legacy fuel designs in the current CSA. The revised analysis shows that the effective neutron multiplication factor (k_{eff}) in the SFP racks fully loaded with fuel of the highest anticipated reactivity, at a temperature corresponding to the highest reactivity, is less than 0.95 with a 95% probability at a 95% confidence level. Reactivity effects of abnormal and accident conditions are also evaluated to assure that under all credible abnormal and accident conditions, the reactivity will not exceed the regulatory limit.

The analysis is performed consistent with existing applicable regulatory requirements and guidance. The calculations are performed using either the worst case bounding approach or the statistical analysis approach with respect to the various calculation parameters. The proposed CSA has been performed using NRC reviewed and approved methodologies.

Proposed Changes to Technical Specifications

The DNPS, Units 2 and 3 TS requirements related to spent fuel storage are contained in TS Section 4.3, "Fuel Storage." TS 4.3.1 identifies requirements pertaining to the design of the SFP storage racks. Specifically, TS 4.3.1.1.a currently requires k_{eff} to be ≤ 0.95 if fully flooded

with unborated water, which includes an allowance for uncertainties as described in Section 9.1.2 of the Updated Final Safety Analysis Report (UFSAR). TS 4.3.1.1.b currently requires a nominal 6.30-inch center-to-center distance between fuel assemblies placed in the SFP storage racks.

No changes to the existing TS 4.3.1.1.a or 4.3.1.1.b are proposed in this license amendment request. The proposed changes in this license amendment request include one new TS requirement, 4.3.1.1.c. This proposed change is as follows:

"c. The combination of U-235 enrichment and gadolinia loading shall be limited to ensure fuel assemblies have a maximum k-infinity of 0.8895 as determined at 39.2°F in the normal spent fuel pool in-rack configuration."

A mark-up of the proposed TS changes is provided in Attachment 2. The UFSAR will also be revised, upon implementation of the approved amendment, as part of EGC's configuration control process.

The current DNPS TS were based on the Standard TS for General Electric BWR/4s in NUREG-1433, "Standard Technical Specifications General Electric Plants, BWR/4," Revision 1, April 1995, with exceptions as approved during the DNPS, Units 2 and 3 TS conversion (see NRC Safety Evaluation Report dated March 30, 2001, ADAMS Accession No. ML011130121). NUREG-1433, Revision 1 (and the most recent revision; i.e., Revision 4) provide an option to include either the maximum k-infinity in the normal reactor core configuration at cold conditions; or the maximum average U-235 enrichment as part of TS 4.3.1.1. Neither of these options is included in these proposed TS changes as this exception was approved during the DNPS TS conversion referenced above. An in-rack k-infinity limit is included in proposed TS 4.3.1.1.c for DNPS, Units 2 and 3 in this amendment request.

The in-rack k-infinity limit is an effective limiting specification because it accounts for the principal fuel assembly reactivity drivers of U-235 enrichment and gadolinia loading. Enrichment and gadolinia loading can vary from assembly design to assembly design. However, compliance with the in-rack k-infinity limit in proposed TS 4.3.1.1.c ensures peak in-rack reactivity does not exceed the design basis supporting the TS limit. Using the in-rack k-infinity limit ensures that the SFP criticality analysis remains bounding. This is the same protection offered by the in-core k-infinity limit proposed in the Standard Technical Specifications.

3.0 TECHNICAL EVALUATION

As described in the DNPS Updated Final Safety Analysis Report (UFSAR) Section 9.1.2, "Spent Fuel Storage," the design objectives of the DNPS spent fuel storage system are as follows:

A. To provide a maximum underwater storage capability for 7074 fuel assemblies;

B. To provide for underwater storage of reactor vessel internals; and

C. To provide adequate protection against the loss of water from the fuel pools.

D. To safely store fuel in Dry Cask Storage (DCS) systems per 10 CFR 72.

To achieve these objectives, the spent fuel storage system is designed using the following bases:

A. There will be no release of contamination or exposure of personnel to radiation in excess of 10 CFR 20 limits.

B. The storage space in each of the Unit 2 and Unit 3 spent fuel pools is designed for a maximum of 3537 irradiated fuel assemblies.

C. It is possible, at any time, to perform limited work on irradiated components.

D. Space is provided for used control rods, flow channels, and other reactor components.

E. The spent fuel pool is designed to withstand earthquake loadings of a Class I structure.

F. The spent fuel assembly racks are designed to ensure subcriticality in the storage pool. A maximum K_{eff} of 0.95 is maintained with the racks fully loaded with fuel of the highest anticipated reactivity and flooded with unborated water at a temperature corresponding to the highest reactivity.

G. Spent fuel storage in Dry Cask Storage (DCS) systems per 10 CFR 72.

Each SFP contains 33 high-density spent fuel storage racks which provide storage for 3537 fuel assemblies. There are 18 racks arranged in a 9x11 array and 15 racks arranged in a 9x13 array. The racks are constructed to form tubes of adequate size for fuel storage. The tubes are welded together along their length with angles or clips to provide the inter-tube connection. The center-to-center distance between assemblies stored in the tubes is 6.30 in. x 6.30 in.

The fuel storage tube is constructed of stainless-steel-bearing Boral neutron absorbing material. Boral is a sandwich-type plate that has outer surfaces of Type 1100 aluminum and a core of boron carbide (B4C) uniformly dispersed in a matrix of Type 1100 aluminum. These plates are enclosed by inner and outer tubes made of Type 304 stainless steel designed to permit spent fuel pool water to enter and exit the Boral area. The inner and outer tubes maintain the Boral plate structural integrity during vibratory events. The plates are not required to carry load. The individual neutron absorbing tubes are connected in a checkerboard pattern forming the rack assembly. Along the side of the racks, a filler plate assembly is welded between the absorber tube assemblies to enclose the space between neutron absorbing tubes.

The high density spent fuel storage racks were installed at DNPS in the early 1980s. At that time, a Boral coupon surveillance program was implemented to monitor the condition of the Boral in the racks. EGC continues to monitor the condition of the Boral in the high density spent fuel storage racks under the DNPS Boral coupon surveillance program. The proposed amendment does not modify this monitoring program in any way and DNPS intends to continue monitoring the Boral condition in accordance with this program subsequent to approval of the proposed amendment.

Thirteen Boral coupons have been tested since installation of the high density spent fuel storage racks at DNPS. Blistering has only been seen on two of the coupons, with each coupon containing two blisters. The largest blister had a 1 inch diameter. Corrosion pits have also been seen on some of the coupons. The blistering and pitting does not impact the neutron

attenuation properties of the coupons. All coupons tested have an areal density of 0.03g B-10/cm^2 or greater. Additionally, the areal density of all the coupons tested has exceeded the minimum certified areal density for the DNPS SFP racks of 0.02g B-10/cm^2.

There are various legacy fuel assembly designs, including the current Optima2 design and the future ATRIUM 10XM design, to be qualified for storage in the DNPS Units 2 and 3 SFPs. In addition, to support future operations, the ATRIUM 10XM fuel assembly is designed to be compatible with the DNPS reactor core and co-resident legacy fuel. The ATRIUM 10XM fuel assembly is constructed of similar materials within a spatial envelope that is similar to the currently licensed Westinghouse Optima2 legacy fuel type.

A CSA for the DNPS, Units 2 and 3 SFPs has been performed to support the planned transition to ATRIUM 10XM fuel. A summary of that analysis is provided as Attachment 3. The CSA was performed using a peak reactivity lattice. This peak reactivity lattice bounds the lattice reactivity of any fuel assembly stored in either the Unit 2 or Unit 3 SFP and operating in either the Unit 2 or Unit 3 reactor, to assure compliance with the spent fuel criticality control requirements in 10 CFR 50.68(b) and Interim Staff Guidance (ISG) DSS-ISG-2010-01, "Staff Guidance Regarding the Nuclear Criticality Safety Analysis for Spent Fuel Pools," Revision 0 (Reference 2). The CSA uses a Boron areal density of 0.020g B-10/cm^2 in the Boral panels at DNPS.

In the CSA, the term "peak reactivity" is defined as the reactivity of a fuel assembly lattice in the SFP storage rack geometry as determined by the three-dimensional Monte Carlo computer code MCNP5-1.51 (using the two-dimensional multigroup transport theory computer code CASMO-4 depletion calculation isotopic compositions). This peak reactivity considers nominal fuel assembly and storage rack dimensions and bounding core operating parameters.

The reactivity of the DNPS, Units 2 and 3 SFP storage racks has been calculated using the computer codes CASMO-4 and MCNP5 (see Attachment 3). MCNP5 has been validated and verified for SFP storage rack evaluations by benchmarking calculations of light water reactor (LWR) critical experiments as discussed in Attachment 3, Section 2.2 Computer Codes and Cross Section Libraries, Subsection, 2.2.1, "MCNP5-1.51." The benchmarking report for the MCNP5-1.51 code, which is a three-dimensional Monte Carlo code, is included in Attachment 4, Holtec International Report No. HI-2104790, Revision 1, "Nuclear Group Computer Code Benchmark Calculations."

The NRC has previously approved the use of the CASMO-4 code (see Reference 3) for reactor analysis (i.e., depletion) when providing reactivity data for specific 3D simulator codes as noted in Attachment 3, Section 2.2.2, "CASMO-4."

NRC DSS-ISG-2010-01 (Reference 2) was reviewed and addressed, as applicable, in the criticality analyses. Guidance pertaining to soluble boron in the SFP is not applicable because DNPS is a BWR plant and has no soluble boron in the SFP. Table 1 below provides a cross-reference between the ISG technical guidance topic and the location where this topic is addressed in the criticality analysis.

TABLE 1
NRC DSS-ISG-2010-01 Cross-Reference to Criticality Analyses

ISG Section	Technical Guidance Topic	Criticality Analysis Section (Attachment 3)
1	Fuel Assembly Selection	2.3.1 5.1 Appendix A Appendix B
2 – Depletion Analysis		
2.a	Depletion Uncertainty	2.3.9 Table C.7
2.b	Reactor Parameters	2.3.2 5.2 Tables 5.2(a) and 5.2(c) Table C.1
2.c	Burnable Absorbers	2.3.1.1 2.3.3
2.d	Rodded Operation	2.3.2 5.2 Tables 5.2(b) and 5.2(c) Table C.1
3 – Criticality Analysis		
3.a	Axial Burnup Profile	2.3.1
3.b	Rack Model	5.3 Table 5.3
3.c	Interfaces	2.3.12 Table C.10
3.d	Normal conditions	2.3.5 2.3.6 2.3.11 2.3.14 2.3.16 Table 5.2(a) Appendix C
3.e	Accident Conditions	2.3.15 Tables C.4 and C.11
4 – Criticality Code Validation		
4.a	Area of Applicability	2.2.1.1 Table 2.1(a)
4.b	Trend Analysis	2.2.1.1 Table 2.1(b)
4.c	Statistical Treatment	2.2.1.1
4.d	Lumped Fission Products	2.3.10
4.e	Code-to-Code Comparisons	N/A[1]

TABLE 1 (Continued)
NRC DSS-ISG-2010-01 Cross-Reference to Criticality Analyses

ISG Section	Technical Guidance Topic	Criticality Analysis Section (Attachment 3)
5 - Miscellaneous		
5.a	Precedents	N/A[2]
5.b	References	Throughout
5.c	Assumptions	Throughout

NOTES:
1. Not used in this analysis.
2. This analysis is a complete, stand-alone analysis and does not cite any precedents.

The spent fuel rack configuration was analyzed for credible accident scenarios. The scenarios considered are presented in the bulleted list that follows and are discussed in Section 2.3.15 of Attachment 3.

- SFP temperature exceeding the normal range
- Dropped assemblies
- Missing BORAL Panel
- Rack movement
- Mislocated fuel assembly (a fuel assembly in the wrong location outside the storage rack, including the platform area)

The criticality analysis for the storage of BWR assemblies in the DNPS SFP racks with BORAL has been performed. The results for the normal condition show that k_{eff} is < 0.95 with the storage racks fully loaded with fuel of the highest anticipated reactivity, at a temperature corresponding to the highest reactivity. The results for the bounding accident condition, i.e. the Mislocated in the Corner of Three Racks, Closed Rack Gaps, Eccentric Fuel (Case 2.3.15.6.3.4), also show that k_{eff} is < 0.95 with the storage racks fully loaded with fuel of the highest anticipated reactivity, at a temperature corresponding to the highest reactivity.

Reactivity effects of abnormal and accident conditions have been evaluated to assure that under all credible abnormal and accident conditions, the reactivity will not exceed the regulatory limit of 0.95 with a 95% probability at a 95% confidence level.

4.0 REGULATORY EVALUATION

4.1 Applicable Regulatory Requirements/Criteria

10 CFR 50.68, "Criticality accident requirements," paragraph (b)(4) states that the k_{eff} of the spent fuel storage racks loaded with fuel of the maximum fuel assembly reactivity and flooded with unborated water must not exceed 0.95, at a 95 percent probability, 95 percent confidence

level. The DNPS SFP criticality analysis, provided as Attachment 3 to this submittal, demonstrates that this requirement is met.

Paragraph (b)(7) of 10 CFR 50.68 states that the maximum nominal U-235 enrichment of the fresh fuel assemblies is limited to 5.0 percent by weight. DNPS new fuel is below 5.0 percent by weight U-235 enrichment.

The following General Design Criterion (GDC) is applicable to this amendment request. It should be noted that, although DNPS is not formally committed to the GDC due to the vintage of the station, an evaluation was performed addressing the DNPS conformance with the GDC. This evaluation is documented in the UFSAR Section 3.1, "Conformance with NRC General Design Criteria." This evaluation concluded that DNPS fully satisfies the intent of the (then draft) GDC.

GDC 62, "Prevention of criticality in fuel storage and handling," states that criticality in the fuel storage and handling system shall be prevented by physical systems or processes, preferably by use of geometrically safe configurations. The evaluation of DNPS's conformance with GDC 62 is discussed in Section 9.1.2, "Spent Fuel Storage," of the DNPS UFSAR. The racks in which spent fuel assemblies are placed, are designed and arranged to ensure subcriticality in the storage pool. The DNPS criticality analysis has been performed to demonstrate that, given the current spent fuel storage system design, k_{eff} will remain less than or equal to 0.95 for legacy fuel types in addition to the new ATRIUM 10XM fuel design.

4.2 No Significant Hazards Consideration

In accordance with 10 CFR 50.90, "Application for amendment of license, construction permit, or early site permit," Exelon Generation Company, LLC (EGC) requests an amendment to Renewed Facility Operating License Nos. DPR-19 and DPR-25 for Dresden Nuclear Power Station (DNPS), Units 2 and 3, respectively. Specifically, EGC is utilizing a new Criticality Safety Analysis (CSA) methodology for performing the criticality safety evaluation for legacy fuel types in addition to the new ATRIUM 10XM fuel design in the spent fuel pool (SFP). In addition, EGC is proposing a change to the DNPS Technical Specification (TS) 4.3.1, "Criticality," in support of the new CSA. EGC proposes to add a new TS 4.3.1.1.c that will require an in-rack k-infinity limit for the fuel assemblies that are allowed to be stored in the DNPS Units 2 and 3 SFPs storage racks.

According to 10 CFR 50.92, "Issuance of amendment," paragraph (c), a proposed amendment to an operating license involves no significant hazards consideration if operation of the facility in accordance with the proposed amendment would not:

(1) Involve a significant increase in the probability or consequences of an accident previously evaluated; or

(2) Create the possibility of a new or different kind of accident from any accident previously evaluated; or

(3) Involve a significant reduction in a margin of safety.

EGC has evaluated the proposed change for DNPS using the criteria in 10 CFR 50.92, and has determined that the proposed change does not involve a significant hazards consideration. The following information is provided to support a finding of no significant hazards consideration.

1. Does the proposed amendment involve a significant increase in the probability or consequences of an accident previously evaluated?

   Response: No

   The proposed amendment involves a revised CSA for the DNPS Units 2 and 3 SFPs using a new methodology and proposes a new TS requirement limiting the maximum in-rack k-infinity. The proposed amendment does not change or modify the fuel, fuel handling processes, spent fuel storage racks, number of fuel assemblies that may be stored in the SFP, decay heat generation rate, or the SFP cooling and cleanup system.

   The proposed amendment was evaluated for impact on the following previously evaluated events and accidents:

   - A fuel handling accident (FHA),
   - A fuel mispositioning event,
   - A seismic event, and
   - A loss of SFP cooling event

   The probability of a FHA is not increased because implementation of the proposed amendment will employ the same equipment and processes to handle fuel assemblies that are currently used. The FHA radiological consequences are not increased because the methodology used in support of the CSA does not impact the radiological source term of a single fuel assembly. Therefore, the proposed amendment does not significantly increase the probability or consequences of an FHA.

   Operation in accordance with the proposed amendment will not significantly increase the probability of a fuel mispositioning event because fuel movement will continue to be controlled by approved fuel handling procedures. These procedures continue to require identification of the initial and target locations for each fuel assembly that is moved. The consequences of a fuel mispositioning event are not changed because the reactivity analysis demonstrates that the new subcriticality criteria and requirements will be met for the worst-case fuel mispositioning event.

   Operation in accordance with the proposed amendment will not change the probability of a seismic event. The consequences of a seismic event are not increased because the forcing functions for seismic excitation are not increased and because the mass of storage racks has not changed.

   Operation in accordance with the proposed amendment will not change the probability of a loss of SFP cooling event because the systems and events that could affect SFP cooling are unchanged. The consequences are not significantly increased because there are no changes in the SFP heat load or SFP cooling systems, structures or components due to the proposed change in CSA methodology. Furthermore, conservative analyses indicate

that the current design requirements and criteria continue to be met with the presence of Boral blisters.

Therefore, the proposed change does not involve a significant increase in the probability or consequences of an accident previously evaluated.

2. Does the proposed amendment create the possibility of a new or different kind of accident from any accident previously evaluated?

Response: No

Onsite storage of spent fuel assemblies in the DNPS, Units 2 and 3 SFPs is a normal activity for which DNPS has been designed and licensed. As part of assuring that this normal activity can be performed without endangering the public health and safety, the ability to safely accommodate different possible accidents in the spent fuel pool have been previously analyzed. These analyses address accidents such as radiological releases due to dropping a fuel assembly; and potential inadvertent criticality due to misloading a fuel assembly. The proposed amendment does not change the method of fuel movement or spent fuel storage and does not create the potential for a new accident.

The proposed use of a new methodology for performing the DNPS SFP CSA and addition of a new TS requirement limiting the maximum in-rack k-infinity does not change or modify the fuel, fuel handling processes, spent fuel racks, number of fuel assemblies that may be stored in the pool, decay heat generation rate, or the SFP cooling and cleanup system. The potential for blistering on the Boral has been evaluated and the neutron poison will continue to fulfill its function.

The limiting fuel assembly mispositioning event does not represent a new or different type of accident. The mispositioning of a fuel assembly within the fuel storage racks has always been possible. The proposed amendment involves a revised CSA for the DNPS Units 2 and 3 SFPs using a new methodology. The associated analysis results show that the storage racks remain sub-critical, with substantial margin, following a worst-case fuel misloading event.

Therefore, the proposed change does not create the possibility of a new or different kind of accident from any previously evaluated.

3. Does the proposed amendment involve a significant reduction in a margin of safety?

Response: No

The proposed amendment involves a revised CSA for the DNPS Units 2 and 3 SFPs using a new methodology and proposes a new TS requirement limiting the maximum in-rack k-infinity. This change was evaluated for its effect on margins of safety related to criticality and spent fuel heat removal capability.

DNPS TS 4.3, "Fuel Storage," Specification 4.3.1.1.a requires the spent fuel storage racks to maintain the effective neutron multiplication factor, k_{eff}, less than or equal to 0.95 when

fully flooded with unborated water, which includes an allowance for uncertainties. Therefore, for spent fuel pool criticality considerations, the required safety margin is 5 percent.

The proposed change ensures, as verified by the associated criticality analysis, that k_{eff} continues to be less than or equal to 0.95, thus preserving the required safety margin of 5 percent. In addition, using the in-rack k-infinity limit ensures that the SFP criticality analysis remains bounding and provides adequate protection to ensure public health and safety in that it determines the reactivity limit for the fuel assemblies that are allowed to be stored in the SFP storage racks.

The proposed use of a new methodology for performing the DNPS SFP CSA does not affect spent fuel heat generation or the spent fuel cooling systems. A conservative analysis indicates that the design basis requirements and criteria for spent fuel cooling continue to be met with Boral blistering considered.

In addition, the radiological consequences of a dropped fuel assembly remain unchanged as the anticipated fuel damage due to a fuel handling accident is unaffected by the use of a new methodology to perform the CSA. The proposed change also does not increase the capacity of the Unit 2 and Unit 3 spent fuel pools beyond the current capacity of not more than 3537 fuel assemblies.

Based on the above, EGC concludes that the proposed amendment does not involve a significant hazards consideration under the standards set forth in 10 CFR 50.92(c), and, accordingly, a finding of no significant hazards consideration is justified.

4.3 Conclusions

In conclusion, based on the considerations discussed above, (1) there is reasonable assurance that the health and safety of the public will not be endangered by operation in the proposed manner, (2) such activities will be conducted in compliance with the Commission's regulations, and (3) the issuance of the amendment will not be inimical to the common defense and security or to the health and safety of the public.

5.0 ENVIRONMENTAL CONSIDERATION

EGC has evaluated this proposed operating license amendment consistent with the criteria for identification of licensing and regulatory actions requiring environmental assessment in accordance with 10 CFR 51.21, "Criteria for and identification of licensing and regulatory actions requiring environmental assessments." EGC has determined that these proposed changes meet the criteria for a categorical exclusion set forth in paragraph (c)(9) of 10 CFR 51.22, "Criterion for categorical exclusion; identification of licensing and regulatory actions eligible for categorical exclusion or otherwise not requiring environmental review," and as such, has determined that no irreversible consequences exist in accordance with paragraph (b) of 10 CFR 50.92, "Issuance of amendment." This determination is based on the fact that these changes are being proposed as an amendment to the license issued pursuant to 10 CFR 50, "Domestic Licensing of Production and Utilization Facilities," which changes a requirement with respect to

installation or use of a facility component located within the restricted area, as defined in 10 CFR 20, "Standards for Protection Against Radiation," or which changes an inspection or a surveillance requirement, and the amendment meets the following specific criteria:

(i) The amendment involves no significant hazards consideration.
(ii) There is no significant change in the types or significant increase in the amounts of any effluent that may be released offsite.
(iii) There is no significant increase in individual or cumulative occupational radiation exposure.

Therefore, in accordance with 10 CFR 51.22, paragraph (b), no environmental impact statement or environmental assessment need be prepared in connection with the proposed amendment.

6.0 REFERENCES

1. L. I. Kopp, "Guidance on the Regulatory Requirements for Criticality Analysis of Fuel Storage at Light-Water Reactor Power Plants," NRC Memorandum from L. Kopp to T. Collins, August 19, 1998

2. DSS-ISG-2010-01, "Staff Guidance Regarding the Nuclear Criticality Safety Analysis for Spent Fuel Pools," Revision 0

3. Letter from T. J. Orf (NRC) to M. Nazar (Florida Power and Light Company), "St. Lucie Plant, Unit 2 - Issuance of Amendment Regarding New Fuel Vault and Spent Nuclear Fuel Pool Nuclear Criticality Analysis (TAC No. ME8782)," dated September 19, 2012 (ADAMS Accession No. ML12263A224)

ATTACHMENT 2

Mark-up of Technical Specifications Page

TS Page 4.0-2 (Units 2 and 3)

4.0 DESIGN FEATURES (continued)

4.3 Fuel Storage

4.3.1 Criticality

4.3.1.1 The spent fuel storage racks are designed and shall be maintained with:

a. $k_{eff} \leq 0.95$ if fully flooded with unborated water, which includes an allowance for uncertainties as described in Section 9.1.2 of the UFSAR; and

b. A nominal 6.30 inch center to center distance between fuel assemblies placed in the storage racks.

c. The combination of U-235 enrichment and gadolinia loading shall be limited to ensure fuel assemblies have a maximum k-infinity of 0.8895 as determined at 39.2°F in the normal spent fuel pool in-rack configuration

4.3.2 Drainage

The spent fuel storage pool is designed and shall be maintained to prevent inadvertent draining of the pool below elevation 589 ft 2.5 inches.

4.3.3 Capacity

The spent fuel storage pool is designed and shall be maintained with a storage capacity limited to no more than 3537 fuel assemblies.

ATTACHMENT 5

Holtec International Affidavit Requesting
Proprietary Report be Withheld from Public Disclosure

HOLTEC INTERNATIONAL

Holtec Center, 555 Lincoln Drive West, Marlton, NJ 08053
Telephone (856) 797-0900
Fax (856) 797-0909

Holtec International Document ID 2393-AFFI-01

AFFIDAVIT PURSUANT TO 10 CFR 2.390

I, Debabrata (Debu) Mitra Majumdar, being duly sworn, depose and state as follows:

(1) I have reviewed the information described in paragraph (2) which is sought to be withheld, and am authorized to apply for its withholding.

(2) The information sought to be withheld is information provided in the following reports.

a. Holtec International Report No. HI-2146153, "Licensing Report for the Criticality Analysis of the Dresden Unit 2 and 3 SFP for ATRIUM 10XM Fuel Design", Revision 1 (Proprietary Version).

b. Holtec International Report No. HI-2104790, Revision 1, "Nuclear Group Computer Code Benchmark Calculations" (Proprietary).

These reports contain Holtec proprietary information.

(3) In making this application for withholding of proprietary information of which it is the owner, Holtec International relies upon the exemption from disclosure set forth in the Freedom of Information Act ("FOIA"), 5 USC Sec. 552(b)(4) and the Trade Secrets Act, 18 USC Sec. 1905, and NRC regulations 10CFR Part 9.17(a)(4), 2.390(a)(4), and 2.390(b)(1) for "trade secrets and commercial or financial information obtained from a person and privileged or confidential" (Exemption 4). The material for which exemption from disclosure is here sought is all "confidential commercial information", and some portions also qualify under the narrower definition of "trade secret", within the meanings assigned to those terms for purposes of FOIA Exemption 4 in, respectively, Critical Mass Energy Project v. Nuclear Regulatory Commission, 975F2d871 (DC Cir. 1992), and Public Citizen Health Research Group v. FDA, 704F2d1280 (DC Cir. 1983).

(4) Some examples of categories of information which fit into the definition of proprietary information are:

a. Information that discloses a process, method, or apparatus, including supporting data and analyses, where prevention of its use by Holtec's competitors without license from Holtec International constitutes a competitive economic advantage over other companies;

b. Information which, if used by a competitor, would reduce his expenditure of resources or improve his competitive position in the design, manufacture, shipment, installation, assurance of quality, or licensing of a similar product.

c. Information which reveals cost or price information, production, capacities, budget levels, or commercial strategies of Holtec International, its customers, or its suppliers;

d. Information which reveals aspects of past, present, or future Holtec International customer-funded development plans and programs of potential commercial value to Holtec International;

e. Information which discloses patentable subject matter for which it may be desirable to obtain patent protection.

The information sought to be withheld is considered to be proprietary for the reasons set forth in paragraph 4.b, above.

(5) The information sought to be withheld is being submitted to the NRC in confidence. The information (including that compiled from many sources) is of a sort customarily held in confidence by Holtec International, and is in fact so held. The information sought to be withheld has, to the best of my knowledge and belief, consistently been held in confidence by Holtec International. No public disclosure has been made, and it is not available in public sources. All disclosures to third parties, including any required transmittals to the NRC, have been made, or must be made, pursuant to regulatory provisions or proprietary

agreements which provide for maintenance of the information in confidence. Its initial designation as proprietary information, and the subsequent steps taken to prevent its unauthorized disclosure, are as set forth in paragraphs (6) and (7) following.

(6) Initial approval of proprietary treatment of a document is made by the manager of the originating component, the person most likely to be acquainted with the value and sensitivity of the information in relation to industry knowledge. Access to such documents within Holtec International is limited on a "need to know" basis.

(7) The procedure for approval of external release of such a document typically requires review by the staff manager, project manager, principal scientist or other equivalent authority, by the manager of the cognizant marketing function (or his designee), and by the Legal Operation, for technical content, competitive effect, and determination of the accuracy of the proprietary designation. Disclosures outside Holtec International are limited to regulatory bodies, customers, and potential customers, and their agents, suppliers, and licensees, and others with a legitimate need for the information, and then only in accordance with appropriate regulatory provisions or proprietary agreements.

(8) The information classified as proprietary was developed and compiled by Holtec International at a significant cost to Holtec International. This information is classified as proprietary because it contains detailed descriptions of analytical approaches and methodologies not available elsewhere. This information would provide other parties, including competitors, with information from Holtec International's technical database and the results of evaluations performed by Holtec International. A substantial effort has been expended by Holtec International to develop this information. Release of this information would improve a competitor's position because it would enable Holtec's competitor to copy our technology and offer it for sale in competition with our company, causing us financial injury.

(9) Public disclosure of the information sought to be withheld is likely to cause substantial harm to Holtec International's competitive position and foreclose or reduce the availability of profit-making opportunities. The information is part of Holtec International's comprehensive spent fuel storage technology base, and its commercial value extends beyond the original development cost. The value of the technology base goes beyond the extensive physical database and analytical methodology, and includes development of the expertise to determine and apply the appropriate evaluation process.

The research, development, engineering, and analytical costs comprise a substantial investment of time and money by Holtec International.

The precise value of the expertise to devise an evaluation process and apply the correct analytical methodology is difficult to quantify, but it clearly is substantial.

Holtec International's competitive advantage will be lost if its competitors are able to use the results of the Holtec International experience to normalize or verify their own process or if they are able to claim an equivalent understanding by demonstrating that they can arrive at the same or similar conclusions.

The value of this information to Holtec International would be lost if the information were disclosed to the public. Making such information available to competitors without their having been required to undertake a similar expenditure of resources would unfairly provide competitors with a windfall, and deprive Holtec International of the opportunity to exercise its competitive advantage to seek an adequate return on its large investment in developing these very valuable analytical tools.

AFFIDAVIT PURSUANT TO 10 CFR 2.390

STATE OF NEW JERSEY)
) ss:
COUNTY OF BURLINGTON)

Mr. Debabrata (Debu) Mitra Majumdar, being duly sworn, deposes and says:

That he has read the foregoing affidavit and the matters stated therein are true and correct to the best of her knowledge, information, and belief.

Executed at Marlton, New Jersey, this 24th day of October, 2014.

Debabrata (Debu) Mitra Majumdar, Ph.D.
Holtec International

Subscribed and sworn before me this 24 day of October, 2014.

MARIA C. MASSI
NOTARY PUBLIC OF NEW JERSEY
My Commission Expires April 25, 2015

ATTACHMENT 6

Holtec International Report No. HI-2146153, "Licensing Report for the Criticality Analysis of the Dresden Unit 2 and 3 SFP for ATRIUM 10XM Fuel Design"
(Non-Proprietary Version)

HOLTEC
INTERNATIONAL

Holtec Center, One Holtec Drive, Marlton, NJ 08053
Telephone (856) 797- 0900
Fax (856) 797 - 0909

Licensing Report for the Criticality Analysis of the Dresden Unit 2 and 3 SFP for ATRIUM 10XM Fuel Design - Non Proprietary Version

FOR

Exelon

Holtec Report No: HI-2146153

Holtec Project No: 2393

Sponsoring Holtec Division: HTS

Report Class : SAFETY RELATED

Summary of Revisions:

Revision 0: Original Issue

Revision 1: Minor editorial changes incorporated.

Table of Contents

[redacted]

1. INTRODUCTION

This report documents the criticality safety evaluation for the storage of BWR fuel in the Unit 2 and Unit 3 spent fuel pools (SFPs) at the Dresden Station operated by Exelon. The Unit 2 and Unit 3 SFP racks are identical and are designed to accommodate BWR fuel. Currently, the SFP racks credit BORAL for reactivity control. This analysis will include a new fuel design, ATRIUM 10XM. This analysis will show that the effective neutron multiplication factor (k_{eff}) in the SFP racks fully loaded with fuel of the highest reactivity, at a temperature corresponding to the highest reactivity, is less than 0.95 with a 95% probability at a 95% confidence level. Reactivity effects of abnormal and accident conditions are also evaluated to assure that under all credible abnormal and accident conditions, the reactivity will not exceed the regulatory limit.

Criticality control in the SFP, as credited in this analysis, relies on the following:

- Fixed neutron absorbers
  - BORAL fixed to the SFP rack cell walls
- Integrated neutron absorbers
  - Gadolinium (Gd) in the fuel (peak reactivity isotopic composition).

Criticality control in the SFP, as credited in this analysis, does not rely on the following:

- Crediting burnup

2. METHODOLOGY

2.1 *General Approach*

The analysis is performed consistent with regulatory requirements and guidance. The calculations are performed using either the worst case bounding approach or the statistical analysis approach with respect to the various calculation parameters. The approach considered for each parameter is discussed below.

2.2 *Computer Codes and Cross Section Libraries*

2.2.1 MCNP5-1.51

MCNP5-1.51 is a three-dimensional Monte Carlo code developed at the Los Alamos National Laboratory [1]. MCNP5-1.51 calculations use continuous energy cross-section data based on ENDF/B-VII. MCNP is selected because it has history of successful use in fuel storage criticality analyses and has most of the necessary features (except for fuel depletion analysis) for the analysis to be performed for Dresden Station SFP.

The convergence of a Monte Carlo criticality problem is sensitive to the following parameters: (1) number of histories per cycle, (2) the number of cycles skipped before averaging, (3) the total number of cycles and (4) the initial source distribution. All MCNP5 calculations are performed with a minimum of 12,000 histories per cycle, a minimum of 300 skipped cycles before averaging, and a minimum of 300 cycles that are accumulated. The initial source is specified as uniform over the fueled regions (assemblies). [redacted]

2.2.1.1 MCNP5-1.51 Validation

[redacted]

[1] A positive bias which results in decrease in reactivity is truncated to zero [3].

[redacted]

2.2.2 CASMO-4

Fuel depletion analyses during core operation are performed with CASMO-4 Version 2.05.14 (using the 70-group cross-section library), which has been approved by the NRC for reactor analysis (depletion) when providing reactivity data for specific 3D simulator codes. CASMO-4 is a two-dimensional multigroup transport theory code based on the Method of Characteristics and it is developed by Studsvik of Sweden [4]. CASMO-4 is used to perform depletion calculations and to perform various sensitivity studies. The uncertainty on the isotopic composition of the fuel (i.e., the number density) is considered as discussed below (see Section 2.3.9). A validation for CASMO-4 to develop a bias and bias uncertainty is not necessary because the results of the CASMO-4 sensitivity studies are not used as input into the k_{eff} calculations. However, the code authors have validated CASMO-4 against MCNP and various critical experiments [5].

2.3 *Analysis Methods*

2.3.1 Design Basis Fuel Assembly

There are various fuel designs stored in the Dresden SFP. For the purpose of this analysis, the reactivity of each design is evaluated and the most reactive fuel bundle lattice is determined for use as the design basis fuel assembly (a single lattice (most reactive) along the entire active length) to determine k_{eff} at the 95/95 level. This approach follows the guidance in [6] and [7], and is further described below.

2.3.1.1 Peak Reactivity

The BWR fuel designs used at the Dresden Station use Gd as an integral burnable absorber. Initially, the Gd in the fuel assembly holds down the fresh fuel assembly reactivity and then, as core depletion occurs, the Gd begins to burnout until it is essentially fully depleted. As the Gd depletes the reactivity of the fuel assembly increases until it reaches a peak. This peak reactivity is the fuel assembly's most reactive condition. Note that most BWR fuel designs are composed of various axial lattices (including blankets) that can have different axial lengths, uranium loadings, fuel pin arrangements including partial or part-length rods, Gd pin locations and loading, etc. These various lattice components can all effect at what burnup the peak reactivity occurs and the magnitude of the peak reactivity. The axial lattices within a single fuel assembly can therefore all have different peak reactivity. Therefore, for each fuel design type, an assessment is made of every lattice to determine the bounding lattice (highest peak reactivity). These are the screening calculations described in Section 2.3.1.2 and are performed with CASMO-4 only. Note that using the CASMO-4 code is appropriate since all lattices are compared as axially infinite models.

Note that for the purposes of this analysis, the term "peak reactivity" is defined as the reactivity of a fuel assembly lattice in the SFP storage rack geometry as determined by MCNP5-1.51 (using CASMO-4 depletion calculation isotopic compositions [redacted]). This peak reactivity considers nominal fuel assembly and storage rack dimensions. For the purpose of determining the design basis fuel assembly and its bounding lattice (see Section 2.3.1.2 and Section 2.3.1.3), the core operating parameters (COP) are varied using four sets. For all further calculations using the design basis fuel assembly lattice bounding core operating parameters are used (see Section 2.3.2). Note that the fuel assembly orientation in the core with respect to its control blade does not change and therefore the CASMO-4 depletion calculations consider the only possible configuration.

2.3.1.1.1 Peak Reactivity and Fuel Assembly Burnup

Typically, a spent fuel assembly is characterized by its assembly average burnup (over all lattices or nodes). In this analysis methodology the fuel assembly average burnup is of no concern and is not credited for reactivity control. Rather, the methodology credits the residual Gd and other depletion isotopic compositions at the fuel assembly peak reactivity (most reactive lattice peak reactivity). While the peak reactivity occurs at some specific *lattice burnup*, the peak reactivity lattice burnup varies from lattice to lattice within a fuel design. Therefore, independent calculations with MCNP5-1.51 [redacted] (see Section 2.3.1.1.2) are performed for *every lattice* that is selected as a result of the screening calculations (see Section 2.3.1.2) and all further design basis calculations using MCNP5-1.51. The MCNP5-1.51 calculations are performed over a burnup range to determine the burnup at peak reactivity for every lattice in the storage rack geometry. Since each lattice is considered at its peak reactivity (and therefore the lattice or nodal burnup at which that occurs), the fuel assembly average burnup or fuel assembly burnup profile is not applicable because the analysis already considers each lattice at its most reactive composition, independent of the fuel assembly average burnup.

[redacted]

2.3.1.2 Screening Calculations for the Design Basis Fuel Assembly

The SFP holds various legacy fuel assemblies designs, the current Optima2 design and the future ATRIUM 10XM design to be qualified for storage. For many of the legacy fuel designs, it is not necessary to perform calculations because they have a very low lattice average enrichment. Since it is known that the design basis lattice will have a high lattice average enrichment, a simple assessment of the legacy fuel population is all that is required to determine that they are bounded by the design basis lattice. Therefore, for legacy fuel designs with low lattice enrichments (i.e. less than about 4.3 % U-235), engineering judgment is used to determine that these designs will not need screening calculations since they are well bounded by the more recent fuel designs with much higher lattice average enrichments.

For all of fuel design lattices that require screening calculations, the first step (Step 1) is to perform CASMO-4 calculations to determine the lattices that have the highest peak reactivity in the storage rack geometry (see Appendix A). For Step 1, an arbitrary value of $k_{inf} > 0.8500$ is used to determine the lattices that have the highest peak reactivity in the storage rack geometry. This arbitrary value was selected using engineering judgment.

Each of the Step 1 screening calculations using CASMO-4 includes the in core depletion and restart in SFP rack cell. Note that for the core depletion calculations, four sets of core operating parameters are used and the maximum reactivity over all four is determined (see Section A.2). These four sets of core operating parameters are presented in Table 5.2.(c) and have been selected to bound the effects of the most important parameters (i.e. void fraction, control blade use and temperatures).

Based on the results of Step 1, the most reactive fuel lattices are identified by selecting the subset of lattices that have a reactivity greater than 0.8500 (see Appendix A). The lattices which meet this criteria are then used for Step 2 calculations as described below.

2.3.1.3 Determination of the Design Basis Fuel Assembly Lattice

As discussed in Section 2.3.1.2, the Step 1 screening calculations are performed with CASMO-4 for each of the selected lattices. Based on the results of these screening calculations, the most reactive lattices are determined by comparison to the criteria of $k_{inf} > 0.8500$. Step 2 calculations are then performed using in-rack MCNP5-1.51 to determine the peak reactivity for each of the most reactive lattices selected in Step 1. See Appendix B.

Step 2 determines the peak reactivity for the most reactive lattices using MCNP5-1.51 calculations in the storage rack geometry. Note that the peak reactivity of the CASMO-4 depletion calculation model is used only for the screening calculations and is not the peak reactivity as determined by MCNP5-1.51 in rack models. MCNP5-1.51 calculations are performed over a burnup range to independently determine the peak reactivity.

[redacted]

The result of the Step 2 calculations are then compared, and the most reactive fuel assembly lattice is determined. Note that the results of the Step 2 lattice calculations in MCNP5-1.51 are useful to show important trends in the reactivity effect of lattice enrichment, Gd rod location, number and loading. These trends are expected to show that the most reactive lattices are those with the highest lattice average enrichment, lowest number of Gd rods and lowest Gd rod loading. The most reactive lattice is then used to construct a new lattice that is much more bounding by increasing the lattice average enrichment to the maximum value (i.e. 4.95 wt% U-235), decreasing the number of Gd rods to the minimum expected (i.e. 10) with the minimum expected Gd loading (i.e. 3%). This new constructed lattice is then used as the design basis fuel assembly lattice and is modeled along the entire active length for all calculations used to determine k_{eff} at the 95/95 level.

2.3.1.4 Design Basis Model

The analysis design basis MCNP5-1.51 model is a 2x2 array (and larger array sizes as noted below) that considers the formed and fabricated cell design of the storage racks. The storage rack cell wall, poison, and sheathing are all explicitly modeled along the active length of the design basis lattice. The BORAL panels are considered at their minimum thickness and loading. The design basis model explicitly considers the fuel pellet, pellet to cladding gap, cladding, water box and fuel assembly channel (unless otherwise noted below). Various studies are performed with the design basis model to determine the reactivity effect of SFP water, radial position of the fuel assembly within the storage cell, and radial orientation of the fuel in the 2x2 array with respect to the corner of the bundle which was adjacent to the control blade in the core. The reactivity impacts from these studies are discussed in detail in the sections below. The MCNP5-1.51 model uses periodic boundary conditions radially and 12 inches of water as axial reflectors. The assembly lattice is considered along the full active length. The storage rack is considered along the full active fuel length only.

The design basis model is used for all calculations used to show compliance with the regulatory limit. All calculations with the design basis model are presented in Appendix C. The design basis model differs slightly from the model used to determine the bounding lattice (i.e., [redacted] (see Appendix B).

Calculations are performed with the design basis model for the four sets of COP to confirm the selection of the bounding set from Appendix B. The design basis MCNP5-1.51 model is

presented in Figure 2.2. Note that all calculations are performed at zero hours cooling time. Justification of this cooling time is also presented in Appendix C.

The following cases are considered:

- Case 2.3.1.4.1: This is the design basis model. It is a 2x2 array cases MCNP5-1.51 with the fuel assembly centered in the rack cell. The COP used is the "min" set (see Table 5.2(c)). See Figure 2.2.

- Case 2.3.1.4.2: Same as Case 2.3.1.4.1 except that the COP used are in "nom" set.

- Case 2.3.1.4.3: Same as Case 2.3.1.4.1 except that the COP used are in "max" set.

- Case 2.3.1.4.4: Same as Case 2.3.1.4.1 except that the COP used are in "minr" set.

- Case 2.3.1.4.5: Same as Case 2.3.1.4.1 except that the isotopic compositions are at 72 hours cooling time.

The results of these calculations are presented in Table C.1. The results presented in Table C.1 also provide the bounding case from Appendix B so that a comparison can be made between the two calculations.

2.3.2 Core Operating Parameters

As previously discussed, CASMO-4 is used to perform depletion calculations to determine the spent fuel isotopic composition. The operating parameters for spent fuel depletion calculations are discussed in this Section. The core operating parameters which may have a significant impact on BWR spent fuel isotopic composition are void fraction, control blade history, moderator temperature, fuel temperature, and power density. Other parameters such as the effect of burnable absorbers and axial enrichment distribution are discussed in Section 2.3.3 and Section 2.3.4, respectively. For the purpose of determining the bounding set of COP for each lattice, four sets of COP are used (see Table 5.2(c)). The bounding set of COP is determined using both CASMO-4 and MCNP5-1.51 calculations (see Appendix A and Appendix B),. The bounding set of COP for the design basis lattice is used for all design basis lattice calculations (see Appendix C).

2.3.3 Integral Reactivity Control Devices

The only type of burnable absorber used for the fuel assemblies covered in this analysis is Gd. The use of Gd does not increase the reactivity of the assembly, compared to an assembly lattice where all rods contain fuel and no Gd. As discussed in Section 2.3.1.1.1, the Gd in the fuel assembly holds down the fresh fuel assembly reactivity and then, as core depletion occurs, the Gd begins to burnout until it is essentially fully depleted. As the Gd depletes the reactivity of the fuel assembly increases until it reaches a peak. This peak reactivity is the fuel assembly's most reactive condition, which is used for design basis condition.

2.3.4 Axial and Planar Enrichment Variations

All calculations were performed with the design basis fuel assembly lattice pin specific enrichment(s), without any axial variation.

2.3.5 Fuel Assembly Eccentric Positioning and Fuel Assembly De-Channeling

The BWR fuel that is loaded in the SFP racks may not rest exactly in the center of the storage cell, therefore the potential reactivity effect of this eccentric positioning should be evaluated. The ATRIUM 10XM fuel assembly (the most reactive fuel assembly, as will be shown in Section 7) may be de-channeled, therefore the potential reactivity effect of de-channeling should be evaluated. These two parameters, storage cell eccentric positioning and the fuel assembly de-channeling may occur simultaneously and may impact the reactivity effect of each other. Therefore the two parameters should be evaluated together. Evaluations are therefore performed to determine the most limiting fuel radial location for fuel with and without a channel.

The following cases with the fuel assembly channel present are analyzed:

- Case 2.3.5.1: This is the reference for the 2x2 array cases, Case 2.3.5.2 and Case 2.3.5.3. The MCNP5-1.51 model used herein is a 2x2 array with the fuel assembly centered in the rack cell. This model is the same model as the design basis model. See Figure 2.2.

- Case 2.3.5.2: Every fuel assembly is positioned toward the center as shown in Figure 2.3.

- Case 2.3.5.3: Every fuel assembly is positioned toward one corner as shown in Figure 2.4.

- Case 2.3.5.4: This is the reference for Case 2.3.5.5 and Case 2.3.5.6. The MCNP5-1.51 model used herein is an 8x8 array with the fuel assembly centered in the rack cell. The model is the same as the design basis model but the array size is larger.

- Case 2.3.5.5: Every fuel assembly is positioned toward the center as shown in Figure 2.5.

- Case 2.3.5.6: Every fuel assembly is positioned toward one corner as shown in Figure 2.6.

The following cases with the fuel assembly channel NOT present are analyzed:

- Case 2.3.5.7: This is the reference for the 2x2 array cases, Case 2.3.5.8 and Case 2.3.5.9. The MCNP5-1.51 model used herein is a 2x2 array with the fuel assembly centered in the rack cell. This model is the same model as the design basis model except that the fuel channel has been removed.

- Case 2.3.5.8: Every fuel assembly is positioned toward the center as shown in Figure 2.7.

- Case 2.3.5.9: Every fuel assembly is positioned toward one corner as shown in Figure 2.8.

- Case 2.3.5.10: This is the reference for Case 2.3.5.11 and Case 2.3.5.12. The MCNP5-1.51 model used herein is an 8x8 array with the fuel assembly centered in the rack cell. The model is the same as the design basis model but the array size is larger.

- Case 2.3.5.11: Every fuel assembly is positioned toward the center as shown in Figure 2.9.

- Case 2.3.5.12: Every fuel assembly is positioned toward one corner as shown in Figure 2.10.

The maximum positive reactivity effect of the MCNP5-1.51 calculations for the fuel eccentric positioning and de-channeling is added as the bias and the corresponding 95/95 uncertainty is statistically combined with other uncertainties to determine k_{eff}.

2.3.6 Fuel Bundle Orientation in SFP Rack Cell

As described in Section 2.3.1.1.2, fuel assemblies have various radial fuel enrichments and gadolinium distribution. Also, one corner of each fuel assembly is adjacent to the control blade during the depletion in the core. As a result, the fuel depletion is not uniform and therefore one fuel assembly corner may be more reactive than other corners and the fuel assembly orientation in the SFP storage cell may have an impact on reactivity.

Five cases are analyzed to assess the fuel assembly orientation variations and to determine the most limiting fuel orientation in SFP rack cell.

The MCNP5-1.51 model of the reference case is the design basis fuel in the 2x2 array, as shown in Figure 2.2. The MCNP5.1.51 models of the other four cases are the same as that of the reference case, except with different orientations. The following cases are considered:

- Case 2.3.6.1: This is the reference for the 2x2 array cases, Case 2.3.6.2 through Case 2.3.6.5. This model is the same model as the design basis model where the corner of the lattice adjacent to the control blades in the core is oriented towards the north west. See Figure 2.2.

- Case 2.3.6.2: The fuel assembly in each cell in the 2x2 array is oriented as shown in Figure 2.11.

- Case 2.3.6.3: The fuel assembly in each cell in the 2x2 array is oriented as shown in Figure 2.12.

- Case 2.3.6.4: The fuel assembly in each cell in the 2x2 array is oriented as shown in Figure 2.13.

- Case 2.3.6.5: The fuel assembly in each cell in the 2x2 array is oriented as shown in Figure 2.14.

Note that the evaluations use the same MCNP5-1.51 models with periodic boundary conditions used in the design basis calculation. The isotopic compositions of the fuel rods are the same as those of the design basis fuel assembly.

The maximum positive reactivity effect of the MCNP5-1.51 calculations for the fuel bundle orientation is added as the bias and the corresponding 95/95 uncertainty is statistically combined with other uncertainties to determine k_{eff}.

2.3.7 Reactivity Effect of Spent Fuel Pool Water Temperature

The Dresden Station SFP has a normal pool water temperature operating range below 150 °F. For the nominal condition, the criticality analyses are to be performed at the most reactive temperature and density [6]. Also, there are temperature-dependent cross section effects in MCNP5-1.51 that need to be considered. In general, both density and cross section effects may not have the same reactivity effect for all storage rack scenarios, since configurations with strong neutron absorbers typically show a higher reactivity at lower water temperature, while configurations without such neutron absorbers typically show a higher reactivity at a higher water temperature. For the SFP racks which credit neutron absorbers, the most reactive SFP water temperature and density is expected to be at 39.2 °F and 1 g/cc, respectively.

The standard cross section temperature in MCNP5-1.51 is 293.6 K. Cross sections are also available at other temperatures; however, not usually at the desired temperature for SFP criticality analysis. MCNP5-1.51 has the ability to automatically adjust the cross sections to the specified temperature when using the TMP card. Furthermore, MCNP5-1.51 has the ability to make a molecular energy adjustment for select materials (such as water) by using the S(α,β) card. The S(α,β) card is provided for certain fixed temperatures which are not always applicable to SFP criticality analysis. Rather, there are limited temperature options, i.e., 293.6 K and 350 K, etc. Additionally, MCNP5-1.51 does not have the ability to adjust the S(α,β) card for temperatures as it does for the TMP card discussed above. Therefore, additional studies are performed to show the impact of the S(α,β) card at the two available temperatures.

To determine the water temperature and density which result in the maximum reactivity, MCNP5-1.51 calculations are run using the bounding values. Additionally, S(α,β) calculations are performed for both upper and lower bounding S(α,β) values, if needed. Additional cases are added to cover the potential increase in temperature beyond normal conditions (i.e. accident condition).

The following cases are considered:

- Case 2.3.7.1 (reference case): Temperature of 39.2 °F (277.15 K) and a density of 1.0 g/cc are used to determine the reactivity at the low end of the temperature range. The S(α,β) card corresponds to a temperature of 68.81 °F (293.6 K).

- Case 2.3.7.2: Temperature of 150 °F (338.71 K) and a corresponding density of 0.98026 g/cc are used to determine the reactivity at the high end of the temperature range. The S(α,β) card corresponds to a temperature of 68.81 °F (293.6 K).

- Case 2.3.7.3: Temperature of 150 °F (338.71 K) and a corresponding density of 0.98026 g/cc. The S(α,β) card corresponds to a temperature of 170.33 °F (350 K).

- Case 2.3.7.4: Temperature of 212 °F (373.15 K) and a corresponding density of 0.95837 g/cc. The S(α,β) card corresponds to a temperature of 170.33 °F (350 K). This is a SFP water temperature accident condition.

- Case 2.3.7.5: Temperature of 212 °F (373.15 K) and a corresponding density of 0.95837 g/cc. The S(α,β) card corresponds to a temperature of 260.33 °F (400 K). This is a SFP water temperature accident condition.

- Case 2.3.7.6: Temperature of 255 °F (397.04 K) and a corresponding density of 0.84591 g/cc. The S(α,β) card corresponds to a temperature of 260.33 °F (400 K). In this model, it is assumed that the water modeled includes 10% void. Void is modeled as 10% decrease in density, compared to the density of water at 255 °F. This is a SFP water temperature accident condition.

The bounding water temperature and density (the temperature and its corresponding density which result in the maximum reactivity) of the above cases are applied to all further calculations so that the most reactive water temperature and density is considered. Note that the evaluations use the same MCNP5-1.51 models used in the design basis calculation. The pin specific isotopic compositions of the fuel rods are the same as those of the design basis fuel assembly.

2.3.8 Fuel and Storage Rack Manufacturing Tolerances

In order to determine the k_{eff} of the SFP at a 95% probability at a 95% confidence level, consideration is given to the effect of the BWR fuel and SFP storage rack manufacturing tolerances on reactivity. The reactivity effects of significant independent tolerance variations are combined statistically [6]. The evaluations use the same MCNP5-1.51 models used in the design basis calculation.

2.3.8.1 Fuel Manufacturing Tolerances

The BWR fuel tolerances for ATRIUM 10XM design basis lattice (which is the most reactive fuel design evaluated herein) are presented in Table 5.1(h). Fuel tolerance calculations are performed using the design basis fuel assembly lattice only because the reactivity of the design basis lattice is much greater than lattices from other fuel bundle designs. Therefore, only the tolerances applicable to that lattice are applicable. Separate CASMO-4 depletion calculations are performed for each fuel tolerance and the full value of the tolerance is applied for each case in both the depletion and in rack calculations. Pin specific compositions are used. The MCNP5-1.51 tolerance calculation is compared to the MCNP5-1.51 reference case (nominal parameter values) at the 95% probability at a 95% confidence level using the following equation:

$$\text{delta-}k_{calc} = (k_{calc2} - k_{calc1}) \pm 2 * \sqrt{(\sigma_1^2 + \sigma_2^2)}$$

The following fuel manufacturing tolerances cases are considered in this analysis:

- Case 2.3.8.1.1 (reference case): This is the reference for all the other fuel tolerance cases. This MCNP5-1.51 model is the same model as the design basis model. See Figure 2.2.
- Case 2.3.8.1.2: This is the fuel pellet density increase tolerance.
- Case 2.3.8.1.3: This is the fuel pellet diameter increase tolerance.
- Case 2.3.8.1.4: This is the fuel pellet diameter decrease tolerance.
- Case 2.3.8.1.5: This is the minimum cladding thickness tolerance. In this model, the maximum cladding inner diameter and minimum cladding outer diameter are applied together.
- Case 2.3.8.1.6: This is the increased rod pitch tolerance.
- Case 2.3.8.1.7: This is the decreased rod pitch tolerance.
- Case 2.3.8.1.8: This is the increased channel thickness tolerance.
- Case 2.3.8.1.9: This is the decreased channel thickness tolerance.
- Case 2.3.8.1.10: This is the increased fuel enrichment tolerance. All fuel pins have an increase in U-235 enrichment, including the Gd rods, of 0.05 wt% U-235.
- Case 2.3.8.1.11: This is the decreased Gd loading tolerance.

The maximum positive reactivity effect of the MCNP5-1.51 calculations for each tolerance is statistically combined with the other tolerance results, and this result is then statistically combined with other uncertainties when determining the k_{eff} value.

2.3.8.2 SFP Storage Rack Manufacturing Tolerances

The SFP rack tolerances are presented in Table 5.3. The full value of the tolerance is applied for each case. The MCNP5-1.51 tolerance calculation is compared to the MCNP5-1.51 reference case with a 95% probability at a 95% confidence level using the following equation:

$$\text{delta-}k_{calc} = (k_{calc2} - k_{calc1}) \pm 2 * \sqrt{(\sigma_1^2 + \sigma_2^2)}$$

The following rack manufacturing tolerances cases are considered in this analysis:

- Case 2.3.8.2.1 (reference case): This is the reference for all the other rack tolerance cases.

This MCNP5-1.51 model is the same model as the design basis model. See Figure 2.2.

- Case 2.3.8.2.2: This is the increased storage cell inner diameter (ID) tolerance.
- Case 2.3.8.2.3: This is the decreased storage cell inner diameter tolerance.
- Case 2.3.8.2.4: This is the increased wall thickness tolerance. Note that the tolerance associated with the wall thickness is assumed to be 10% of the wall thickness.
- Case 2.3.8.2.5: This is the decreased wall thickness tolerance. Note that the tolerance associated with the wall thickness is assumed to be 10% of the wall thickness.
- Case 2.3.8.2.6: This is the increased storage cell pitch tolerance.
- Case 2.3.8.2.7: This is the decreased storage cell pitch tolerance.
- Case 2.3.8.2.8: This is the increased BORAL width tolerance.
- Case 2.3.8.2.9: This is the decreased BORAL width tolerance.

The maximum positive reactivity effect of the MCNP5-1.51 calculations for each tolerance is statistically combined with the other tolerance results, and this result is then statistically combined with other uncertainties when determining the k_{eff} value.

The evaluations use the same MCNP5-1.51 models used in the design basis calculation. The isotopic compositions of the fuel rods are the same as those of the design basis fuel assembly.

The poison thickness and loading are used at their minimum values for all calculations; i.e., they are treated as a bias instead of uncertainty, for conservatism and simplification.

2.3.9 Fuel Depletion Calculation Uncertainty

To account for the uncertainty of the number densities in the depletion calculations performed in CASMO-4, a 5% depletion uncertainty factor as described in [6] and [7] is used. Note that an additional uncertainty factor is used to account for the uncertainty in the cross sections; for fission products see Section 2.3.10.

The depletion uncertainty is applied by multiplying it with the reactivity difference (at 95%/95%) between the MCNP5-1.51 calculation with spent fuel at peak reactivity (includes residual Gd) and a corresponding MCNP5-1.51 calculation with fresh fuel (without Gd_2O_3).

The uncertainty is determined by the following:

$$\text{Uncertainty}_{\text{Isotopics}} = [\ (k_{\text{calc-2}} - k_{\text{calc-1}}) + 2 * \sqrt{(\sigma_{\text{calc-1}}^2 + \sigma_{\text{calc-2}}^2)}\ ] * 0.05$$

with

k_{calc-1} = k_{calc} with spent fuel
k_{calc-2} = k_{calc} with fresh fuel
σ_{calc-1} = Standard deviation of k_{calc-1}
σ_{calc-2} = Standard deviation of k_{calc-2}

The following case is considered:

- Case 2.3.9.1 (reference case): This is the reference case. This MCNP5-1.51 model is the same model as the design basis model. See Figure 2.2.

- Case 2.3.9.2: This is the fresh fuel with no Gd case.

The result of the MCNP5-1.51 calculation for the fuel depletion calculation uncertainty is statistically combined with other uncertainties to determine k_{eff}.

[redacted]

2.3.11 Depletion Related Fuel Assembly Geometry Changes

During irradiation the BWR fuel assembly may experience depletion related fuel geometry changes. These changes can be fuel rod growth and cladding creep, crud buildup, fuel rod bow and the fuel channel may bow and bulge. These fuel assembly geometry changes can affect the neutron spectrum during depletion by changing the fuel to moderator ratio. In the spent fuel pool, there are two potential impacts from the depletion related fuel geometry changes: first, the effect during depletion may lead to a different isotopic composition, second, the fuel geometry change itself can also impact reactivity by the change in the fuel to moderator ratio. The effect of these possible fuel geometry changes on the reactivity of the fuel in the SFP are discussed below.

Note that since the peak reactivity for the design basis fuel assembly is below 20 GWd/mtU (i.e. is about 11 GWd/mtU), there is no expected significant reactivity impact associated with any minimal fuel geometry changes which occur below that exposure value.

2.3.11.1 Fuel Rod Geometry Changes

Possible changes to the fuel rod geometry may occur as a result of fuel rod growth, cladding creep, and crud buildup. These geometry changes have the potential to change the fuel-to-moderator ratio in the geometry, thus potentially increasing reactivity, and are therefore discussed below.

2.3.11.1.1 Fuel Rod Growth and Cladding Creep

Fuel rod growth and cladding creep is not expected for the design basis lattice at the peak reactivity burnup (i.e. about 11 GWd/mtU). Therefore, no additional calculations are performed.

2.3.11.1.2 Fuel Rod Crud Buildup

Crud buildup on the fuel rod cladding decreases the amount of water around the fuel rods and thus increases the fuel-to-moderator ratio. The amount of crud buildup at peak reactivity is not expected to be significant. Therefore, no further evaluations are performed.

2.3.11.1.3 Fuel Rod Bow

Fuel rod bow is a depletion related geometry change that alters the fuel rod pitch. The effect of the fuel rod bow is similar to the fuel rod crud buildup (see Section 2.3.11.1.2). The reactivity impact of this geometry change to the fuel in the SFP is evaluated using the depletion related fuel rod pitch positive tolerance provided in Table 5.1(h).

The following fuel rod bow cases are considered:

- Case 2.3.11.1.3.1 (reference case): This is the reference case. This MCNP5-1.51 model is the same model as the design basis model. See Figure 2.2.

- Case 2.3.11.1.3.2: This is the fuel rod bow case. The isotopic compositions are taken from CASMO4 runs with this geometry change included. The geometry change is also included in the geometry of the MCNP5-1.51 model.

The results of the MCNP5-1.51 calculations are used to determine a bias and bias uncertainty. The bias and bias uncertainty are applied to the design basis results as discussed in Section 2.3.13.

The maximum positive reactivity effect of the MCNP5-1.51 calculations for the fuel rod bow is added as the bias and the corresponding 95/95 uncertainty is statistically combined with other uncertainties to determine k_{eff}.

2.3.11.2 Fuel Channel Bulging and Bowing

Fuel channel bulging and bowing is a depletion related geometry change that changes the proximity of the channel to the fuel rods. Since the proximity of the channel relative to the fuel rods may change, the temperature and density of the moderator during depletion may change (volume of moderator inside the channel may change). The reactivity effect of fuel channel bulging and bowing is evaluated using the channel outer exposed width tolerance presented in Table 5.1(h).

The following fuel channel bulging and bowing cases are considered:

- Case 2.3.11.2.1: This is the fuel channel bulging and bow case. The isotopic compositions are taken from CASMO4 runs with this geometry change included. The geometry change is also included in the geometry of the MCNP5-1.51 model.

The results of the MCNP5-1.51 calculations are used to determine a bias and bias uncertainty. The bias and bias uncertainty are applied to the design basis results as discussed in Section 2.3.13.

The maximum positive reactivity effect of the MCNP5-1.51 calculations for the fuel channel bulging and bowing is added as the bias and the corresponding 95/95 uncertainty is statistically combined with other uncertainties to determine k_{eff}.

2.3.12 SFP Storage Rack Interfaces

The Dresden SFP storage racks are all the high density egg crate design. BORAL panels are fixed to the outside of all fabricated cells and these fabricated cells are joined to create formed cells. Along the outside of each rack module, BORAL panels are not fixed to the locations where the formed cells reach the edge, thus there is no BORAL panel every other location. For each rack module, the fabricated cell is placed in each corner of the module so that there is always a BORAL panel beginning and ending each rack module edge. For the location where the formed cell is along the rack module edge there is a steel filler plate welded to cover the hole.

The rack design method creates a configuration where there may be no BORAL between two fuel bundles in adjacent rack modules, only the steel filler plates. Therefore, the reactivity effect of this interface condition is evaluated.

The following interface cases are considered:

- Case 2.3.12.1. The MCNP5-1.51 model is a 16x16 array model. The array is the same as the design basis model except that along every 8 columns of cells every other location has both BORAL panels removed. The two steel sheathings were left in the model to represent the steel plate. Thus, the steel plate thickness considered in the model is thinner than the actual steel plate (see Table 5.3). Note that in this model the gap between racks is not included in the model at all. All fuel is cell centered. See Figure 2.15.

- Case 2.3.12.2: This is the same as Case 2.3.12.1 except the fuel is eccentric towards the center of the model.

For the purpose of the interface calculations, two 16x16 array models that are larger arrays of the design basis model (one cell centered and one with the fuel eccentric towards the center of the model), are used as reference cases. The results of the MCNP5-1.51 calculations are used to determine a bias and bias uncertainty.

The maximum positive reactivity effect of the MCNP5-1.51 calculations for the storage rack interface is added as the bias and the corresponding 95/95 uncertainty is statistically combined with other uncertainties to determine k_{eff}.

2.3.13 Maximum k_{eff} Calculation for Normal Conditions

The calculation of the maximum k_{eff} of the SFP storage racks fully loaded with design basis fuel assemblies at their maximum reactivity is determined by adding all uncertainties and biases to the calculated reactivity. Note that the BORAL thickness and its B-10 loading are taken at their worst case values in all design basis cases.

k_{eff} is determined by the following equation:

$k_{eff} = k_{calc}$ + uncertainty + bias

where uncertainty includes:

- Fuel manufacturing tolerances
- SFP storage rack manufacturing tolerances
- Fuel eccentricity bias uncertainty
- Fuel orientation bias uncertainty
- Fuel channel bow bias uncertainty
- Fuel rod bow bias uncertainty
- Depletion calculation uncertainty
- [redacted]
- MCNP5-1.51 bias uncertainty (95% probability at a 95% confidence level)
- MCNP5-1.51 calculations statistics (95% probability at a 95% confidence level, 2σ)
- Interface bias uncertainty

and the bias includes

- Fuel eccentricity bias
- Fuel orientation bias
- Fuel channel bow bias
- Fuel rod bow bias
- MCNP5-1.51 bias
- Interface bias

Note that each uncertainty is statistically combined with other uncertainties, while biases are added together in order to determine k_{eff}.

[redacted]

2.3.14 Fuel Movement, Inspection and Reconstitution Operations

Fuel movement procedures govern the movement and inspection of the fuel at all times that the fuel is onsite. The new fuel enters the SFP via the fuel prep machine (FPM). The FPM has a single fuel assembly capacity. There are two FPMs in each SFP, which could be loaded with fuel at the same time. However, the FPMs are greater than six feet apart, which is a low reactivity

configuration because of the distance between either FPM so no further analysis beyond the normal condition is necessary. The fuel is then picked up by the refueling platform, which also has a single fuel assembly capacity at any given time, and moved into a storage location in the storage rack. The fuel is always moved above the rack and never moved along the side of the rack. From the storage rack, the fuel is picked up by the refueling platform and moved through the refueling slot for transport to the core. The return trip uses the same process in reverse. All of these fuel movement operations involve a single fuel assembly that is never in close enough (i.e., directly adjacent) proximity to any other fuel that the configuration is not bounded by the analysis for normal conditions.

The FPM is not considered to be a long-term storage location for fuel but it is physically possible that a fuel assembly in the FPM could be approached by another fuel assembly in the refueling platform. The FPM is only single capacity; therefore, once a fuel assembly is in the FPM there is no normal operation that would allow the presence of another fuel assembly in close proximity to the FPM. This configuration (i.e., two fuel bundles in or around a FPM) is not considered a normal configuration.

Due to the location of the FPM, only one of the two refueling platforms can ever physically use the FPM at any given time. Furthermore, dimensions for distance from the FPMs to the nearest SFP rack is 7 inches, which is more than the dimensions of a fuel assembly.

2.3.15 Accident Condition

The accidents considered are:

- SFP temperature exceeding the normal range
- Dropped assemblies
- Missing BORAL Panel
- Rack movement
- Mislocated fuel assembly (a fuel assembly in the wrong location outside the storage rack, including the platform area)

Those are briefly discussed in the following sections.

Note that the double contingency principle as stated in [6] specifies that "two unlikely independent and concurrent incidents or postulated accidents are beyond the scope of the required analysis." This principle precludes the necessity of considering the simultaneous occurrence of multiple accident conditions. The k_{eff} calculations performed for the accident conditions are done with a 95% probability at a 95% confidence level.

The accident conditions are considered at the 95/95 level using the total corrections from the design basis case. Note that the design basis lattice is used for the accident analyses.

2.3.15.1 Temperature and Water Density Effects

The SFP water temperature accident conditions for consideration are the increase in SFP water temperature above the maximum SFP operating temperature of 150 °F (the decrease in temperature was already considered for the temperature coefficient determination as discussed in Section 2.3.7). The increase in SFP temperature accident cases are discussed in Section 2.3.7 and are bounded by the calculations at reduced temperature.

2.3.15.2 Dropped Assembly – Horizontal

For the case in which a fuel assembly is assumed to be dropped on top of a rack, the fuel assembly will come to rest horizontally on top of the rack with a separation distance between the fueled portions of the two assemblies of more than 12 inches. Thus, the horizontally dropped assembly is decoupled from the fuel assemblies in the rack. This accident is also bounded by the mislocated case, where the mislocated assembly is closer to the assembly in the racks. Therefore, the horizontally dropped fuel assembly is not evaluated further in the report.

2.3.15.3 Dropped Assembly – Vertical into an Empty Storage Cell

It is also physically possible to vertically drop an assembly into a location that might be empty and such a drop may result in deformation of the rack baseplate. In that case some part of the active fuel length may extend beyond the BORAL panel out of the bottom of the rack. This potential configuration is physically similar to the normal condition of insertion and removal of fuel from the storage rack. In the normal condition of insertion and removal of a fuel assembly from the storage cell, the active fuel in the rack remains well within the length of the BORAL panels, while the part of the moving fuel bundle that is above the length of the BORAL panel is physically separated from the fuel in the rack by a sufficient amount of water to preclude neutron coupling. For the case where the fuel assembly is dropped into an empty cell, the fuel assembly could potentially break through the baseplate. The design of the rack is such that each storage cell location has a baseplate that is not connected with the adjacent cells. Therefore, this accident condition is physically the same as the normal condition of insertion and removal of fuel in the rack. However, this case is considered to show that there is no reactivity effect associated with this configuration.

The following vertical drop cases are considered:

- Case 2.3.15.3.1: This MCNP5-1.51 model is the same model as the design basis model but the array is 16x16. In the center location, the active length is extended below the active length of the other fuel by the thickness of the baseplate and the distance from the baseplate to the pool floor (see Table 5.3). All fuel is centered in the storage cell. See Figure 2.16.

- Case 2.3.15.3.2: Same as Case 2.3.15.3.1 but the fuel is eccentric in the storage cell towards the dropped fuel.

2.3.15.4 Missing BORAL Panel

The missing BORAL panel accident is considered to cover the potential that a BORAL panel may have been inadvertently not installed during construction of the rack or that a panel might become dislodged by some other accident force.

The following cases are considered:

- Case 2.3.15.4.1: This MCNP5-1.51 model is the same model as the design basis model but the array is 8x8. The cell in the center of the model has 1 BORAL panel removed. All fuel is centered in the storage cell. See Figure 2.17.

- Case 2.3.15.4.2: This is the same as Case 2.3.15.4.1 but the fuel is eccentric toward the missing BORAL panel.

2.3.15.5 Rack movement

The racks may move due to seismic activity and the gaps between racks may close. However, the design basis analysis already considers the interface of the racks without any gap, and therefore this condition is already analyzed.

2.3.15.6 Mislocated Fuel Assembly

The Dresden SFP layout was reviewed to determine the possible worst case locations for a mislocated fuel assembly. Five hypothetical locations where a fuel assembly may be mislocated are:

- Adjacent to the storage rack side where there is no BORAL panel
- In the corner between two racks
- In the corner between three racks
- Between the SFP rack and the FPM
- Between the two locations on the FPM.

The cited scenarios are evaluated, as follows.

2.3.15.6.1 Mislocated Fuel Assembly Adjacent to the Storage Rack

A fuel assembly may be mislocated adjacent to the storage rack in one of the alternating locations where there is no BORAL panel. The reactivity effect of this accident is discussed below.

The following cases are considered:

- Case 2.3.15.6.1.1: This MCNP5-1.51 model is the same model as the design basis model but the array is 80x80. The mislocated fuel assembly is placed adjacent to the storage rack on one side, aligned vertically with the fuel in the storage rack and in a location that is face adjacent to a location with no BORAL panel. The fuel in the storage rack is cell centered.

- Case 2.3.15.6.1.2: This is the same as Case 2.3.15.6.1.1 but the fuel in the storage rack is eccentrically positioned toward the center of the model.

2.3.15.6.2 Mislocated Fuel Assembly in the Corner between Two Racks

There are some places in the SFP, but outside of the racks, where the mislocated fuel assembly may be in the corner between two racks (thus the mislocated fuel assembly would be adjacent to the fuel assemblies in racks from two sides). To evaluate the effect of the mislocated fuel assembly in the corner between two racks, the following cases are evaluated:

- Case 2.3.15.6.2.1: This MCNP5-1.51 model is the same model as the design basis model but the array is 80x80 with a corner cut out to model the junction of two racks. The mislocated fuel assembly is in the corner between two racks. The two rack faces where the fuel assembly is mislocated do not have BORAL panels. This configuration is not physically possible because the racks are designed so that the BORAL panels are always in the first location along the outer edge. However, this model is conservative. The fuel in the storage rack is cell centered. See Figure 2.18.

- Case 2.3.15.6.2.2: The MCNP5-1.51 model is the same as Case 2.3.15.6.2.1, except with all fuel assemblies in the storage rack eccentric toward the misplaced fuel assembly.

2.3.15.6.3 Mislocated Fuel Assembly in the Corner between Three Racks

There is a location in the SFP where the mislocated fuel assembly may be in the corner between three racks (thus the mislocated fuel assembly would be adjacent to the fuel assemblies in racks from three sides, although there is a significant gap for the third face). To evaluate the effect of the mislocated fuel assembly in the corner between three racks, the following cases are evaluated:

- Case 2.3.15.6.3.1: This MCNP5-1.51 model is the same model as the design basis model but the array is 80x80 with a corner cut out to model the junction of three racks. The mislocated fuel assembly is in the corner between the three racks. The two rack faces where the fuel assembly is mislocated do not have BORAL panels. This configuration is not physically possible because the racks are designed so that the BORAL panels are always in the first location along the outer edge. However, this model is conservative. The fuel in the storage rack is cell centered. See Figure 2.19.

- Case 2.3.15.6.3.2: The MCNP5-1.51 model is the same as Case 2.3.15.6.3.1, except with all fuel assemblies in the storage rack eccentric toward the misplaced fuel assembly.

- Case 2.3.15.6.3.3: The MCNP5-1.51 model is the same as Case 2.3.15.6.3.1, except that the gap between the mislocated fuel assembly and the third rack is closed.

- Case 2.3.15.6.3.4: The MCNP5-1.51 model is the same as Case 2.3.15.6.3.3, except with all fuel assemblies in the storage rack eccentric toward the misplaced fuel assembly.

2.3.15.6.4 Mislocated Fuel Assembly in the FPM

The FPM is located adjacent to the SFP storage racks. The FPM has a fuel assembly capacity of two, where the pitch between the two locations on the FPM is specified in Table 5.3. There is a possibility that a fuel assembly could be mislocated between the two FPM locations or between the FPM locations and the storage rack. Note that the pitch is large enough to preclude neutron coupling between FPM locations. However, for conservatism, the evaluation of this potential mislocated fuel assembly accident condition considers that the distance between the two FPM locations is reduced to about 12 inches and one of them is face adjacent to a missing BORAL panel location. The gap between the FPM location and the storage rack is 7 inches.

The following FPM mislocated fuel assembly accident cases are considered:

- Case 2.3.15.6.4.1: The FPM mislocated MCNP5-1.51 model is a large 80x80 array. The model includes two FPM fuel assemblies. No FPM structural materials are considered. The mislocated fuel assembly is placed between the two FPM fuel assemblies with a small gap (position 1) to the closest location. The fuel is centered in the SFP storage rack cells. See Figure 2.20.

- Case 2.3.15.6.4.2: This is the same as Case 2.3.15.6.4.1 but the fuel is eccentric in the SFP storage rack cells toward the FPM.

- Case 2.3.15.6.4.3: This is the same as Case 2.3.15.6.4.1 but the mislocated fuel is at a distance (position 2) from the closest FPM location.

- Case 2.3.15.6.4.4: This is the same as Case 2.3.15.6.4.3 but the fuel is eccentric in the SFP storage rack cells towards the mislocated fuel assembly.

- Case 2.3.15.6.4.5: This is the same as Case 2.3.15.6.4.1 but the mislocated fuel is at a distance (position 3) from the closest FPM location.

- Case 2.3.15.6.4.6: This is the same as Case 2.3.15.6.4.5 but the fuel is eccentric in the SFP storage rack cells toward the mislocated fuel assembly.

- Case 2.3.15.6.4.7: This is the same as Case 2.3.15.6.4.1 but the mislocated fuel is at a distance (position 4) from the closest FPM location.

- Case 2.3.15.6.4.8: This is the same as Case 2.3.15.6.4.7 but the fuel is eccentric in the SFP storage rack cells toward the mislocated fuel assembly.

- Case 2.3.15.6.4.9: This is the same as Case 2.3.15.6.4.1 but the mislocated fuel is directly adjacent to the closest FPM location (position 5). See Figure 2.21

- Case 2.3.15.6.4.10: This is the same as Case 2.3.15.6.4.9 but the fuel is eccentric in the SFP storage rack cells toward the mislocated fuel assembly.

- Case 2.3.15.6.4.11: This is the same as Case 2.3.15.6.4.1 but the mislocated fuel is between the SFP rack and the FPM fuel. The mislocated fuel is directly adjacent to the SFP storage rack location without a BORAL panel (position 6). See Figure 2.22.

- Case 2.3.15.6.4.12: This is the same as Case 2.3.15.6.4.11 but the fuel is eccentric in the SFP storage rack cells toward the mislocated fuel assembly.

- Case 2.3.15.6.4.13: This is the same as Case 2.3.15.6.4.11 but the mislocated fuel is directly adjacent to the closest FPM location (position 7). See Figure 2.23.

- Case 2.3.15.6.4.14: This is the same as Case 2.3.15.6.4.13 but the fuel is eccentric in the SFP storage rack cells toward the mislocated fuel assembly.

2.3.16 Reconstituted Fuel Assemblies

The SFP contains various reconstituted assemblies. The entire population of previously reconstituted fuel has been examined to determine if the reconstitution may have created a more reactive lattice than those which have been evaluated for this analysis. The evaluation of the population of reconstituted fuel shows that most of the fuel is very old low reactivity legacy fuel and that there has been no reconstituted bundles that may pose a risk of not being bounded by the analysis. The evaluation also showed that there is a small set of newer Optima2 fuel bundles that have been reconstituted. However, the enrichment of these bundles is less than 4.2 wt% U-235, and therefore clearly bounded by the analysis. Therefore, all previously reconstituted fuel is considered bounded by the analysis and no further analysis is required. All future reconstituted bundles will have to be evaluated to determine if they are bounded by the analysis.

3. ACCEPTANCE CRITERIA

Codes, standard, and regulations or pertinent sections thereof that are applicable to these analyses include the following:

- Code of Federal Regulations, Title 10, Part 50, Appendix A, General Design Criterion 62, "Prevention of Criticality in Fuel Storage and Handling."
- Code of Federal Regulations, Title 10, Part 50.68, "Criticality Accident Requirements."
- USNRC Standard Review Plan, NUREG-0800, Section 9.1.1, Criticality Safety of Fresh and Spent Fuel Storage and Handling, Revision 3 – March 2007.
- L. Kopp, "Guidance on the Regulatory Requirements for Criticality Analysis of Fuel Storage at Light-Water Reactor Power Plants," NRC Memorandum from L. Kopp to T. Collins, August 19, 1998.
- ANSI ANS-8.17-1984, Criticality Safety Criteria for the Handling, Storage and Transportation of LWR Fuel Outside Reactors (withdrawn in 2004).
- USNRC, NUREG/CR-6698, Guide for Validation of Nuclear Criticality Safety Calculational Methodology, January 2001.
- DSS-ISG-2010-01, Revision 0, Staff Guidance Regarding the Nuclear Criticality Safety Analysis for Spent Fuel Pools.

4. ASSUMPTIONS

The analyses apply a number of assumptions, either for conservatism or to simplify the calculation approach. Important aspects of applying those assumptions are as follows:

1. Bounding or sufficiently conservative inputs and assumptions are used essentially throughout the entire analyses, and as necessary studies are presented to show that the selected inputs and parameters are in fact conservative or bounding.
2. Neutron absorption in minor structural members of the fuel assembly is neglected, e.g., spacer grids are replaced by water.
3. The neutron absorber length in the rack is more than the active region of the fuel, but it is modeled to be the same length.
4. The fuel density is assumed to be equal to the pellet density for the design basis calculations, and is conservatively modeled as a solid right cylinder over the entire active length, neglecting dishing and chamfering. This is acceptable since the amount of fuel modeled is more than the actual amount.
5. All models are laterally infinite arrays of the respective configuration, neglecting lateral leakage. The exception is where the model boundaries are water, as specified.
6. All fuel cladding materials are modeled as pure zirconium, while the actual fuel cladding consists of one of several zirconium alloys. This is acceptable since the model neglects the trace elements in the alloy which provide additional neutron absorption.
7. The SFP storage rack cell ID and cell wall thickness tolerances are assumed values presented in Table 5.3.

5. INPUT DATA

5.1 *Fuel Assembly Specification*

The SFP racks are designed to accommodate various fuel assembly types used in Dresden Unit 2 and Unit 3. A subset of these fuel designs are presented here for information purposes (the much older fuel designs are not shown):

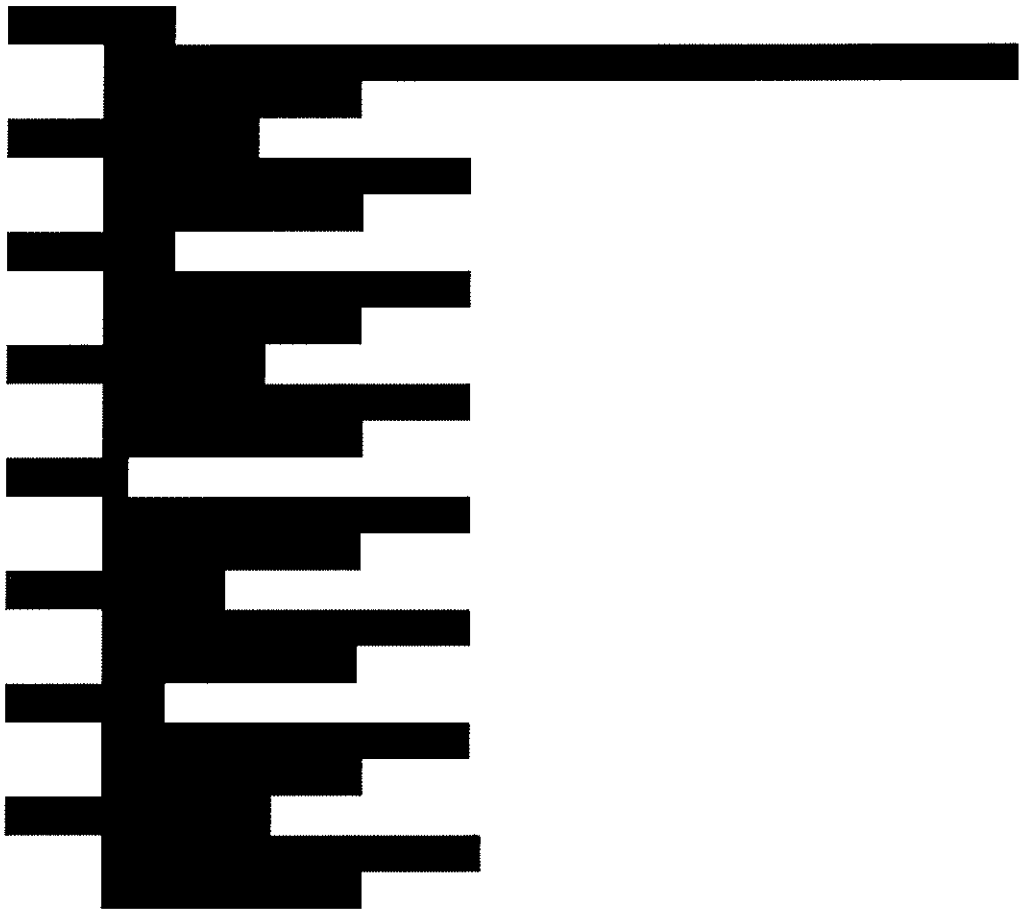

The specifications for the above fuel assemblies designs are presented in Table 5.1. Note that the fuel assembly tolerance information is provided for the bounding fuel design only. As it can be seen in Section 7.1, the reactivity difference between the reactivity of the bounding lattice from the most reactive fuel design and the next most reactive design is large enough to preclude tolerance calculations for both designs.

Additional Specification of the ATRIUM 10XM

[redacted]

[2] Note: This is the expected actual IMPAE; the design basis lattice uses 4.95 wt% U-235.

5.2 *Reactor and SFP Operating Parameters*

The reactor core and SFP operating parameters are provided in Table 5.2(a). The reactor control blade data are provided in Table 5.2(b). The reactor control parameters used in CASMO-4 screening and design basis calculations are provided in Table 5.2(c).

5.3 *Storage Rack Specification*

The spent fuel pool rack parameters are provided in Table 5.3. The rack cells are constructed by fixing BORAL panels to the outside of a fabricated steel cell box with sheathing. The fabricated cells are then joined to create formed cells. On the exterior of every rack module, the location of the formed cells along the exterior without BORAL is closed with a filler plate. Thus, beginning at the corner of each module, the first location has BORAL and then every other location does not have BORAL.

The SFP layout is shown in Figure 5.1.

5.4 *Material Compositions*

The MCNP5-1.51 material specification is provided in Table 5.4(a) for non-fuel materials, and Table 5.4(b) specifies isotopes followed in the fuel pellet.

6. COMPUTER CODES

The following computer codes were used in this analysis.

- MCNP5-1.51 [1] is a three-dimensional continuous energy Monte Carlo code developed at Los Alamos National Laboratory. This code offers the capability of performing full three dimensional calculations for the loaded storage racks. MCNP5-1.51 was run on the PCs at Holtec.
- CASMO-4 [4] is a two-dimensional multigroup transport theory code developed by Studsvik. CASMO-4 is used to perform the depletion calculation for the pin-specific approach, and for various studies. CASMO-4 was run on the PCs at Holtec.

7. ANALYSIS RESULTS

7.1 *Determination of the Design Basis Fuel Assembly Lattice*

As discussed in Section 2.3.1, a complete evaluation of the legacy fuel bundles, current fuel bundle designs and future fuel bundle designs (i.e. the ATRIUM 10XM design) has been performed. Based on the method described in Section 2.3.1, and the discussion presented in Appendix A, CASMO-4 screening calculations were performed for all Optima2 lattices, all ATRIUM 10XM lattices, three ATRIUM 9B lattices and one GE14 lattice. The results of the screening calculations determined a subset of lattices with an in-rack CASMO-4 reactivity greater than 0.8500. The subset of most reactive lattices has been further evaluated using MCNP5-1.51 to determine the bounding lattice. This evaluation is documented in Appendix B.

7.2 *Core Operating Parameters*

As discussed in Section 2.3.2, the effects of the core operating parameters on the reactivity were evaluated both during the design basis lattice screening calculations in Appendix A and Appendix B, as well as in the final design basis models calculations presented in Appendix C, Table C.1. As can be seen from the results in Appendix C, Table C.1 the bounding COP for the design basis lattice is the "min" set (see Table 5.2(c)). Therefore, all design basis calculations use the "min" set of COP. Since the bounding configuration is determined for the various design basis calculations, there is no bias and bias uncertainty associated with COP.

7.3 *Fuel Assembly Eccentric Positioning and Fuel Assembly De-Channeling*

As discussed in Section 2.3.5, the reactivity effect of the fuel assembly position in the storage cell and the reactivity effect of the channel have been evaluated. The results of these calculations are presented in Appendix C, Table C.2. The result show that the bounding fuel assembly position is cell centered and the bounding condition is channeled fuel. Therefore, all

design basis calculations consider the fuel cell centered and with a channel with the exception of specific cases that are otherwise noted. Since the bounding configuration is determined for the various design basis calculations, there is no bias and bias uncertainty associated with fuel assembly eccentric positioning and fuel assembly de-channeling (i.e. the value is zero as presented in Table 7.1 and 7.2).

7.4 *Fuel Bundle Orientation in the SFP Rack Cell*

As discussed in Section 2.3.6, the reactivity effect of the fuel assembly orientation (i.e. orientation of the in core control blade corner) has been evaluated. The results of these calculations are presented in Appendix C, Table C.3. The results of these calculations show that Case 2.3.6.2 has a small bias and bias uncertainty. This small bias and bias uncertainty are therefore considered in the determination of k_{eff} (see Table 7.1 and 7.2).

7.5 *Reactivity Effect of Spent Fuel Pool Water Temperature*

As discussed in Section 2.3.7, the effects of water temperature, and the corresponding water density and temperature adjustments ($S(\alpha,\beta)$) were evaluated for SFP racks. The results of these calculations are presented in Appendix C, Table C.4.

The results of the SFP temperature and density calculations show that as expected (for poisoned racks) the most reactive water temperature and density for the SFP racks is a temperature of 39.2 ^{o}F at a density of 1 g/cc, and these values are used for all calculations in SFP racks with the exception of specific accident conditions.

7.6 *Fuel and Storage Rack Manufacturing Tolerances*

7.6.1 Fuel Manufacturing Tolerances

As discussed in Section 2.3.8.1, the effect of the BWR fuel tolerances on reactivity was determined. The results of these calculations are presented in Appendix C, Table C.5. The maximum positive delta-k value for each tolerance is statistically combined.

The maximum statistical combination of fuel assembly tolerances is used to determine k_{eff} in Table 7.1 and Table 7.2.

7.6.2 SFP Storage Rack Manufacturing Tolerances

As discussed in Section 2.3.8.2, the effect of the manufacturing tolerances on reactivity of the SFP racks was determined. The results of these calculations are presented in Appendix C, Table C.6. The maximum positive delta-k value for each tolerance is statistically combined.

The maximum statistical combination of the SFP rack tolerances is used to determine k_{eff} in Table 7.1 and Table 7.2.

7.6.3 Fuel Depletion Calculation Uncertainty

As discussed in Section 2.3.9, the uncertainty of the number densities in the depletion calculations was evaluated. The results of these calculations are presented in Appendix C, Table C.7. As can be seen in Appendix C, Table C.7, the depletion uncertainty is calculated as 5% of the reactivity difference between the design basis case and a calculation with fresh fuel and no Gd.

The depletion uncertainty is included in the statistical combination of uncertainties used to determine k_{eff} in Table 7.1 and Table 7.2.

.

[redacted]

7.6.5 Depletion Related Fuel Assembly Geometry Changes

As discussed in Section 2.3.11, the reactivity effect of depletion related fuel assembly geometry changes has been evaluated. These evaluations are discussed further below.

7.6.5.1 Fuel Rod Geometry Changes

.

As discussed in Section 2.3.11.1, the reactivity effect of fuel rod geometry changes is evaluated. These evaluations consider fuel rod growth and cladding creep, fuel rod crud buildup and fuel rod bow and are discussed below. As previously discussed, the fuel assembly is not expected to undergo significant depletion related geometry changes at peak reactivity (i.e. about 11 GWd/mtU). However, specific effects are evaluated as discussed below.

7.6.5.1.1 Fuel Rod Growth, Cladding Creep and Fuel Rod Crud Buildup

As discussed in Section 2.3.11.1.1 and Section 2.3.11.1.2, the effect of the fuel rod growth, cladding creep and fuel rod crud buildup on reactivity was not evaluated due to the low burnup at peak reactivity.

7.6.5.1.2 Fuel Rod Bow

As discussed in Section 2.3.11.1.3, the reactivity effect of the fuel rod bow was evaluated by calculation. The fuel rod bow calculation results are presented in Appendix C, Table C.9. The

results presented in Appendix C, Table C.9 show a small bias and bias uncertainty. This bias and bias uncertainty are considered in the determine of k_{eff} as presented in Table 7.1 and 7.2.

7.6.5.2 Fuel Channel Bulging and Bowing

As discussed in Section 2.3.11.2, the reactivity effect of fuel channel bulging and bowing was evaluated by calculation. The fuel channel bow calculation results are presented in Appendix C, Table C.9. The results presented in Appendix C, Table C.9 show a small bias and bias uncertainty. This bias and bias uncertainty are considered in the determine of k_{eff} as presented in Table 7.1 and 7.2.

7.7 *SFP Storage Rack Interfaces*

As discussed in Section 2.3.12, the reactivity effect of the SFP storage rack interfaces, specifically the interface of one storage rack module with another storage rack model has been evaluated. The calculation results are presented in Appendix C, Table C.10. The results presented in Appendix C, Table C.10 show a bias and bias uncertainty. This bias and bias uncertainty are considered in the determine of k_{eff} as presented in Table 7.1 and 7.2.

7.8 *Maximum k_{eff} Calculations for Normal Conditions*

As discussed in Section 2.3.13, the maximum k_{eff} for normal conditions is calculated. The results are tabulated in Table 7.1. The results show that the maximum k_{eff} for the normal conditions in the SFP racks is less than 0.95 at a 95% probability and at a 95% confidence level.

7.9 *Fuel Movement, Inspection and Reconstitution Operation.*

As discussed in Section 2.3.14, the fuel movement, inspection and reconstitution operations are normal conditions that are bounded by the analysis. No further evaluations are required.

7.10 *Abnormal and Accident Conditions*

As discussed in Sections 2.3.15, the effects of various accident conditions has been evaluated. The results of these calculations are presented in Appendix C, Table C.4 (increased SFP temperature only) and Appendix C, Table C.11 (all other accidents). The maximum reactivity accident has been determined to be Case 2.3.15.6.3.4, "Mislocated in the Corner of Three Racks, Closed Rack Gaps, Eccentric Fuel". The calculated results of this accident are used, along with all applicable biases and uncertainties, to show compliance with the regulatory limit in Table 7.2. As it can be seen in Table 7.2, the maximum calculated reactivity is less than 0.95 at a 95% probability and at a 95% confidence level.

8. CONCLUSION

The criticality analysis for the storage of BWR assemblies in the Dresden SFP racks with BORAL has been performed. The results for the normal condition show that k_{eff} is [redacted] with the storage racks fully loaded with fuel of the highest anticipated reactivity, which is the [redacted], at a temperature corresponding to the highest reactivity. The results for the bounding accident condition, i.e. the Mislocated in the Corner of Three Racks, Closed Rack Gaps, Eccentric Fuel (Case 2.3.15.6.3.4), show that k_{eff} is [redacted] with the storage racks fully loaded with fuel of the highest anticipated reactivity, which is [redacted], at a temperature corresponding to the highest reactivity. The maximum calculated reactivity for both normal and accident conditions include a margin for uncertainty in reactivity calculations with a 95% probability at a 95% confidence level. Reactivity effects of abnormal and accident conditions have been evaluated to assure that under all credible abnormal and accident conditions, the reactivity will not exceed the regulatory limit of 0.95.

9. REFERENCES

[1] "MCNP - A General Monte Carlo N-Particle Transport Code, Version 5," Los Alamos National Laboratory, LA-UR-03-1987, April 24, 2003 (Revised 2/1/2008).

[2] "Nuclear Group Computer Code Benchmark Calculations," Holtec Report HI-2104790 Revision 1.

[3] Guide for Validation of Nuclear Criticality Safety Calculational Methodology, NUREG/CR-6698, January 2001.

[4] M. Edenius, K. Ekberg, B.H. Forssén, and D. Knott, "CASMO-4 A Fuel Assembly Burnup Program User's Manual," Studsvik/SOA-95/1; and J. Rhodes, K Smith, "CASMO-4 A Fuel Assembly Burnup Program User's Manual," SSP-01/400, Revision 5, Studsvik of America, Inc. and Studsvik Core Analysis AB (proprietary).

[5] D. Knott, "CASMO-4 Benchmark Against Critical Experiments," SOA-94/13, Studsvik of America, Inc., (proprietary); and D. Knott, "CASMO-4 Benchmark Against MCNP," SOA-94/12, Studsvik of America, Inc., (proprietary).

[6] L.I. Kopp, "Guidance on the Regulatory Requirements for Criticality Analysis of Fuel Storage at Light-Water Reactor Power Plants," NRC Memorandum from L. Kopp to T. Collins, August 19, 1998.

[7] DSS-ISG-2010-01, Staff Guidance Regarding the Nuclear Criticality Safety Analysis for Spent Fuel Pools, Revision 0.

[8] HI-2002444, Latest Revision, "Final Safety Analysis Report for the HI-STORM 100 Cask System", USNRC Docket 72-1014.

[9] "Atlas of Neutron Resonances", S.F. Mughabghab, 5th Edition, National Nuclear Data Center, Brookhaven National Laboratory, Upton, USA.

[10] "Sensitivity Studies to Support Criticality Analysis Methodology," HI-2104598 Rev. 1, October 2010.

[11] "Spent Nuclear Fuel Burnup Credit Analysis Validation", ORNL Presentation to NRC, September 21, 2010.

[12] An Approach for Validating Actinide and Fission Product Burnup Credit Criticality Safety Analyses—Criticality (k_{eff}) Predictions, NUREG/CR-7109, April 2012.

Table 2.1(a)

[redacted]

[redacted]

Table 2.1(b)
Analysis of the MCNP5-1.51 calculations [2]

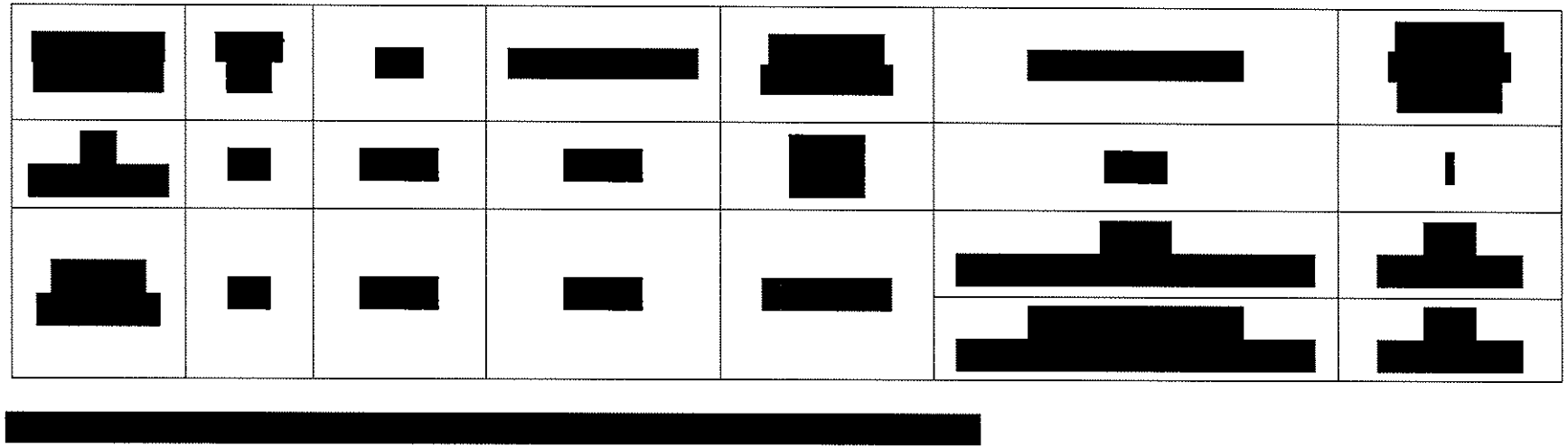

Table 2.1(c)
Bias and Bias Uncertainty as a Function of Independent Parameter for SFP Racks Filled with Pure Water [2]

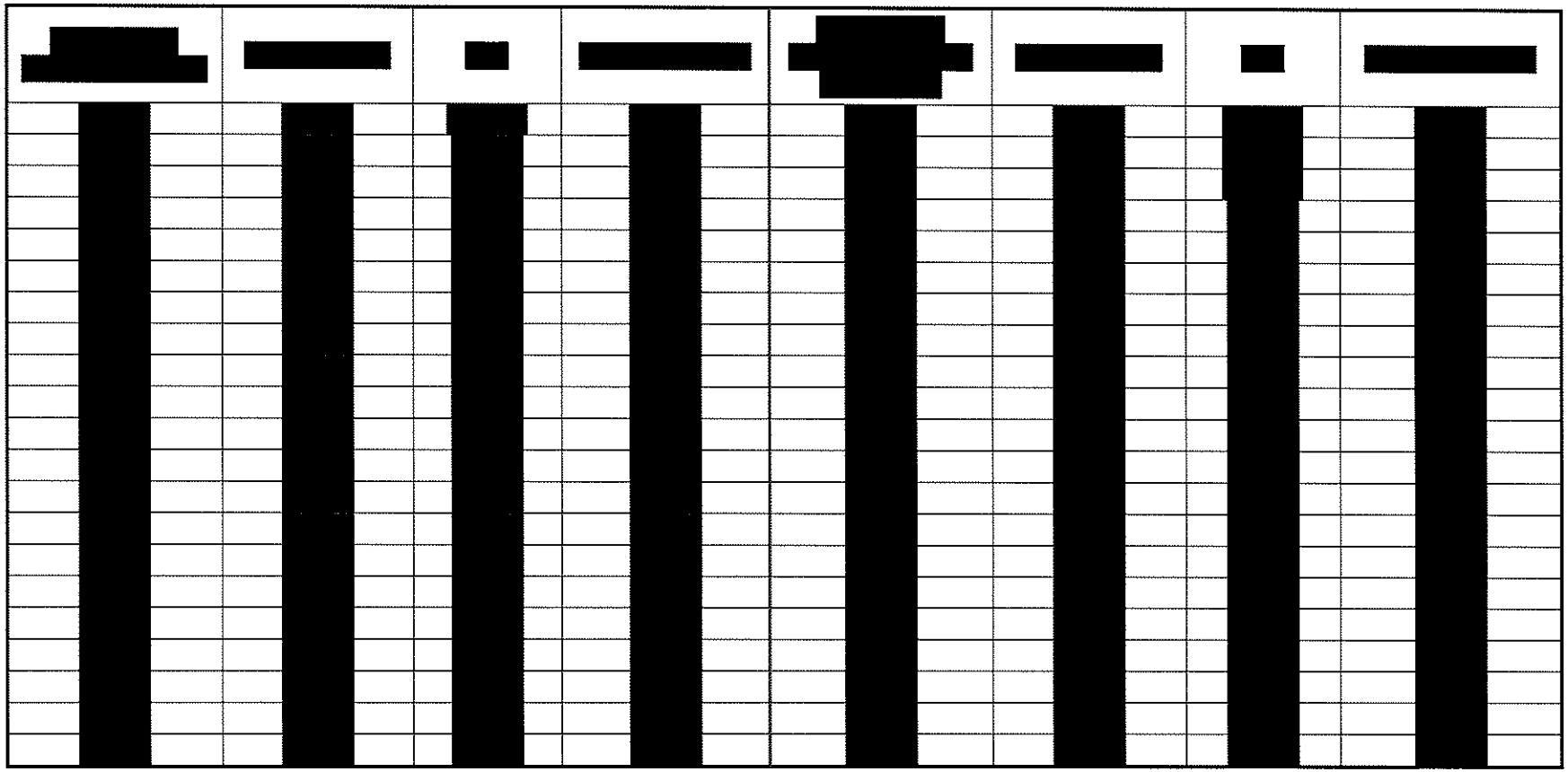

Table 5.1(a)

[redacted]

Table 5.1(b)

[redacted]

Table 5.1(c)

[redacted]

Table 5.1(d)

[redacted]

Table 5.1(e)

[redacted]

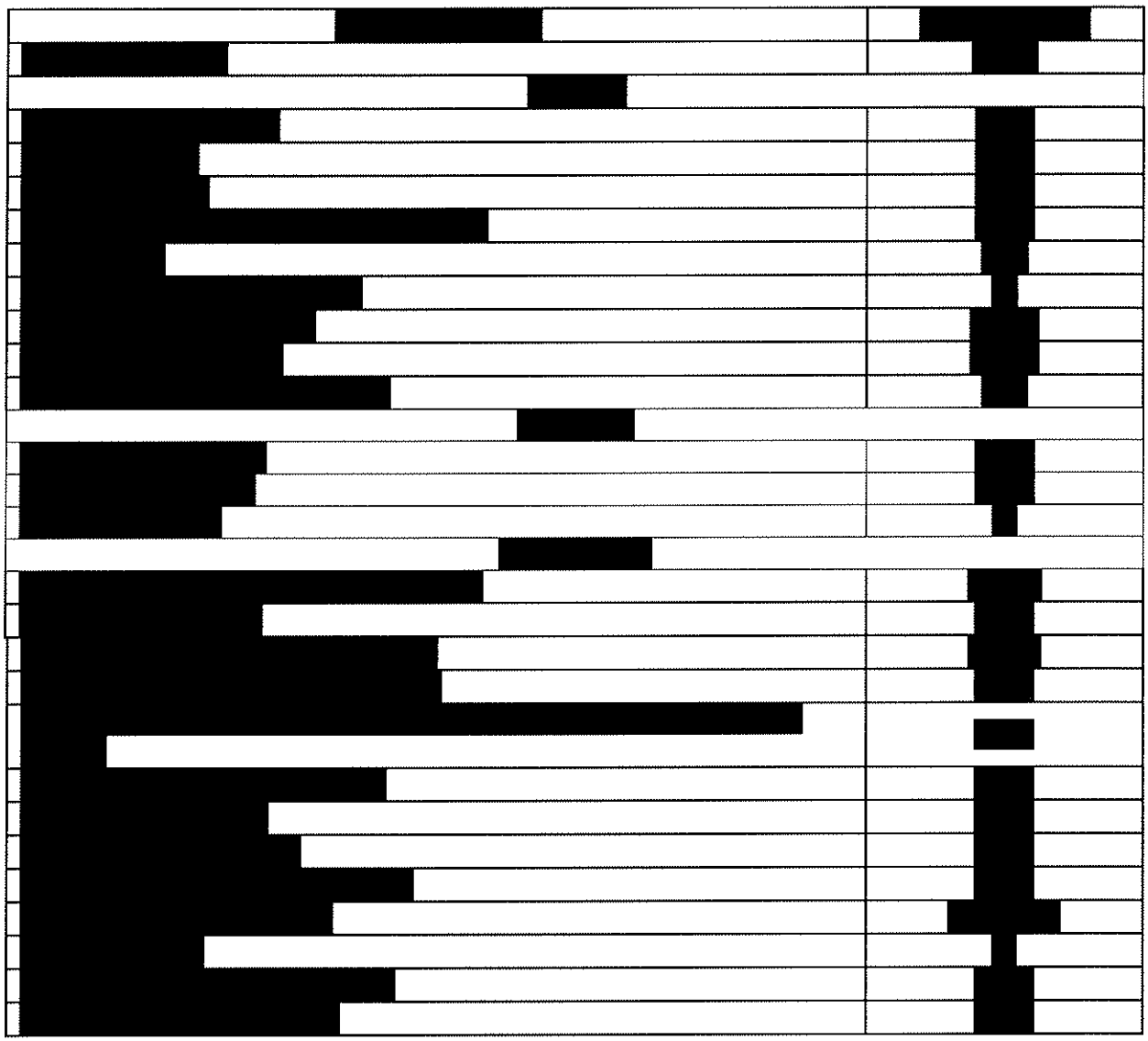

Table 5.1(f)

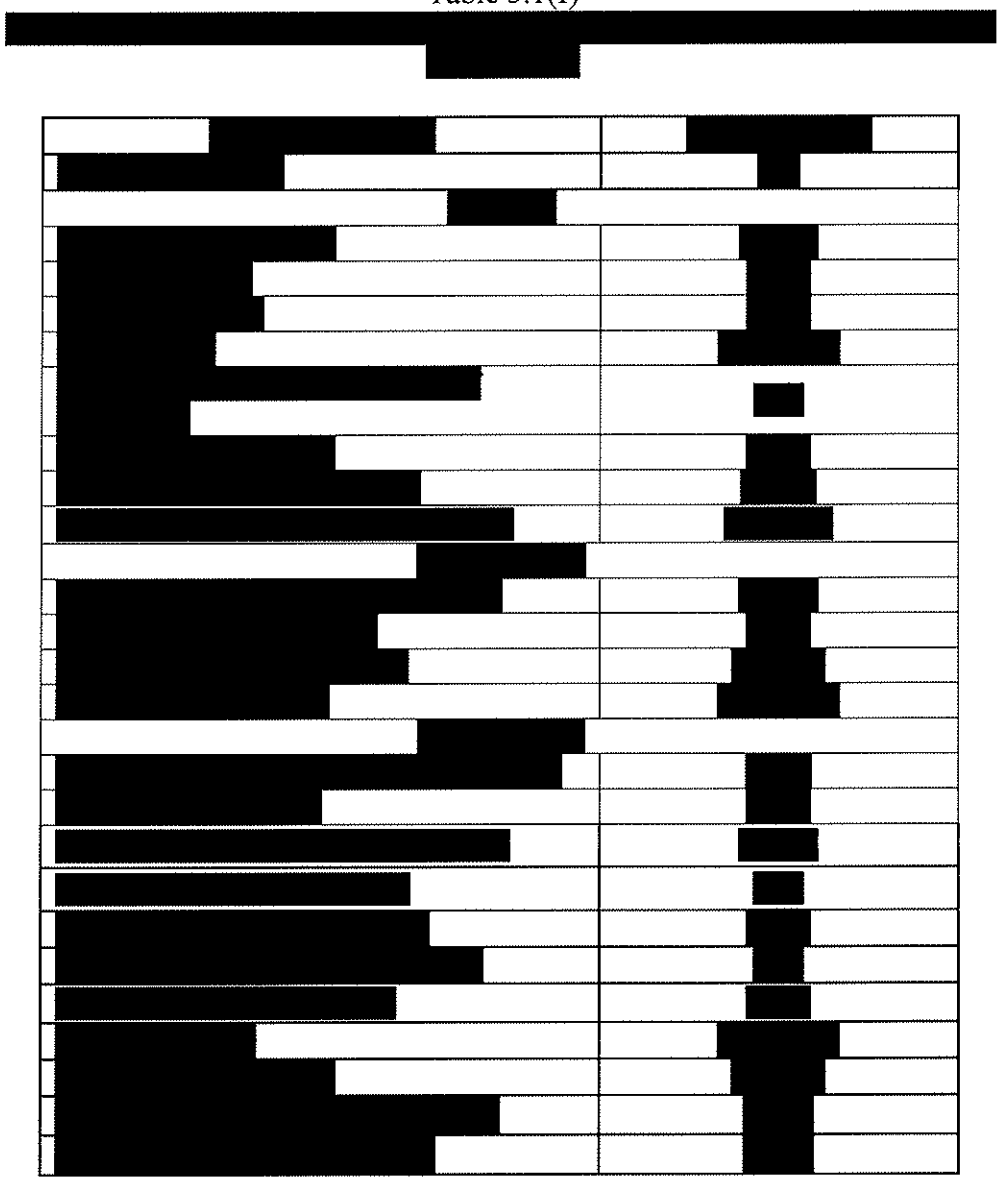

Table 5.1(g)

[redacted]

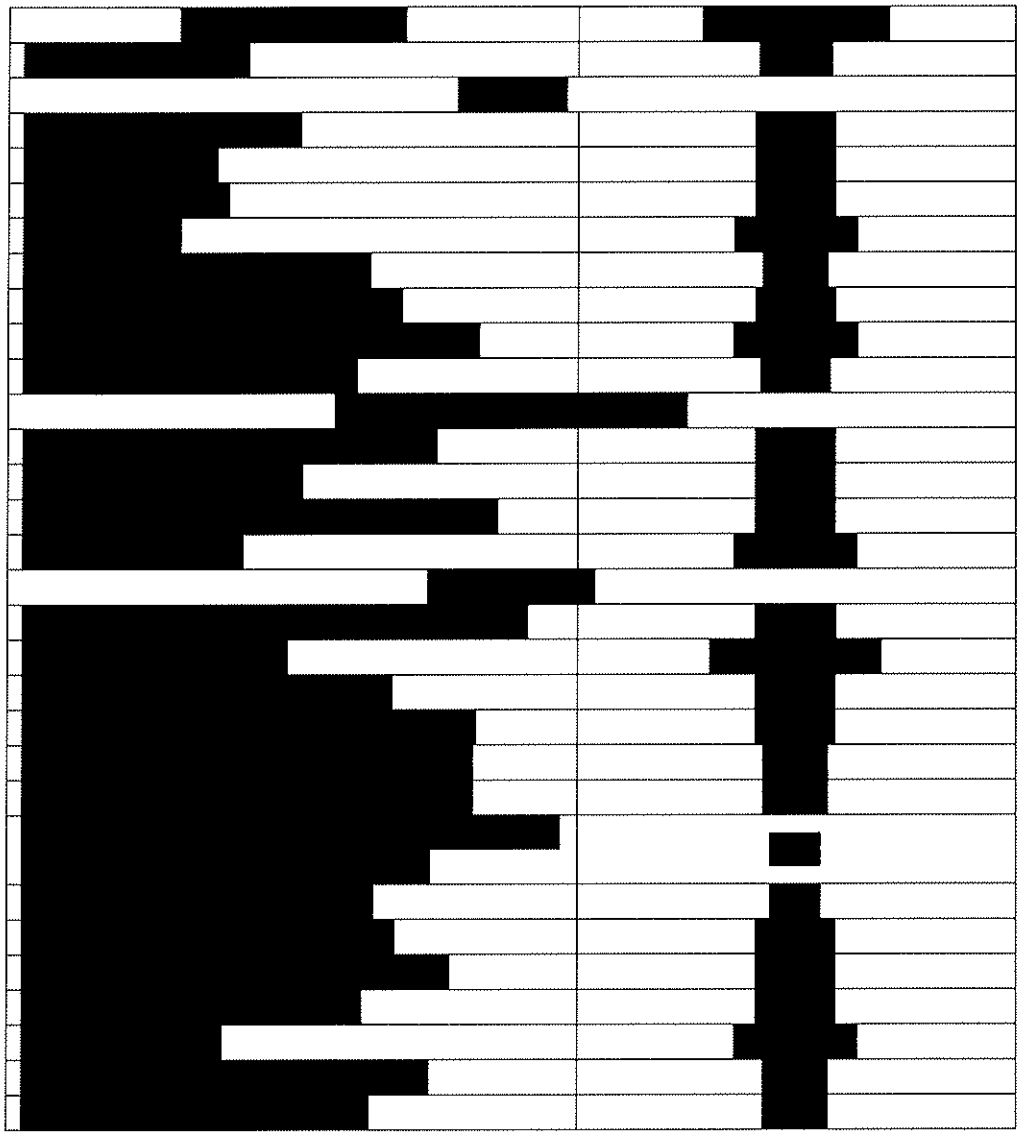

[redacted]

Table 5.1(h)

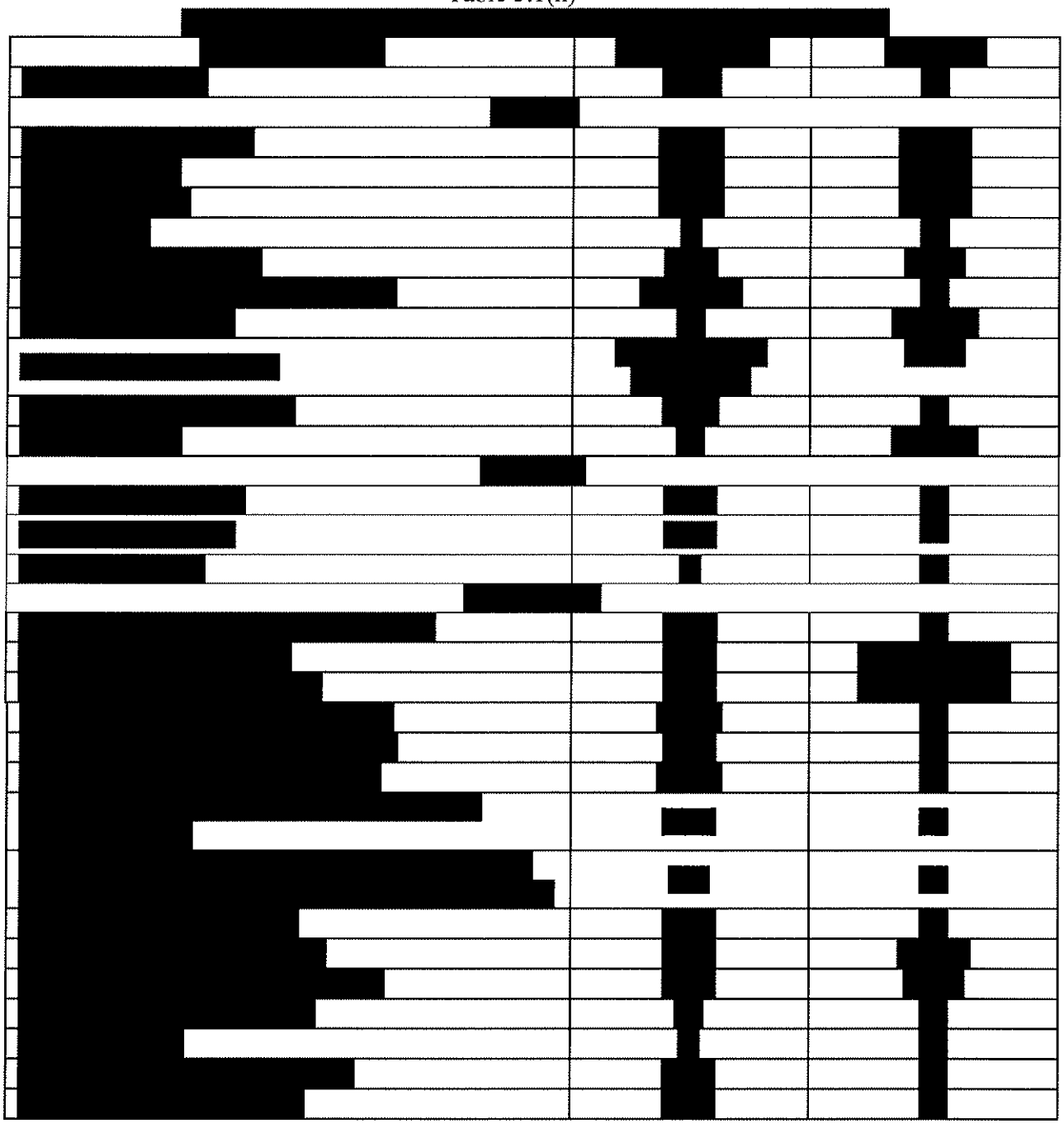

Table 5.2(a)
Reactor Core and Spent Fuel Pool Parameters

Description (Unit)	Value
Reactor	
Licensed thermal power (MW_{th})	[redacted]
Power density (W/gU)	[redacted]
Maximum fuel pin temperature (K)	[redacted]
Moderator temperature range (°F)	[redacted]
Moderator saturation temperature (°F)	[redacted]
Design basis core average void fraction (%)	[redacted]
Maximum bundle core exit void fraction (%)	[redacted]
Spent fuel pool	
Maximum temperature (°F)	[redacted]

Table 5.2(b)
Reactor Control Blade Data

Description (Unit)	Nominal Value
GE standard initial equipment	
[redacted]	

Table 5.2(c)
Reactor Core Parameters used for CASMO-4 Screening and Design Basis Calculations

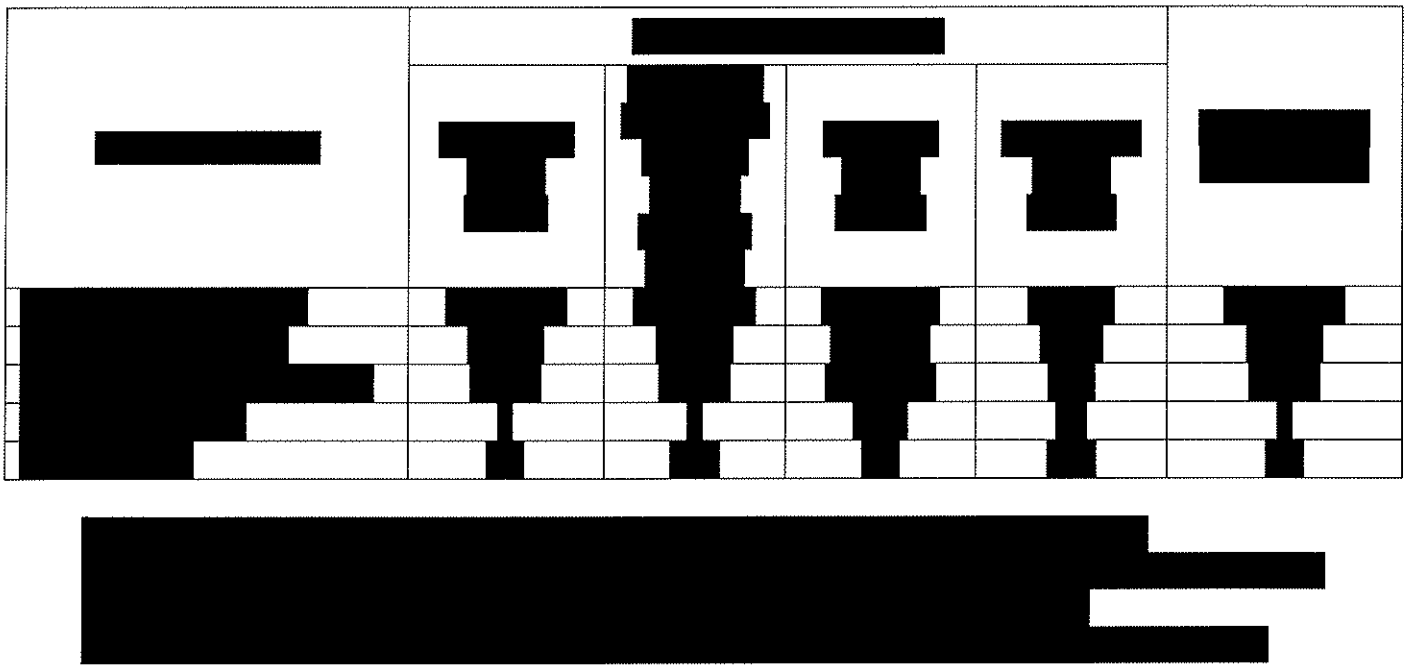

Table 5.3
SFP Storage Rack Parameters and Dimensions

†These are assumed values.
††This is the design value. The value used in the interface model (see Section 2.3.12) is [redacted] inches.
††† This representation of the fuel prep machine (FPM) is a simplification. There are two physically separate FMPs in the SFP each with a capacity of one assembly.

Table 5.4(a)
Non-Fuel Material Compositions

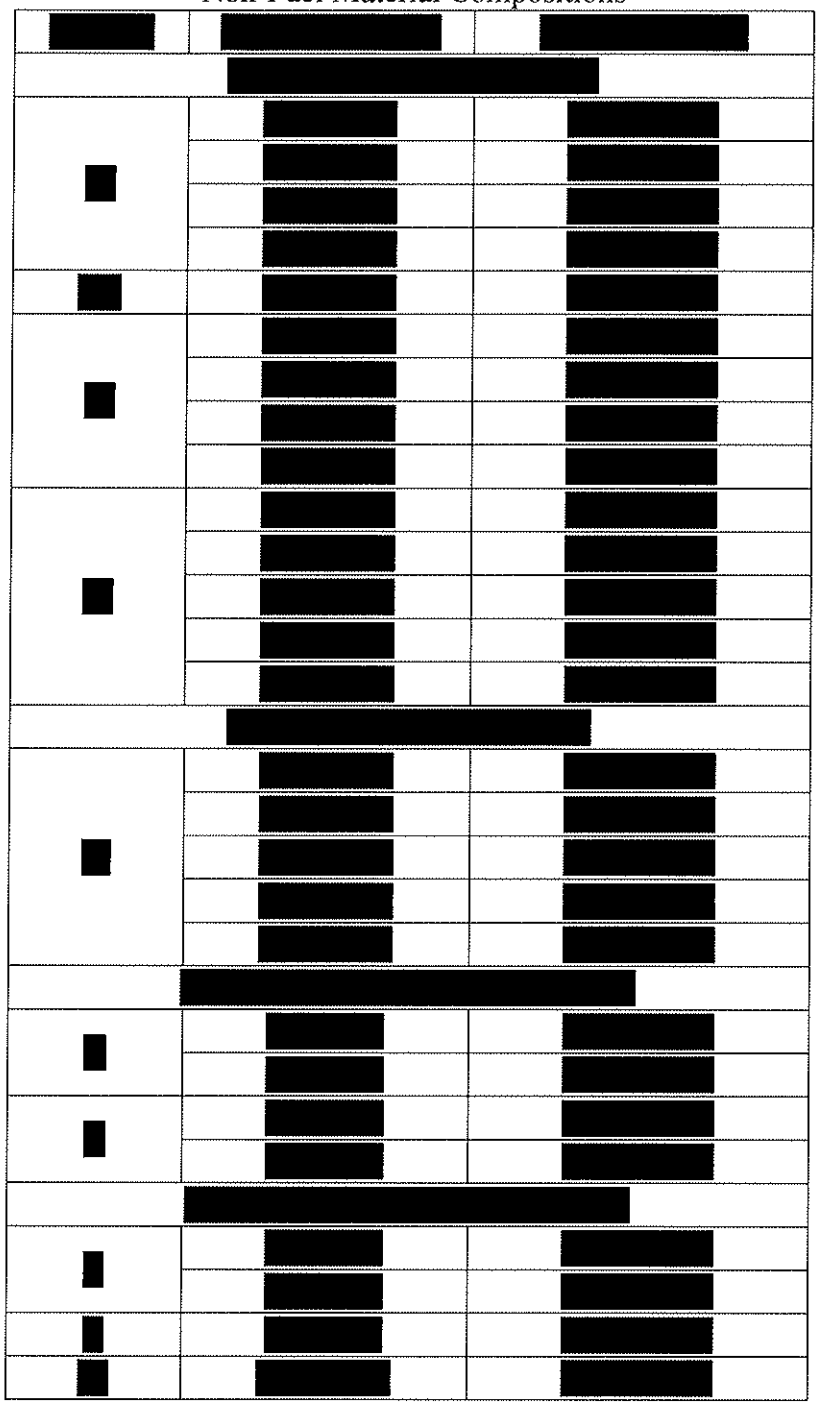

† The material composition was expanded to represent the full list of natural isotopes for each chemical element.

Table 5.4(b)
Summary of the Fuel and Fission Product Isotopes Used in Calculations

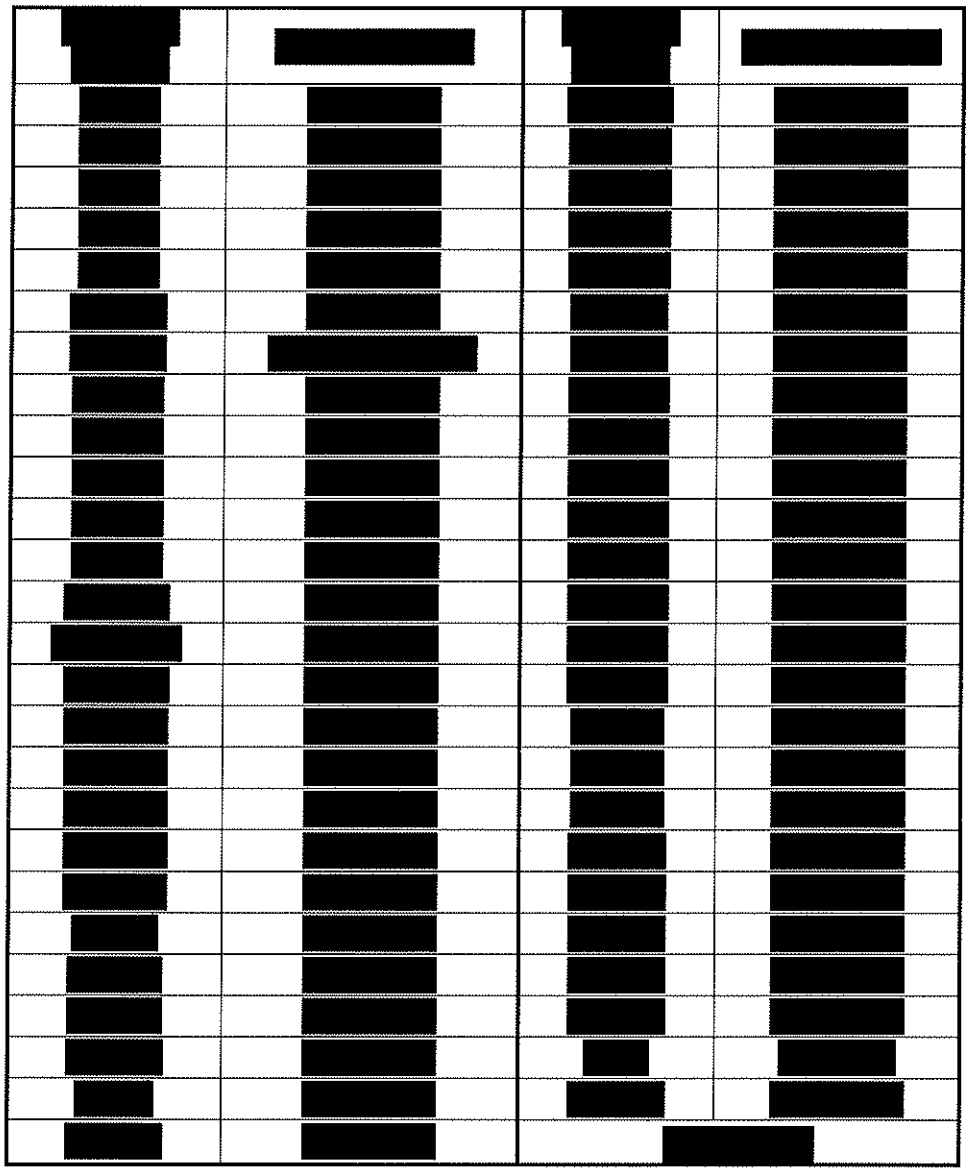

Table 7.1
Maximum k_{eff} Calculation for Normal Conditions in SFP Racks

Parameter	Value
Uncertainties[†]	
Fuel tolerance uncertainty, from Table C.5	[redacted]
Rack tolerance uncertainty, from Table C.6	[redacted]
Fuel eccentricity and de-channeling bias uncertainty, from Table C.2	[redacted]
Fuel orientation bias uncertainty, from Table C.3	[redacted]
Fuel channel bow bias uncertainty, from Table C.9	[redacted]
Fuel rod bow bias uncertainty, from Table C.9	[redacted]
Depletion uncertainty, from Table C.7	[redacted]
[redacted]	[redacted]
MCNP5-1.51 code bias uncertainty (95%/95%), from Table 2.1(b)	[redacted]
MCNP5-1.51 calculations statistics (95%/95%, 2σ), from Table C.1	[redacted]
Interface bias uncertainty, from Table C.10	[redacted]
Statistical combination of uncertainties	[redacted]
Biases	
Fuel eccentricity and de-channeling bias, from Table C.2	[redacted]
Fuel orientation bias, from Table C.3	[redacted]
Fuel channel bow bias, from Table C.9	[redacted]
Fuel rod bow bias, from Table C.9	[redacted]
MCNP5-1.51 code bias, from Table 2.1(b)	[redacted]
Interface bias, from Table C.10	[redacted]
Determination of k_{eff}	
Calculated MCNP5-1.51 k_{calc}, from Table C.1	[redacted]
Maximum k_{eff}	[redacted]
Regulatory Limit	[redacted]
Margin to Limit	[redacted]

[†] The provided value is the 95%/95% delta k_{calc} uncertainty.

Note 1: The negative biases were conservatively truncated.

Table 7.2

Maximum k_{eff} Calculation for Abnormal and Accident Conditions in SFP Racks

Parameter	Value
Uncertainties[†]	
Fuel tolerance uncertainty, from Table C.5	[redacted]
Rack tolerance uncertainty, from Table C.6	[redacted]
Fuel eccentricity and de-channeling bias uncertainty, from Table C.2	[redacted]
Fuel orientation bias uncertainty, from Table C.3	[redacted]
Fuel channel bow bias uncertainty, from Table C.9	[redacted]
Fuel rod bow bias uncertainty, from Table C.9	[redacted]
Depletion uncertainty, from Table C.7	[redacted]
[redacted]	[redacted]
MCNP5-1.51 code bias uncertainty (95%/95%), from Table 2.1(b)	[redacted]
MCNP5-1.51 calculations statistics (95%/95%, 2σ), from Table C.11	[redacted]
Interface bias uncertainty, from Table C.10	[redacted]
Statistical combination of uncertainties	[redacted]
Biases	
Fuel eccentricity and de-channeling bias, from Table C.2	[redacted]
Fuel orientation bias, from Table C.3	[redacted]
Fuel channel bow bias, from Table C.9	[redacted]
Fuel rod bow bias, from Table C.9	[redacted]
MCNP5-1.51 code bias, from Table 2.1(b)	[redacted]
Interface bias, from Table C.10	[redacted]
Determination of k_{eff}	
Calculated MCNP5-1.51 k_{calc}, from Table C.11	[redacted]
Maximum k_{eff}	[redacted]
Regulatory Limit	[redacted]
Margin to Limit	[redacted]

[†] The provided value is the 95%/95% delta k_{calc} uncertainty.

Note 1: The negative biases were conservatively truncated.

Figure 2.1
A representation of the Design Basis CASMO-4 Model with the Design Basis Lattice.

The figure is proprietary

Figure 2.2
A 2-D Representation of the MCNP5-1.51 Design Basis Model with the Design Basis Lattice, Case 2.3.1.4.1

The figure is proprietary

Figure 2.3
A 2-D Representation of the 2x2 Channeled Fuel Eccentric Positioning MCNP5-1.51 Model, Case 2.3.5.2

The figure is proprietary

Figure 2.4
A 2-D Representation of the 2x2 Channeled Fuel Eccentric Positioning MCNP5-1.51 Model, Case 2.3.5.3

The figure is proprietary

Figure 2.5
A 2-D Representation of the 8x8 Channeled Fuel Eccentric Positioning MCNP5-1.51 Model, Case 2.3.5.5.

The figure is proprietary

Figure 2.6
A 2-D Representation of the 8x8 Channeled Fuel Eccentric Positioning MCNP5-1.51 Model, Case 2.3.5.6.

The figure is proprietary

Figure 2.7
A 2-D Representation of the 2x2 De-channeled Fuel Eccentric Positioning MCNP5-1.51 Model, Case 2.3.5.8.

The figure is proprietary

Figure 2.8
A 2-D Representation of the 2x2 De-channeled Fuel Eccentric Positioning MCNP5-1.51 Model, Case 2.3.5.9.

The figure is proprietary

Figure 2.9
A 2-D Representation of the 8x8 De-channeled Fuel Eccentric Positioning MCNP5-1.51 Model, Case 2.3.5.11

The figure is proprietary

Figure 2.10
A 2-D Representation of the 8x8 De-channeled Fuel Eccentric Positioning MCNP5-1.51 Model, Case 2.3.5.12

The figure is proprietary

Figure 2.11
A 2-D Representation of the 4x4 Fuel Orientation MCNP5-1.51 Model, Case 2.3.6.2

The figure is proprietary

Figure 2.12
A 2-D Representation of the 4x4 Fuel Orientation MCNP5-1.51 Model, Case 2.3.6.3

The figure is proprietary

Figure 2.13
A 2-D Representation of the 4x4 Fuel Orientation MCNP5-1.51 Model, Case 2.3.6.4

The figure is proprietary

Figure 2.14
A 2-D Representation of the 4x4 Fuel Orientation MCNP5-1.51 Model, Case 2.3.6.5

The figure is proprietary

Figure 2.15
A Partial 2-D Representation of the MCNP5-1.51 Interface Model, Case 2.3.12.1

The figure is proprietary

Figure 2.16
A partial 2-D Representation of the 16x16 Vertical Fuel Drop Accident MCNP5-1.51 Model, Case 2.3.15.3.1

The figure is proprietary

Figure 2.17

A partial 2-D Representation of the 8x8 Missing BORAL Panel Accident MCNP5-1.51 Model, Case 2.3.15.4.1

The figure is proprietary

Figure 2.18
A partial 2-D Representation of the 80x80 Mislocated in a Corner of Two Racks Accident
MCNP5-1.51 Model, Case 2.3.15.6.2.1

The figure is proprietary

Figure 2.19
A partial 2-D Representation of the 80x80 Mislocated in a Corner of Three Racks Accident
MCNP5-1.51 Model, Case 2.3.15.6.3.1

The figure is proprietary

Figure 2.20
A partial 2D representation of the SFP Platform Mislocated Fuel Assembly Accident MCNP5-1.51 Model, Position 1 (Case 2.3.15.6.4.1)

The figure is proprietary

Figure 2.21
A partial 2D representation of the SFP Platform Mislocated Fuel Assembly Accident MCNP5-1.51 Model, Position 5 (Case 2.3.15.6.4.9)

The figure is proprietary

Figure 2.22
A partial 2D representation of the SFP Platform Mislocated Fuel Assembly Accident MCNP5-1.51 Model, Position 6 (Case 2.3.15.6.4.11)

The figure is proprietary

Figure 2.23
A partial 2D representation of the SFP Platform Mislocated Fuel Assembly Accident MCNP5-1.51 Model, Position 7 (Case 2.3.15.6.4.13)

The figure is proprietary

Figure 5.1
Layout of the SFP

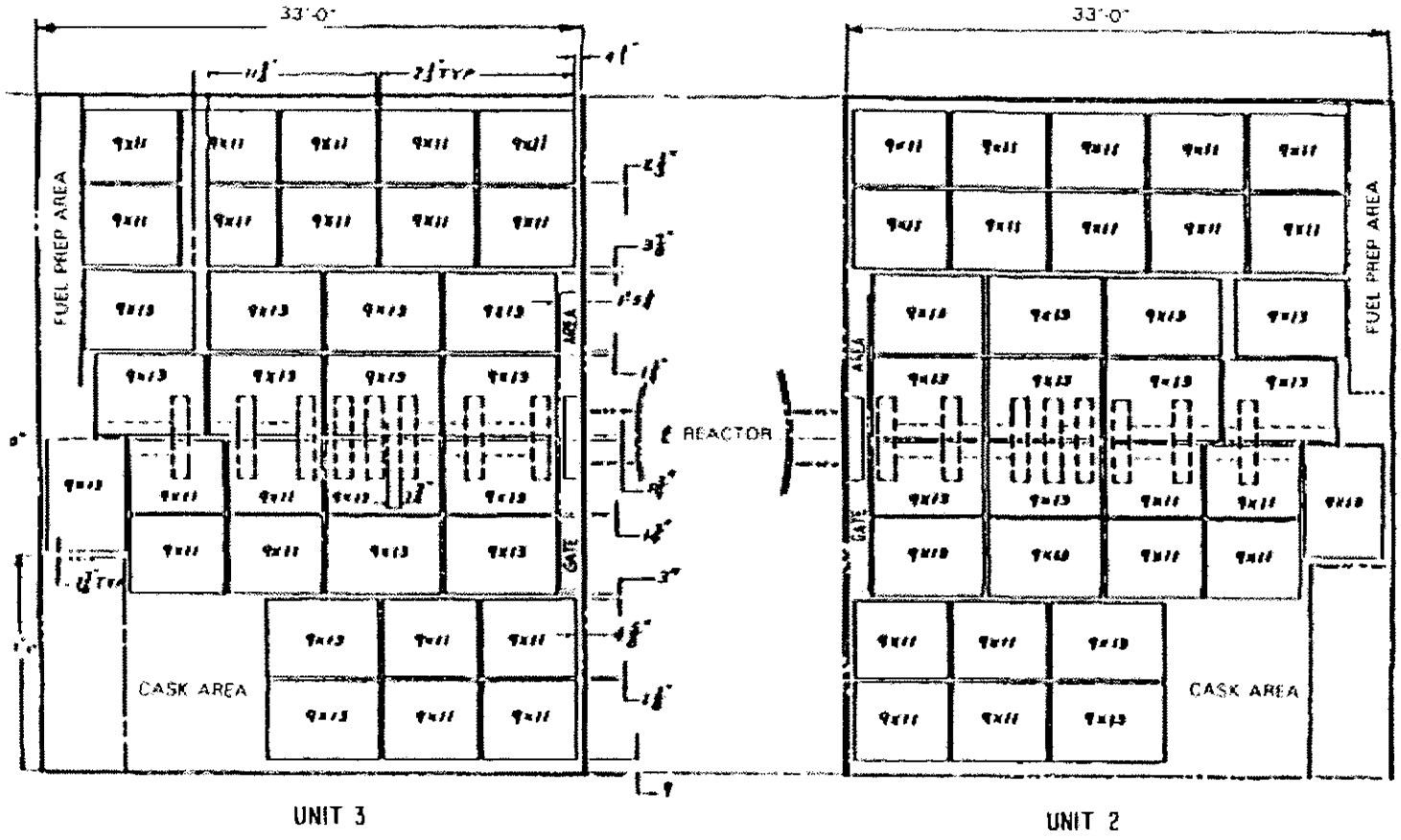

Figure 7.1

The figure is proprietary

Figure 7.2

The figure is proprietary

Figure 7.3

The figure is proprietary

Appendix A

The appendix is proprietary.

Appendix B

The appendix is proprietary.

Appendix C

The appendix is proprietary.

ATTACHMENT 7

Holtec International Report No. HI-2104790, Revision 1,
"Nuclear Group Computer Code Benchmark Calculations"
(Non-Proprietary Version)

HOLTEC
INTERNATIONAL

Holtec Center, One Holtec Drive, Marlton, NJ 08053
Telephone (856) 797- 0900
Fax (856) 797 - 0909

Nuclear Group Computer Code Benchmark Calculations

FOR

GENERIC: NON-PROPRIETARY VERSION

Holtec Report No: HI-2104790

Holtec Project No: GENERIC

Sponsoring Holtec Division: HTS

Report Class : SAFETY RELATED

Summary of Revisions

Revision 0

Original Issue

Revision 1

Additional criticality experiments were added to Appendix B. The index numbers of criticality experiments in Appendix C were updated to be consistent with a new revision of Appendix B. The benchmark of MCNP5-1.51 with ENDF/B-VII was added in Appendix D.

Table of Contents

1.0 Introduction

This report documents the criticality experiment benchmark validation calculations for the following computer codes and libraries combinations and establishes the criticality code bias and bias uncertainty for these codes:

MCNP5-1.51 with ENDF/B-V (Appendix C)
MCNP5-1.51 with ENDF/B-VII (Appendix D)

For that purpose, results from the codes are compared to the critical experiments referred to as the Haut Taux de Combustion (HTC) experiments and to the selected critical, presented in Appendix B, with geometric and material characteristics similar to that of spent fuel storage and transport casks. The simulated fuel rods used in these experiments contained uranium or mixture of uranium and plutonium oxides. In the HTC experiments the plutonium-to-uranium ratio and the isotopic compositions of both the uranium and plutonium were designed to be similar to what would be found in a typical pressurized-water reactor (PWR) fuel assembly that initially had an enrichment of 4.5 wt % ^{235}U and was burned to 37,500 MWd/MTU.

The purpose of the calculation is to determine the code bias and bias uncertainty consistent with standards such as ANSI/ANS-8.1 [1] and ANSI/ANS-8.17 [2]. Criticality safety standards ANSI/ANS-8.1 and ANSI/ANS-8.17 apply to criticality methods validation and to criticality evaluations, respectively. ANSI/ANS-8.1 requires that a validation be performed on the method used to calculate criticality safety margins and that the validation must be documented in a written report describing the method, computer program and cross section libraries used, the experimental data, the areas of applicability and the bias and margins of safety. ANSI/ANS-8.17 prescribes the criteria to establish sub-criticality safety margins.

2.0 Methodology

Validation of the computer code and continuous energy data library to perform criticality safety calculation has been performed following reference [5] methodology. The validation allows the understanding of the accuracy of the calculational methodology to predict subcriticality. Validation includes identification of the difference between calculated and experimental neutron effective multiplication factor (k_{eff}), called the bias. A set of appropriate critical experiments are selected so bias trends can be drawn through statistical analyses. The range of the benchmark parameters used to validate the calculational methodology primarily defines the area of applicability (AOA), which establishes the limits of the systems that can be analyzed using the validated criticality safety methodology.

Determination of Bias and Bias Uncertainty

Following reference [5] guide, the statistical analysis to determine the mean multiplication factor ($\overline{k_{eff}}$) and the bias uncertainty (S_p) approach involves determining the weighted mean that incorporates the uncertainty from both, measurements and calculation method as follows:

$$\sigma_i = \sqrt{\sigma_{calc-i}^2 + \sigma_{exp}^2} \quad (2\text{-}1)$$

where σ_i is the uncertainty for the ith k_{eff}, σ_{exp} is the measurement uncertainty and $\sigma_{calc\text{-}i}$ is the calculation uncertainty. Then, the weighted mean multiplication factor $\overline{k_{eff}}$ and the bias uncertainty (S_p) are given by:

$$\overline{k_{eff}} = \frac{\sum \frac{1}{\sigma_i^2}(k_{eff-i})}{\sum \frac{1}{\sigma_i^2}} \quad (2\text{-}2)$$

$$S_p = \sqrt{s^2 + \bar{\sigma}^2} \quad (2\text{-}3)$$

where s^2 is the variance about the mean and $\bar{\sigma}^2$ is the average total uncertainty, given by:

$$s^2 = \frac{\left(\frac{1}{n-1}\right)\sum \frac{1}{\sigma_i^2}\left(k_{eff-i} - \overline{k_{eff}}\right)^2}{\frac{1}{n}\sum \frac{1}{\sigma_i^2}} \quad (2\text{-}4)$$

$$\bar{\sigma}^2 = \frac{n}{\sum \frac{1}{\sigma_i^2}} \quad (2\text{-}5)$$

where n is the number of critical experiments used in the validation and $k_{eff\text{-}i}$ is the ith value of the multiplication factor.

Bias is determined by the relation:

$$Bias = \overline{k_{eff}} - 1 \quad \text{if } \overline{k_{eff}} \text{ is less than 1, otherwise } Bias = 0 \quad (2\text{-}6)$$

Because a positive bias may be nonconservative, a bias is set to zero if the calculated average k_{eff} is greater than one.

Statistical Methods

Single Sided Tolerance Limit Method

If the benchmark calculated neutron multiplication factor does not exhibit trends with the parameters, the lower tolerance limit or single sided tolerance limit method can be used. A weighted lower limit tolerance (K_L) is a single lower limit above which a defined fraction of the population of k_{eff} is expected to lie, with a prescribed confidence and within the area of the applicability. The term "weighted" refers to a specific statistical technique where the

uncertainties in the data are used to weight the data point. Data with high uncertainties will have less "weight" than data with small uncertainties.

A lower tolerance limit can be used when there are no trends apparent in the critical experiment results and the critical experiment results have a normal distribution. The method is applicable only within the limits of the validation data without extrapolating the AOA. The single sided lower tolerance limit is defined by the equation:

$$K_L = \overline{k_{eff}} - U \times S_p \tag{2-7}$$

$$If\ \overline{k_{eff}} \geq 1,\ then\ K_L = 1 - U \times S_p \tag{2-8}$$

where S_p is the square root of the pooled variance used as the mean bias uncertainty when applying the single sided tolerance limit for a normally distributed data and U is the single sided lower tolerance factor, determined from the following equations [6]. Note that for groups with larger than 50 samples, the single sided lower tolerance factor for 50 samples was conservatively used.

$$\boldsymbol{U = \frac{z_{1-p} + \sqrt{z_{1-p}^2 - ab}}{a}} \tag{2-9}$$

$$\boldsymbol{a = 1 - \frac{z_{1-\gamma}^2}{2(N-1)}} \tag{2-10}$$

$$\boldsymbol{b = z_{1-p}^2 - \frac{z_{1-\gamma}^2}{N}} \tag{2-11}$$

where z_{1-p} is the critical value from the normal distribution that is exceeded with probability $1-p$ and $z_{1-\gamma}$ is the critical value from the normal distribution that is exceeded with probability $1-\gamma$.

Confidence Band with Administrative Margin Method

If the benchmarks calculated neutron multiplication factor exhibit a trend with a given parameter, the method based on a confidence band with administrative margin can be used. This method applies a statistical calculation of the bias and its uncertainty plus an administrative margin to a linear fit of the critical experiment benchmark data.

The confidence band W is defined for a confidence level of $(1-\gamma)$ using the relationship:

$$W = \max\{w(x_{min}), w(x_{max})\} \tag{2-12}$$

where

$$w(x) = t_{1-\gamma} \times S_p \sqrt{1 + \frac{1}{n} + \frac{(x - \bar{x})^2}{\sum_{i=1,n}(x - \bar{x})^2}} \qquad (2\text{-}13)$$

and

n is the number of critical experiments used in establishing $k_{cal(x)}$,

$t_{1-\gamma}$ is the Student-t distribution statistic for $1-\gamma$ and $n-2$ degrees of freedom,

$\bar{x}$ is the mean value of the parameter x in the set of calculations,

x_{min}, x_{max} are the minimum and maximum values of the independent parameter x,

S_p is the pooled standard deviation for the set of criticality calculations given by:

$$S_p = \sqrt{s^2_{k(x)} + s^2_w} \qquad (2\text{-}14)$$

where $S^2_{k(x)}$ is the variance of the regression fit and is given by:

$$s^2_{k(x)} = \frac{1}{(n-2)}\left[\sum_{i=1,n}(k_{eff-i} - \bar{k})^2 - \frac{\{\sum_{i=1,n}(x_i - \bar{x})(k_{eff-i} - \bar{k})\}^2}{\sum_{i=1,n}(x_i - \bar{x})^2}\right] \qquad (2\text{-}15)$$

$\bar{k}$ is the mean value of the calculated k_{eff} and s_w^2 is the within-variance of the data:

$$S^2_w = \frac{1}{n}\sum_{i=1,n}\sigma_i^2 \qquad (2\text{-}16)$$

where $\sigma_i = \sqrt{\sigma^2_{calc-i} + \sigma^2_{exp}}$ is the uncertainty for the ith k_{eff}, σ_{exp} is the measurement uncertainty and $\sigma_{calc\text{-}i}$ is the calculated uncertainty.

Non-parametric Statistical Treatment Method

Data that do not follow a normal distribution can be analyzed by non-parametric techniques. The analysis results in a determination of the degree of confidence that a fraction of the true population of data lies above the smallest observed value. The more data is available in the sample, the higher the degree of confidence.

The following equation determines the percent confidence that a fraction of the population is above the lowest observed value:

$$\beta = 1 - \sum_{j=0}^{m-1} \frac{n!}{j!\,(n-j)!}(1-q)^j q^{n-j}$$

(2-17)

where

q is the desired population fraction (normally 0.95),

n is the number of data in one data sample,

m is the rank order indexing from the smallest sample to the largest (m=1 for the smallest sample; m=2 for the second smallest sample, etc.). Non-parametric techniques do not require reliance upon distributions, but are rather an analysis of ranks. Therefore, the samples are ranked from the smallest to the largest.

For a desired population fraction of 95% and a rank of order of 1 (the smallest data sample), the equation reduces to:

$$\beta = 1 - q^n = 1 - 0.95^n \qquad (2\text{-}18)$$

This information is then used to determine the Non-parametric Margin from Table 2.2 in Reference [5].

For non-parametric data analysis, K_L is determined by:

K_L = Smallest k_{eff} value – Uncertainty for Smallest k_{eff} – Non-parametric Margin (NPM) *(2-19)*

Single-Sided Tolerance Band Method

When a relationship between a calculated k_{eff} and an independent variable can be determined, a single-sided lower tolerance band may be used. This is a conservative method that provides a fitted curve above which the true population of k_{eff} is expected to lie. The tolerance band equation is actually a calibration curve relation.

The equation for the single-sided lower tolerance band is

$$K_L = K_{fit}(x) - S_{P_{fit}} \left\{ \sqrt{2F_a^{(2,n-2)} \left[\frac{1}{n} + \frac{(x-\bar{x})^2}{\sum (x_i - \bar{x})^2} \right]} + z_{2P-1} \sqrt{\frac{(n-2)}{\chi^2_{1-\gamma,n-2}}} \right\}$$

(2-20)

where:

$K_{fit}(x)$ is the function derived from the trend analysis,

p is the desired confidence (0.95),

$F_a^{(fit,n-2)}$ is the F distribution percentile with degree of fit, *n-2* degrees of freedom. The degree of fit is 2 for a linear fit,

n is the number of critical experiment k_{eff} values,

x is the independent fit variable,

x_i is the independent parameter in the data set corresponding to the "ith" k_{eff} value,

$\bar{x}$ is the weighted mean of the independent variables,

z_{2P-1} is the symmetric percentile of the Gaussian or normal distribution that contains the P fraction,

$$\gamma = (1 - p) / 2, \qquad (2\text{-}21)$$

$\chi^2_{1-\gamma,n-2}$ is the upper Chi-square percentile,

$$S_{P_{fit}} = \sqrt{s_{fit}^2 + \bar{\sigma}^2} \qquad (2\text{-}22)$$

$$s_{fit}^2 = \frac{\frac{1}{n-2}\sum\left\{\frac{1}{\sigma_i^2}\left[k_{eff_i} - K_{fit}(x_i)\right]^2\right\}}{\frac{1}{n}\sum\frac{1}{\sigma_i^2}} \qquad (2\text{-}23)$$

Area of Applicability

The area(s) of applicability refers to the key physical parameter(s) that define a particular fissile configuration. This configuration can either be an actual system or a process. The determination of the AOA of the validation is determined following NUREG/CR-6698 steps [5]. The approach used in developing the AOA consists of the following steps:

i. Identification of the key parameters associated with the system to be evaluated.
ii. Establishment a "screening" AOA for critical experiments.
iii. Identification of criticality experiments that are within the "screening" AOA.
iv. Determination of the detailed AOA based on the selected criticality benchmark experiments.
v. Demonstration that the system to be evaluated in within the AOA provided by the critical experiments.

Steps i. and ii. are presented in subsections 2.3.1 and 2.3.2, respectively. Step iii. is presented in Appendix B. Steps iv. and v. are presented in Appendix C and D.

Key Parameters Identification

This validation will cover a number of designs but all the designs will consider the same key parameters in defining the applicability area. These parameters fall into three categories: materials, geometry and neutron energy spectra.

Regarding material, the fuel is a uranium or mixture of uranium and plutonium oxides pellets clad in a zirconium alloy. The moderator and reflector is water which in some cases has dissolved boron or gadolinium solutions. Absorber plates made of borated steel, Boral®, Zircaloy Boroflex or cadmium and absorber rods made of steel, aluminum, Gd_2O_3, Pyrex®, Vicor® or borated aluminum will be included in this validation. Some experiments were performed with steel or lead reflector screens.

Regarding geometry, the fuel in the HTC experiments is in square lattices with pin diameter – 9.5 mm and pitch in the range found on Table B-1 through Table B-6. The geometry parameters of other selected critical experiments are varied in a wide range and they can be found in references [B.6] through [B.12]. The fuel assemblies may be separated by water, water and an absorber plate or water and absorber rods. The system may be water reflected or steel/lead reflected.

Regarding the neutron energy spectra, they are thermal with EALF values in the range of 0.07 and 1.55 eV.

Table 2-1 presents the key physical parameters for AOA selected.

Screening Area of Applicability

For the key parameters selected in section 2.3.1, Table 2-1 summarizes the range of parameters for which the validation applies. These data are the base for the selection of the critical experiments, which span the range of parameters.

3.0 Assumptions

No substantial simplifying assumptions were made in the modeling of the critical experiments used for benchmarking: all experiments were modeled as full three-dimensional geometries, fuel rod arrays were modeled as lattices, all fuel rod details were modeled, and the water between the rods was modeled as specified in the experiment description. However, structures further away from the experiment, such as building walls and foundations, were not included in the models.

4.0 Computer Files

All computer files to support this analysis are provided on the Holtec server in \Projects\0\Reports\HI-2104790 and its subdirectories.

5.0 Summary

The criticality experiment benchmark validation calculations for the computer codes and libraries shown in Section 1.0 were performed for the validation of the Holtec International

criticality safety methodology. The results of calculations and the criticality code bias and bias uncertainty for these codes are presented in appropriate appendices. The similarity between the chosen experiments and the actual systems has been based on a set of screening criteria as is stated in the NUREG/CR-6698 [5].

The summary of biases and bias uncertainties for the validated computer codes is shown in Table 5.1.

6.0 References

[1] ANSI/ANS 8.1-1983, American National Standard For Nuclear Criticality Safety In Operations With Fissionable Materials Outside Reactors, American Nuclear Society, La Grange Park, Illinois.

[2] ANSI/ANS-8.17, "American National Standard for Criticality Safety Criteria for the Handling, Storage, and Transportation of LWR Fuel Outside Reactors," American Nuclear Society, La Grange Park, Illinois.

[3] Criticality Benchmark Guide for Light Water Reactor Fuel in Transportation and Storage Packages, NUREG/CR-6361 (ORNL/TM-13211), U.S. Nuclear Regulatory Commission, March 1997.

[4] J.R. Taylor, An Introduction to Error Analysis (University Science Books, Mill Valley, California, 1982).

[5] Guide for Validation of Nuclear Criticality Safety Calculational Methodology, NUREG/CR-6698, U.S. Nuclear Regulatory Commission, January 2001.

[6] M.G. Natrella, Experimental Statistics, National Bureau of Standards, Handbook 91, August 1963.

Table 2-1 Key Criticality System Parameters and Range of those Parameters in Expected Designs

Parameter	Critical Experiment Requirement	Range of Key Parameters
Fissionable Material	^{235}U, ^{239}Pu, ^{241}Pu	^{235}U, ^{239}Pu, ^{241}Pu
Isotopic Composition		
$^{235}U/U_t$	< 5.0wt%	0.16wt% to 5.74wt%
Pu/(U+Pu)	< 20wt%	1.104wt% to 20wt%
Physical Form	UO_2, MOX	UO_2, MOX
Moderator Material (coolant)	H	H
Physical Form	H_20	H_20
Density	Normal pressure & temperature condition	around 1.0 g/cm^3
Reflector Material	H	H
Physical Form	H_20	H_20
Density	Normal pressure & temperature condition	around 1.0 g/cm^3
Interstitial Reflector Material		
Plate	Steel or Lead	Steel or Lead
Absorber Material		
Soluble	None, Boron or Gadolinium	None, Boron (0 to 2550 ppm) or Gadolinium (0 to 197 ppm)
Rods	Boron	Pyrex®, Vicor®, Steel or B-Al
Separating Material		
Plate	Water, B-SS, Boral or Cadmium	Water, B-SS, Boral, Boroflex, Zircaloy or Cadmium
Geometry		
Fuel	Square/Triangle lattice of fuel pins	Square/Triangle lattice of fuel pins
Neutron Energy	Thermal spectrum	Thermal spectrum

Table 5-1 Summary of Biases and Bias Uncertainties for the Validated Computer Codes

Computer Code	Total Bias	Bias Uncertainty
MCNP5-1.51 with ENDF/B-V (Appendix C)	[redacted]	[redacted]
MCNP5-1.51 with ENDF/B-VII (Appendix D)	[redacted]	[redacted]

Appendix A

Holtec Approved Computer Program List

(total number of pages: 5 including this page)

Appendix Proprietary

Appendix B

Description of the Critical Experiments

(total number of pages: 16 including this page)

B.1. Introduction and Purpose

The purpose of this Appendix is to document the description of the full set of critical experiments selected for the benchmark validation of computer codes.

B.2. Physical Description of HTC Critical Experiments

In the 1980s, a series of critical experiments referred to as the Haut Taux de Combustion (HTC) experiments was conducted by the Institut de Radioprotection et de Sûreté Nucléaire (IRSN) at the experimental criticality facility in Valduc, France, between 1988 and 1990. The fuel rods were fabricated specifically for this set of experiments. The fuel consisted of 1-cm-long pellets contained within Zircaloy-4 cladding. The plutonium-to-uranium ratio and the isotopic compositions of both the uranium and plutonium used in the simulated fuel rods were designed to be similar to what would be found in a typical pressurized-water reactor fuel assembly that initially had an enrichment of 4.5 wt % ^{235}U and was burned to 37,500 MWd/MTU. The fuel material also includes ^{241}Am, which is present due to the decay of ^{241}Pu. The fuel rods were held in place by an upper and a lower grid and were contained in one or four assemblies placed into a rectangular tank. The critical approach was accomplished by varying the water or solution level in the tank containing the fuel pin arrays. The critical condition was extrapolated from a subcritical configuration with a multiplication factor within 0.1% of 1.000.

This section provides a summary description of the materials and physical layouts of the 156 critical configurations. Detailed descriptions of the critical experiments are presented in references [B.1] through [B.4]. The HTC experiments include configurations designed to simulate fuel handling activities, pool storage, and transport in casks constructed of thick lead or steel and were categorized into four phases.

B.2.1. Phase 1: Water-Moderated and Reflected Arrays

The first phase included 18 configurations, each involving a single square-pitched array of rods with rod pitch varying from 1.3 to 2.3 cm.

The tank was incrementally filled with water at room temperature, water being injected at the bottom of the tank. A measurement needle provided water height. Therefore, the water was used as core moderator and as reflector beneath the fuel and around the array on four sides. The critical approach parameter was the water level.

Eighteen experiments have been performed with various arrays and all are considered acceptable for use as benchmark experiments:

- 5 square or almost square array - square pitch 1.3, 1.5, 1.7, 1.9, 2.3 cm – 15 experiments,
- 1 rectangular centered array – square pitch 1.7 cm – 2 experiments,
- 1 rectangular no-centered array – square pitch 1.7 cm – 1 experiment.

The experiments key physical parameters are summarized in Table B-1.

B.2.2. Phase 2: Reflected Simple Arrays Moderated by Poisoned Water with Gadolinium or Boron

The second phase included 41 configurations that were similar to the first phase except that the water used as moderator and reflector included either boron or gadolinium in solution at various concentrations.

The tank was incrementally filled with poisoned solution at room temperature, this solution being pumped in the bottom of the tank. A measurement needle provided solution height. The critical approach parameter was the water level.

Forty one experiments are evaluated and all are considered acceptable for use as benchmark experiments. Twenty of them are performed with gadolinium solutions, and the others with boron solutions.

The experiments key physical parameters are summarized in Table B-2 through Table B-3.

B.2.3. Phase 3: Pool Storage

The third phase simulated fuel assembly storage rack conditions and included 26 configurations with 1.6 cm square rods pitch arranged into four assemblies in a 2 × 2 array. These assemblies with, in some cases, canisters, were placed on a pedestal centered inside a parallelepiped tank which was itself located on the floor in the middle (approximately) of a large room. The spacing between assemblies was varied, and some of the assemblies had B-SS, Boral®, or cadmium plates attached to the sides of the four assemblies.

The tank was incrementally filled with water at room temperature, water being pumped in at the bottom of the tank. A measurement needle provided water height. Therefore, the water was used as core moderator and as reflector beneath the fuel and around the array on four sides. The critical approach parameter was the water level.

Twenty six experiments are evaluated and all are considered acceptable for use as benchmark experiments. Eleven of them were performed with neutron absorbing canisters around the four arrays, and the others without any.

The experiments key physical parameters are summarized in Table B-4.

B.2.4. Phase 4: Shipping Cask

The fourth phase simulated cask conditions and included 71 configurations similar to the Phase 3 configurations except thick steel or lead shields were placed around the outside of the 2 × 2 array of fuel assemblies. These assemblies with, in some cases, canisters, were placed on a pedestal centered inside a parallelepiped tank which was itself located on the floor in the middle (approximately) of a large room. Space between assemblies and between assemblies and screen varied from one case to another.

The tank was incrementally filled with water at room temperature, water being pumped in at the bottom of the tank. A measurement needle provided water height. Therefore, the water was used as core moderator and as reflector beneath the fuel and around the array on four sides behind the reflector screens. The critical approach parameter was the water level.

Seventy one experiments are evaluated and all are considered acceptable for use as benchmark experiments. Thirty eight experiments were performed with lead reflector screens and thirty three with steel reflector screens. Twenty six among the former and twenty one among the latter used absorbing canisters around the four arrays, and the others without any.

The experiments key physical parameters are summarized in Table B-5 through Table B-6.

B.3. Physical Description of the Selected Benchmark Critical Experiments

The benchmark experiments are selected to cover a wide range of code applications for fresh and spent fuel storage analysis. This section provides a summary description of the materials and physical layouts of the 135 critical configurations with fresh and selected actinides for spent fuel. For the fresh fuel assumption, the code is compared to the critical experiments of un-irradiated UO_2 systems with geometric and material characteristics similar to that of fuel storage systems. For the spent fuel assumption with burnup credit, additional comparisons are made to un-irradiated mixed-oxide (MOX) fuel of similar characteristics to spent fuel. The UO_2 experiments address ^{234}U, ^{235}U and ^{238}U. The MOX critical experiments address ^{238}Pu, ^{239}Pu, ^{240}Pu, ^{241}Pu, ^{242}Pu and ^{241}Am. Detailed descriptions of the critical experiments are presented in references [B.6] through [B.12].

Description of the selected critical experiments is summarized in Table B-7.

B.4. References

[B.1] F. Fernex, "Programme HTC – Phase 1 : Réseaux de crayons dans l'eau pure (Water-moderated and reflected simple arrays) Réévaluation des expériences," DSU/SEC/T/2005-33/D.R., Institut de Radioprotection et de Sûreté Nucléaire, 2008.

[B.2] F. Fernex, Programme HTC – Phase 2 : Réseaux simples en eau empoisonnée (bore et gadolinium) (Reflected simple arrays moderated by poisoned water with gadolinium or boron) Réévaluation des expériences," DSU/SEC/T/2005-38/D.R., Institut de Radioprotection et de Sûreté Nucléaire, 2008.

[B.3] F. Fernex, "Programme HTC – Phase 3 : Configurations "stockage en piscine" (Pool storage) Réévaluation des expériences," DSU/SEC/T/2005-37/D.R., Institut de Radioprotection et de Sûreté Nucléaire, 2008.

[B.4] F. Fernex, "Programme HTC – Phase 4 : Configurations "châteaux de transport" (Shipping cask) - Réévaluation des expériences," DSU/SEC/T/2005-36/D.R., Institut de Radioprotection et de Sûreté Nucléaire, 2008.

[B.5] C. Portella, C. Woillard “Programme “HTC” - Expériences de criticité avec des crayons combustibles HTC (type REP à haut taux de combustion) - Résultats de l’étude paramétrique avec de l’eau gadoliniée.” [Translation: ““Hbu” program – Criticity Experiments with Hbu fuel rods (LWR type at high burn up) – Results of parametric study with poisoned water with gadolinium.”] Note technique IPSN/SRSC n° 90.01.

[B.6] International Handbook of Evaluated Criticality Safety Benchmark Experiments, NEA/NSC/DOC(95)03, NEA Nuclear Science Committee, September 2008 Edition

[B.7] G.S. Hoovier et al., Critical Experiments Supporting Underwater Storage of Tightly Packed Configurations of Spent Fuel Pins, BAW-1645-4, Babcock & Wilcox Company, November 1991.

[B.8] L.W. Newman et al., Urania Gadolinia: Nuclear Model Development and Critical Experiment Benchmark, BAW-1810, Babcock and Wilcox Company, April 1984.

[B.9] J.C. Manaranche et al., "Dissolution and Storage Experimental Program with 4.75% Enriched Uranium-Oxide Rods," Trans. Am. Nucl. Soc. 33: 362-364 (1979).

[B.10] S.R. Bierman, Criticality Experiments with Neutron Flux Traps Containing Voids, PNL-7167, Battelle Pacific Northwest Laboratory, April 1990.

[B.11] S.R. Bierman, Criticality Experiments with Fast Test Reactor Fuel Pins in Organic Moderator, PNL-5803, Battelle Pacific Northwest Laboratory, December 1986.

[B.12] E.G. Taylor et al., Saxton Plutonium Program Critical Experiments for the Saxton Partial Plutonium core, WCAP-3385-54, Westinghouse Electric Corp., Atomic Power Division, December 1965.

[B.13] Evaluation of the French Haut Taux de Combustion (HTC) Critical Experiment Data, NUREG/CR-6979 (ORNL/TM-2007/083), U.S. Nuclear Regulatory Commission, September 2008.

Table B-1 Key Physical Parameters of the HTC Phase 1 Critical Experiments [B.1]

Case	Reference	Experiment number	Pitch (cm)	Number of Rods		Date of experiment	Temperature (°C)	Critical water height (cm) [(a)]
				Along edge	Total			
1	MIX-COMP-THERM-HTC-001	2327	2.3	50 × 50	2500	05/05/88	22.5	61.41 ± 0.06
2	MIX-COMP-THERM-HTC-002	2335		38 × 37	1406	06/06/88	21.1	87.68 ± 0.06
3	MIX-COMP-THERM-HTC-003	2336		37 × 37	1369	06/07/88	21.0	90.38 ± 0.06
4	MIX-COMP-THERM-HTC-004	2337	1.9	27 × 27	729	06/09/88	20.7	63.77 ± 0.06
5	MIX-COMP-THERM-HTC-005	2339		25 × 25	625	06/13/88	20.5	81.95 ± 0.08
6	MIX-COMP-THERM-HTC-006	2340		25 × 24	600	06/14/88	20.7	90.22 ± 0.06
7	MIX-COMP-THERM-HTC-007	2341	1.7	26 × 26	676	06/15/88	20.2	65.11 ± 0.07
8	MIX-COMP-THERM-HTC-008	2342		25 × 25	625	06/16/88	21.0	74.86 ± 0.06
9	MIX-COMP-THERM-HTC-009	2343		25 × 24	600	06/16/88	20.8	82.25 ± 0.06
10	MIX-COMP-THERM-HTC-010	2345	1.5	29 × 29	841	06/26/88	21.1	59.92 ± 0.06
11	MIX-COMP-THERM-HTC-011	2347		27 × 27	729	06/23/88	21.3	76.72 ± 0.06
12	MIX-COMP-THERM-HTC-012	2348		27 × 26	702	06/23/88	21.1	84.57 ± 0.06
13	MIX-COMP-THERM-HTC-013	2349	1.3	39 × 39	1521	06/29/88	21.3	53.77 ± 0.06
14	MIX-COMP-THERM-HTC-014	2352		34 × 34	1156	07/05/88	21.3	80.16 ± 0.06
15	MIX-COMP-THERM-HTC-015	2353		34 × 33	1122	07/06/88	21.3	86.35 ± 0.06
16	MIX-COMP-THERM-HTC-016	2355	1.7	50 × 18	900	07/19/88	21.0	69.07 ± 0.06
17	MIX-COMP-THERM-HTC-017	2357		50 × 17	850	07/21/88	21.4	83.15 ± 0.08
18	MIX-COMP-THERM-HTC-018	2361		50 × 18 [(b)]	900	07/28/88	22.4	80.16 ± 0.07

(a) given at a level of confidence of 95%

(b) no-centered array

Table B-2 Key Physical Parameters of the HTC Phase 2 Critical Experiments with Gadolinium Solutions [B.2]

Case	Reference	Experiment number	Pitch (cm)	Number of Rods		Date of experiment	Temperature (°C)	Critical water height (cm) [(a)]	Gadolinium conc. (g/l) [(b)]
				Along edge	Total				
19	MIX-COMP-THERM-HTC-019	2405	1.3	38 × 38	1444	01/20/89	20.3	81.86 ± 0.04	0.052
20	MIX-COMP-THERM-HTC-020	2406		38 × 37	1406	01/23/89	19.7	87.16 ± 0.04	0.052
21	MIX-COMP-THERM-HTC-021	2407		42 × 42	1764	01/23/89	20.1	80.13 ± 0.04	0.100
22	MIX-COMP-THERM-HTC-022	2408		42 × 41	1722	01/25/89	19.7	84.38 ± 0.04	0.099
23	MIX-COMP-THERM-HTC-023	2409		41 × 41	1681	01/25/89	19.6	89.54 ± 0.04	0.099
24	MIX-COMP-THERM-HTC-024	2410		46 × 46	2116	01/26/89	20.1	81.33 ± 0.04	0.151
25	MIX-COMP-THERM-HTC-025	2411		45 × 45	2025	01/27/89	20.0	89.49 ± 0.04	0.148
26	MIX-COMP-THERM-HTC-026	2412		50 × 50	2500	01/30/89	20.7	85.83 ± 0.04	0.200
27	MIX-COMP-THERM-HTC-027	2415		50 × 49	2450	02/01/89	19.6	90.03 ± 0.05	0.197
28	MIX-COMP-THERM-HTC-028	2417	1.5	50 × 50	2500	02/09/89	19.6	89.67 ± 0.04	0.196
29	MIX-COMP-THERM-HTC-029	2419		42 × 42	1764	02/14/89	21.4	85.88 ± 0.05	0.147
30	MIX-COMP-THERM-HTC-030	2420		42 × 41	1722	02/15/89	21.0	90.51 ± 0.05	0.147
31	MIX-COMP-THERM-HTC-031	2422		36 × 36	1296	02/21/89	22.1	83.86 ± 0.05	0.098
32	MIX-COMP-THERM-HTC-032	2423		36 × 35	1260	02/21/89	22.6	89.85 ± 0.04	0.098
33	MIX-COMP-THERM-HTC-033	2425		32 × 32	1024	02/24/89	20.9	73.60 ± 0.05	0.048
34	MIX-COMP-THERM-HTC-034	2427		31 × 31	961	02/27/89	20.6	84.14 ± 0.04	0.048
35	MIX-COMP-THERM-HTC-035	2430	1.7	31 × 30	930	03/01/89	21.1	85.87 ± 0.05	0.048
36	MIX-COMP-THERM-HTC-036	2434	1.9	35 × 35	1225	03/08/89	21.7	89.61 ± 0.04	0.048
37	MIX-COMP-THERM-HTC-037	2436	1.7	39 × 39	1521	03/13/89	22.5	85.86 ± 0.05	0.097
38	MIX-COMP-THERM-HTC-038	2433		50 × 23	1150	03/07/89	21.7	84.35 ± 0.04	0.048

(a) given at a level of confidence of 95%

(b) nominal values given in the report [B.5], not retained

Table B-3 Key Physical Parameters of the HTC Phase 2 Critical Experiments with Boron Solutions [B.2]

Case	Reference	Experiment number	Pitch (cm)	Number of Rods		Date of experiment	Temperature (°C)	Critical water height (cm) [(a)]	Boron conc. (g/l)
				Along edge	Total				
39	MIX-COMP-THERM-HTC-039	2437	1.3	37 × 37	1369	04/17/89	23.0	78.80 ± 0.04	0.100 ± 0.001
40	MIX-COMP-THERM-HTC-040	2438		37 × 36	1332	04/18/89	22.8	83.84 ± 0.04	0.106 ± 0.001
41	MIX-COMP-THERM-HTC-041	2441		39 × 39	1521	04/20/89	23.5	84.04 ± 0.04	0.205 ± 0.002
42	MIX-COMP-THERM-HTC-042	2444		42 × 41	1722	04/26/89	23.0	85.40 ± 0.05	0.299 ± 0.003
43	MIX-COMP-THERM-HTC-043	2446		45 × 44	1980	05/09/89	24.2	84.14 ± 0.04	0.400 ± 0.004
44	MIX-COMP-THERM-HTC-044	2447		44 × 44	1936	05/10/89	24.7	88.63 ± 0.05	0.399 ± 0.004
45	MIX-COMP-THERM-HTC-045	2448		47 × 47	2009	05/11/89	26.3	88.44 ± 0.04	0.486 ± 0.005
46	MIX-COMP-THERM-HTC-046	2449		50 × 50	2500	05/17/89	25.1	90.64 ± 0.04	0.587 ± 0.006
47	MIX-COMP-THERM-HTC-047	2459	1.5	49 × 49	2401	06/05/89	24.7	88.88 ± 0.04	0.595 ± 0.006
48	MIX-COMP-THERM-HTC-048	2468		43 × 43	1849	06/15/89	22.7	89.46 ± 0.04	0.499 ± 0.005
49	MIX-COMP-THERM-HTC-049	2470		39 × 39	1521	06/19/89	23.6	85.37 ± 0.05	0.393 ± 0.004
50	MIX-COMP-THERM-HTC-050	2471		35 × 35	1225	06/21/89	23.6	88.90 ± 0.04	0.295 ± 0.003
51	MIX-COMP-THERM-HTC-051	2473		32 × 32	1024	06/27/89	23.5	87.02 ± 0.04	0.200 ± 0.002
52	MIX-COMP-THERM-HTC-052	2475		30 × 29	870	07/03/89	23.6	82.48 ± 0.04	0.089 ± 0.001
53	MIX-COMP-THERM-HTC-053	2478	1.7	28 × 28	784	07/06/89	23.8	85.10 ± 0.04	0.090 ± 0.001
54	MIX-COMP-THERM-HTC-054	2483		32 × 32	1024	07/19/89	24.2	87.06 ± 0.04	0.194 ± 0.002
55	MIX-COMP-THERM-HTC-055	2485		37 × 37	1369	07/21/89	24.5	89.65 ± 0.04	0.286 ± 0.003
56	MIX-COMP-THERM-HTC-056	2487		45 × 44	1980	08/09/89	23.8	88.72 ± 0.04	0.415 ± 0.004
57	MIX-COMP-THERM-HTC-057	2482		50 × 21	1050	07/17/89	24.0	77.74 ± 0.04	0.100 ± 0.001
58	MIX-COMP-THERM-HTC-058	2490	1.9	39 × 38	1482	09/08/89	22.9	88.41 ± 0.04	0.220 ± 0.002
59	MIX-COMP-THERM-HTC-059	2492		31 × 30	930	09/14/89	22.0	86.95 ± 0.04	0.110 ± 0.001

(a) given at a level of confidence of 95%

Table B-4 Key Physical Parameters of the HTC Phase 3 Critical Experiments (pin pitch 1.6 cm) [B.3]

Case	Reference	Experiment number	Canister Type	Number of Rods		Date of experiment	Temperature (°C)	Critical water height (cm) [(a)]	Water Gap (cm)
				Along edge	Total				
60	MIX-COMP-THERM-HTC-060	2518	Borated Steel	25 × 25	625	01/04/90	18.3	88.83 ± 0.34	3.5
61	MIX-COMP-THERM-HTC-061	2520		25 × 24	600	01/09/90	18.7	49.55 ± 0.34	0.0
62	MIX-COMP-THERM-HTC-062	2521		25 × 24	600	01/10/90	18.8	71.45 ± 0.34	2.0
63	MIX-COMP-THERM-HTC-063	2522		25 × 24	600	01/10/90	19.0	89.96 ± 0.34	3.0
64	MIX-COMP-THERM-HTC-064	2523		25 × 24	600	01/12/90	18.9	58.23 ± 0.34	1.0
65	MIX-COMP-THERM-HTC-065	2514	Boral	25 × 25	625	12/28/89	20.6	90.03 ± 0.34	0.0
66	MIX-COMP-THERM-HTC-066	2511	Cadmium	25 × 25	625	12/21/89	21.1	82.16 ± 0.34	2.0
67	MIX-COMP-THERM-HTC-067	2524		25 × 24	600	01/15/90	18.7	55.33 ± 0.34	0.0
68	MIX-COMP-THERM-HTC-068	2525		25 × 24	600	01/16/90	19.0	67.95 ± 0.34	1.0
69	MIX-COMP-THERM-HTC-069	2526		25 × 24	600	01/17/90	19.1	79.83 ± 0.34	1.5
70	MIX-COMP-THERM-HTC-070	2527		25 × 24	600	01/18/90	19.1	58.66 ± 0.34	0.5
71	MIX-COMP-THERM-HTC-071	2509		25 × 25	625	12/19/89	20.9	84.75 ± 0.34	18.0
72	MIX-COMP-THERM-HTC-072	2531		25 × 24	600	01/23/90	19.0	88.2 ± 0.34	14.5
73	MIX-COMP-THERM-HTC-073	2532		24 × 24	576	01/24/90	19.1	81.18 ± 0.34	11.0
74	MIX-COMP-THERM-HTC-074	2533		24 × 23	552	01/25/90	19.3	82.12 ± 0.34	10.0
75	MIX-COMP-THERM-HTC-075	2534		23 × 23	529	01/26/90	19.4	81.2 ± 0.34	9.0
76	MIX-COMP-THERM-HTC-076	2535		22 × 22	484	01/30/90	19.7	86.17 ± 0.34	8.0
77	MIX-COMP-THERM-HTC-077	2536		20 × 20	400	01/31/90	19.7	82.08 ± 0.34	6.0
78	MIX-COMP-THERM-HTC-078	2537		17 × 17	289	02/01/90	19.9	77.92 ± 0.34	4.0
79	MIX-COMP-THERM-HTC-079	2538		17 × 16	272	02/02/90	20.0	90.28 ± 0.34	4.0
80	MIX-COMP-THERM-HTC-080	2539		14 × 14	196	02/05/90	20.2	75.99 ± 0.34	2.0
81	MIX-COMP-THERM-HTC-081	2541		13 × 13	169	02/06/90	20.0	83.17 ± 0.34	1.0
82	MIX-COMP-THERM-HTC-082	2544		13 × 13	169	02/07/90	20.4	79.46 ± 0.34	0.0
83	MIX-COMP-THERM-HTC-083	2547		25 × 25	625	02/19/90	20.9	29.46 ± 0.34	0.0
84	MIX-COMP-THERM-HTC-084	2548		25 × 25	625	02/20/90	20.9	37.96 ± 0.34	4.0
85	MIX-COMP-THERM-HTC-085	2549		25 × 25	625	02/20/90	21.0	64.43 ± 0.34	10.0

(a) given at a level of confidence of 95%

Table B-5 Key Physical Parameters of the HTC Phase 4 Critical Experiments with the Lead Screen (four 25 × 25 arrays with 1.6 cm pitch) [B.4]

Case	Reference	Experiment number	Canister Type	Date of experiment	Temperature (°C)	Water Gap (cm) [(a)]	Screen array distance (cm) [(b)]	Critical water height (cm) [(c)]
86	MIX-COMP-THERM-HTC-086	2562	Borated Steel	03/16/90	22.8	0.0	0.0	42.53 ± 0.34
87	MIX-COMP-THERM-HTC-087	2563		03/19/90	23.1	0.5	0.0	44.79 ± 0.34
88	MIX-COMP-THERM-HTC-088	2564		03/20/90	23.3	1.0	0.0	47.86 ± 0.34
89	MIX-COMP-THERM-HTC-089	2565		03/21/90	23.1	1.5	0.0	51.3 ± 0.34
90	MIX-COMP-THERM-HTC-090	2566		03/22/90	23.3	2.0	0.0	54.65 ± 0.34
91	MIX-COMP-THERM-HTC-091	2567		03/22/90	23.4	3.0	0.0	62.04 ± 0.34
92	MIX-COMP-THERM-HTC-092	2568		03/23/90	23.6	3.5	0.0	66.10 ± 0.34
93	MIX-COMP-THERM-HTC-093	2569		03/26/90	23.5	2.0	0.5	55.87 ± 0.34
94	MIX-COMP-THERM-HTC-094	2570		03/27/90	23.1	2.0	1.0	57.33 ± 0.34
95	MIX-COMP-THERM-HTC-095	2571		03/27/90	23.0	2.0	1.5	58.68 ± 0.34
96	MIX-COMP-THERM-HTC-096	2572		03/28/90	22.9	2.0	2.0	59.78 ± 0.34
97	MIX-COMP-THERM-HTC-097	2586	Boral	04/23/90	21.9	0.0	0.0	72.47 ± 0.34
98	MIX-COMP-THERM-HTC-098	2587		04/24/90	22.0	0.0	0.0	72.49 ± 0.34
99	MIX-COMP-THERM-HTC-099	2588		04/24/90	22.2	0.0	0.5	74.70 ± 0.34
100	MIX-COMP-THERM-HTC-100	2624		07/13/90	21.6	1.0	0.0	86.06 ± 0.34
101	MIX-COMP-THERM-HTC-101	2625		07/18/90	22.4	0.5	0.0	76.69 ± 0.34
102	MIX-COMP-THERM-HTC-102	2577	Cadmium	04/05/90	22.7	0.0	0.0	46.13 ± 0.34
103	MIX-COMP-THERM-HTC-103	2578		04/05/90	22.6	1.0	0.0	52.89 ± 0.34
104	MIX-COMP-THERM-HTC-104	2579		04/06/90	22.6	2.0	0.0	63.52 ± 0.34
105	MIX-COMP-THERM-HTC-105	2580		04/09/90	22.4	2.5	0.0	69.83 ± 0.34
106	MIX-COMP-THERM-HTC-106	2581		04/11/90	22.5	2.0	0.5	65.84 ± 0.34
107	MIX-COMP-THERM-HTC-107	2582		04/11/90	22.5	2.0	1.0	68.63 ± 0.34
108	MIX-COMP-THERM-HTC-108	2583		04/12/90	22.4	2.0	1.5	71.21 ± 0.34

Case	Reference	Experiment number	Canister Type	Date of experiment	Temperature (°C)	Water Gap (cm) [(a)]	Screen array distance (cm) [(b)]	Critical water height (cm) [(c)]
109	MIX-COMP-THERM-HTC-109	2584		04/12/90	22.4	2.0	2.0	73.36 ± 0.34
110	MIX-COMP-THERM-HTC-110	2621		07/03/90	22.3	3.0	0.0	76.25 ± 0.34
111	MIX-COMP-THERM-HTC-111	2622		07/04/90	22.3	3.5	0.0	83.38 ± 0.34
112	MIX-COMP-THERM-HTC-112	2550	No	02/23/90	21.4	0.0	0.0	27.45 ± 0.34
113	MIX-COMP-THERM-HTC-113	2551		02/26/90	22.1	1.0	0.0	28.00 ± 0.34
114	MIX-COMP-THERM-HTC-114	2552		02/28/90	21.8	2.0	0.0	29.37 ± 0.34
115	MIX-COMP-THERM-HTC-115	2553		03/01/90	21.8	4.0	0.0	34.65 ± 0.34
116	MIX-COMP-THERM-HTC-116	2554		03/02/90	21.3	6.0	0.0	41.60 ± 0.34
117	MIX-COMP-THERM-HTC-117	2555		03/05/90	20.7	8.0	0.0	48.65 ± 0.34
118	MIX-COMP-THERM-HTC-118	2556		03/06/90	20.7	10.0	0.0	54.74 ± 0.34
119	MIX-COMP-THERM-HTC-119	2557		03/07/90	20.9	12.0	0.0	59.57 ± 0.34
120	MIX-COMP-THERM-HTC-120	2558		03/09/90	21.3	2.0	0.5	29.43 ± 0.34
121	MIX-COMP-THERM-HTC-121	2559		03/12/90	21.7	2.0	1.0	29.46 ± 0.34
122	MIX-COMP-THERM-HTC-122	2560		03/13/90	21.9	2.0	1.5	29.55 ± 0.34
123	MIX-COMP-THERM-HTC-123	2561		03/14/90	22.3	2.0	2.0	29.62 ± 0.34

(a) Water gap between arrays.

(b) Water gap between screen and array.

(c) Given at a level of confidence of 95%

Table B-6 Key Physical Parameters of the HTC Phase 4 Critical Experiments with the Steel Screen (four 25 × 25 arrays with 1.6 cm pitch) [B.4]

Case	Reference	Experiment number	Canister Type	Date of experiment	Temperature (°C)	Water Gap (cm) [a]	Screen array distance (cm) [b]	Critical water height (cm) [c]
124	MIX-COMP-THERM-HTC-124	2602	Borated Steel	05/21/90	23.6	0.0	0.0	42.11 ± 0.34
125	MIX-COMP-THERM-HTC-125	2603		05/21/90	23.4	0.5	0.0	44.14 ± 0.34
126	MIX-COMP-THERM-HTC-126	2604		05/22/90	22.9	1.0	0.0	46.96 ± 0.34
127	MIX-COMP-THERM-HTC-127	2605		05/29/90	20.4	1.5	0.0	50.16 ± 0.34
128	MIX-COMP-THERM-HTC-128	2606		05/30/90	20.1	2.0	0.0	53.43 ± 0.34
129	MIX-COMP-THERM-HTC-129	2607		05/31/90	20.0	2.0	0.5	54.71 ± 0.34
130	MIX-COMP-THERM-HTC-130	2608		06/05/90	20.2	2.0	1.0	56.32 ± 0.34
131	MIX-COMP-THERM-HTC-131	2609		06/05/90	20.1	2.0	1.5	57.96 ± 0.34
132	MIX-COMP-THERM-HTC-132	2610		06/06/90	19.7	2.0	2.0	59.16 ± 0.34
133	MIX-COMP-THERM-HTC-133	2611		06/08/90	19.5	3.0	0.0	60.38 ± 0.34
134	MIX-COMP-THERM-HTC-134	2612		06/12/90	20.1	3.5	0.0	64.19 ± 0.34
135	MIX-COMP-THERM-HTC-135	2589	Boral	04/26/90	22.4	0.0	0.0	69.82 ± 0.34
136	MIX-COMP-THERM-HTC-136	2626		07/19/90	22.6	0.5	0.0	73.44 ± 0.34
137	MIX-COMP-THERM-HTC-137	2613	Cadmium	06/13/90	20.5	0.0	0.0	44.70 ± 0.34
138	MIX-COMP-THERM-HTC-138	2614		06/13/90	20.6	1.0	0.0	51.00 ± 0.34
139	MIX-COMP-THERM-HTC-139	2615		06/14/90	20.6	2.0	0.0	60.26 ± 0.34
140	MIX-COMP-THERM-HTC-140	2616		06/15/90	20.7	2.0	0.5	62.54 ± 0.34
141	MIX-COMP-THERM-HTC-141	2617		06/18/90	21.0	2.0	1.0	65.85 ± 0.34
142	MIX-COMP-THERM-HTC-142	2618		06/19/90	21.3	2.0	1.5	68.70 ± 0.34
143	MIX-COMP-THERM-HTC-143	2619		06/20/90	21.5	2.0	2.0	71.00 ± 0.34
144	MIX-COMP-THERM-HTC-144	2620		06/21/90	21.7	2.5	0.0	65.76 ± 0.34
145	MIX-COMP-THERM-HTC-145	2590	No	04/27/90	22.4	0.0	0.0	27.77 ± 0.34
146	MIX-COMP-THERM-HTC-146	2591		05/09/90	24.4	1.0	0.0	28.34 ± 0.34

Case	Reference	Experiment number	Canister Type	Date of experiment	Temperature (°C)	Water Gap (cm) [(a)]	Screen array distance (cm) [(b)]	Critical water height (cm) [(c)]
147	MIX-COMP-THERM-HTC-147	2592		05/10/90	24.4	2.0	0.0	29.74 ± 0.34
148	MIX-COMP-THERM-HTC-148	2593		05/10/90	24.3	2.0	0.5	29.68 ± 0.34
149	MIX-COMP-THERM-HTC-149	2594		05/11/90	24.5	2.0	1.0	29.66 ± 0.34
150	MIX-COMP-THERM-HTC-150	2595		05/11/90	24.4	2.0	1.5	29.68 ± 0.34
151	MIX-COMP-THERM-HTC-151	2596		05/14/90	24.7	2.0	2.0	29.76 ± 0.34
152	MIX-COMP-THERM-HTC-152	2597		05/15/90	24.6	4.0	0.0	35.33 ± 0.34
153	MIX-COMP-THERM-HTC-153	2598		05/15/90	24.6	6.0	0.0	43.24 ± 0.34
154	MIX-COMP-THERM-HTC-154	2599		05/16/90	24.7	8.0	0.0	51.30 ± 0.34
155	MIX-COMP-THERM-HTC-155	2600		05/17/90	24.7	10.0	0.0	58.73 ± 0.34
156	MIX-COMP-THERM-HTC-156	2601		05/18/90	24.6	12.0	0.0	64.84 ± 0.34

(a) Water gap between arrays.

(b) Water gap between screen and array.

(c) Given at a level of confidence of 95%

Table B-7 Description of the Selected Benchmark Critical Experiments [B.6]

Case	Reference	Identification	U, wt%	Pu, wt%	
157	LEU-COMP-THERM-011-001	Core I	2.46	-	
158	LEU-COMP-THERM-011-002	Core II	2.46	-	
159	LEU-COMP-THERM-011-004	Core IIIB	2.46	-	
160	LEU-COMP-THERM-011-015	Core IX	2.46	-	
161	LEU-COMP-THERM-051-001	Core X	2.46	-	
162	LEU-COMP-THERM-051-003	Core XIB	2.46	-	
163	LEU-COMP-THERM-051-009	Core XII	2.46	-	
164	LEU-COMP-THERM-051-010	Core XIII	2.46	-	
165	LEU-COMP-THERM-051-012	Core XIV	2.46	-	
166	LEU-COMP-THERM-051-013	Core XV	2.46	-	
167	LEU-COMP-THERM-051-014	Core XVI	2.46	-	
168	LEU-COMP-THERM-051-015	Core XVII	2.46	-	
169	LEU-COMP-THERM-051-016	Core XVIII	2.46	-	
170	LEU-COMP-THERM-051-017	Core XIX	2.46	-	
171	LEU-COMP-THERM-051-018	Core XX	2.46	-	
172	LEU-COMP-THERM-051-019	Core XXI	2.46	-	
173	BAW-1645-4 [B.7]	S-type Fuel, w/886 ppm B	2.46	-	
174	BAW-1645-4 [B.7]	S-type Fuel, w/746 ppm B	2.46	-	
175	BAW-1645-4 [B.7]	SO-type Fuel, w/1156 ppm B	2.46	-	
176	BAW-1810 [B.8]	Case 1 1337 ppm B	2.46	-	
177	BAW-1810 [B.8]	Case 12 1899 ppm B	2.75	-	
178	French [B.9]	Water Moderator 0 gap	4.75	-	
179	French [B.9]	Water Moderator 2.5 cm gap	4.75	-	
180	French [B.9]	Water Moderator 5 cm gap	4.75	-	
181	French [B.9]	Water Moderator 10 cm gap	4.75	-	
182	LEU-COMP-THERM-017-012	Steel Reflector, 1.321 cm separation	2.35	-	
183	LEU-COMP-THERM-017-013	Steel Reflector, 2.616 cm separation	2.35	-	
184	LEU-COMP-THERM-017-014	Steel Reflector, 3.912 cm separation	2.35	-	
185	LEU-COMP-THERM-001-008	Steel Reflector, Infinite separation	2.35	-	
186	LEU-COMP-THERM-010-016	Steel Reflector, 1.321 cm separation	4.306	-	
187	LEU-COMP-THERM-010-018	Steel Reflector, 2.616 cm separation	4.306	-	
188	LEU-COMP-THERM-010-019	Steel Reflector, 5.405 cm separation	4.306	-	
189	LEU-COMP-THERM-004-010	Steel Reflector, Infinite separation	4.306	-	
190	LEU-COMP-THERM-013-003	Steel Reflector, with Boral Sheets	4.306	-	
191	LEU-COMP-THERM-010-021	Lead Reflector, 0.55 cm sepn.	4.306	-	
192	LEU-COMP-THERM-010-022	Lead Reflector, 1.956 cm sepn.	4.306	-	
193	LEU-COMP-THERM-010-023	Lead Reflector, 5.405 cm sepn.	4.306	-	
194	LEU-COMP-THERM-002-004	Experiment 004/032 – no absorber	4.306	-	
195	LEU-COMP-THERM-009-005	Exp. 009 1.05% Boron Steel plates	4.306	-	

Case	Reference	Identification	U, wt%	Pu, wt%
196	LEU-COMP-THERM-009-007	Exp. 009 1.62% Boron Steel plates	4.306	-
197	LEU-COMP-THERM-009-009	Exp. 031 – Boral plates	4.306	-
198	PNL-7167 [B.10]	Experiment 214R – with flux traps	4.306	-
199	PNL-7167 [B.10]	Experiment 214V3 –with flux trap	4.306	-
200	LEU-COMP-THERM-014-001	Case 173 – 0 ppm B	4.306	-
201	LEU-COMP-THERM-014-005	Case 177 – 2550 ppm B	4.306	-
202	PNL-5803 [B.11]	MOX Fuel – Type 3.2 Exp. 21	0.71	20
203	PNL-5803 [B.11]	MOX Fuel – Type 3.2 Exp. 43	0.71	20
204	PNL-5803 [B.11]	MOX Fuel – Type 3.2 Exp. 13	0.71	20
205	PNL-5803 [B.11]	MOX Fuel – Type 3.2 Exp. 32	0.71	20
206	MIX-COMP-THERM-003-001	Saxton Case 52 PuO2 0.52” pitch	0.72	6.6
207	WCAP-3385 [B.12]	Saxton Case 52 U 0.52” pitch	5.74	-
208	MIX-COMP-THERM-003-002	Saxton Case 56 PuO2 0.56” pitch	0.72	6.6
209	MIX-COMP-THERM-003-003	Saxton Case 56 borated PuO2	0.72	6.6
210	WCAP-3385 [B.12]	Saxton Case 56 U 0.56” pitch	5.74	-
211	MIX-COMP-THERM-003-005	Saxton Case 79 PuO2 0.79” pitch	0.72	6.6
212	WCAP-3385 [B.12]	Saxton Case 79 U 0.79” pitch	5.74	-
213	MIX-COMP-THERM-002-030	0.700-in. pitch 0 ppm B	0.72	2.0
214	MIX-COMP-THERM-002-031	0.700-in. pitch 688 ppm B	0.72	2.0
215	MIX-COMP-THERM-002-032	0.870-in. pitch 0 ppm B	0.72	2.0
216	MIX-COMP-THERM-002-033	0.870-in. pitch 1090 ppm B	0.72	2.0
217	MIX-COMP-THERM-002-034	0.990-in. pitch 0 ppm B	0.72	2.0
218	MIX-COMP-THERM-002-035	0.990-in. pitch 767 ppm B	0.72	2.0
219	MIX-COMP-THERM-003-004	Saxton Case PuO2 0.735” pitch	0.72	6.6
220	MIX-COMP-THERM-003-006	Saxton Case PuO2 1.04” pitch	0.72	6.6
221	MIX-COMP-THERM-006-001	8 wt% 240Pu 0.80” pitch	0.71	2.0
222	MIX-COMP-THERM-006-002	8 wt% 240Pu 0.93” pitch	0.71	2.0
223	MIX-COMP-THERM-006-003	8 wt% 240Pu 1.05” pitch	0.71	2.0
224	MIX-COMP-THERM-006-004	8 wt% 240Pu 1.143” pitch	0.71	2.0
225	MIX-COMP-THERM-006-005	8 wt% 240Pu 1.32” pitch	0.71	2.0
226	MIX-COMP-THERM-006-006	8 wt% 240Pu 1.386” pitch	0.71	2.0
227	MIX-COMP-THERM-007-001	16 wt% 240Pu 0.93” pitch	0.72	2.0
228	MIX-COMP-THERM-007-002	16 wt% 240Pu 1.05” pitch	0.72	2.0
229	MIX-COMP-THERM-007-003	16 wt% 240Pu 1.143” pitch	0.72	2.0
230	MIX-COMP-THERM-007-004	16 wt% 240Pu 1.32” pitch	0.72	2.0
231	MIX-COMP-THERM-008-001	24 wt% 240Pu 0.80” pitch	0.72	2.0
232	MIX-COMP-THERM-008-002	24 wt% 240Pu 0.93” pitch	0.72	2.0
233	MIX-COMP-THERM-008-003	24 wt% 240Pu 1.05” pitch	0.72	2.0
234	MIX-COMP-THERM-008-004	24 wt% 240Pu 1.143” pitch	0.72	2.0
235	MIX-COMP-THERM-008-005	24 wt% 240Pu 1.32” pitch	0.72	2.0

Case	Reference	Identification	U, wt%	Pu, wt%	
236	MIX-COMP-THERM-008-006	24 wt% 240Pu 1.386” pitch	0.72	2.0	
237	MIX-COMP-THERM-005-001	18 wt% 240Pu 0.85” pitch	0.72	4.0	
238	MIX-COMP-THERM-005-002	18 wt% 240Pu 0.93” pitch	0.72	4.0	
239	MIX-COMP-THERM-005-003	18 wt% 240Pu 1.05” pitch	0.72	4.0	
240	MIX-COMP-THERM-005-004	18 wt% 240Pu 1.143” pitch	0.72	4.0	
241	MIX-COMP-THERM-005-005	18 wt% 240Pu 1.386” pitch	0.72	4.0	
242	MIX-COMP-THERM-005-006	18 wt% 240Pu 1.60” pitch	0.72	4.0	
243	MIX-COMP-THERM-005-007	18 wt% 240Pu 1.70” pitch	0.72	4.0	
244	LEU-COMP-THERM-001-001	1 Cluster	2.35	-	
245	LEU-COMP-THERM-001-002	3 Clusters, Separation 11.92 cm	2.35	-	
246	LEU-COMP-THERM-001-003	3 Clusters, Separation 8.41 cm	2.35	-	
247	LEU-COMP-THERM-001-004	3 Clusters, Separation 10.05 cm	2.35	-	
248	LEU-COMP-THERM-001-005	3 Clusters, Separation 6.39 cm	2.35	-	
249	LEU-COMP-THERM-001-006	3 Clusters, Separation 9.01 cm	2.35	-	
250	LEU-COMP-THERM-001-007	3 Clusters, Separation 4.46	2.35	-	
251	LEU-COMP-THERM-002-001	1 Cluster, 10x11.51	4.306	-	
252	LEU-COMP-THERM-002-002	1 Cluster, 9x13.35	4.306	-	
253	LEU-COMP-THERM-002-003	1 Cluster, 8x16.37	4.306	-	
254	LEU-COMP-THERM-002-005	3 Clusters, Separation 7.11 cm	4.306	-	
255	LEU-COMP-THERM-003-001	1 Cluster, 614.4 Rods, Gd water impurity	2.35	-	
256	LEU-COMP-THERM-003-002	1 Cluster, 529.3 Rods	2.35	-	
257	LEU-COMP-THERM-003-003	1 Cluster, 523.9 Rods	2.35	-	
258	LEU-COMP-THERM-003-004	1 Cluster, 525.3 Rods	2.35	-	
259	LEU-COMP-THERM-003-005	1 Cluster, 595.4 Rods	2.35	-	
260	LEU-COMP-THERM-003-006	1 Cluster, 485.8 Rods	2.35	-	
261	LEU-COMP-THERM-003-007	1 Cluster, 523.8 Rods	2.35	-	
262	LEU-COMP-THERM-003-008	1 Cluster, 505.4 Rods	2.35	-	
263	LEU-COMP-THERM-003-009	4 Clusters, Separation 2.59 cm	2.35	-	
264	LEU-COMP-THERM-003-010	2 Clusters, Separation 1.68 cm	2.35	-	
265	LEU-COMP-THERM-003-011	4 Clusters, Separation 4.27 cm	2.35	-	
266	LEU-COMP-THERM-003-012	4 Clusters, Separation 5.95 cm	2.35	-	
267	LEU-COMP-THERM-003-013	4 Clusters, Separation 5.11 cm	2.35	-	
268	LEU-COMP-THERM-003-014	4 Clusters, Separation 6.66 cm	2.35	-	
269	LEU-COMP-THERM-003-015	4 Clusters, Separation 7.53 cm	2.35	-	
270	LEU-COMP-THERM-003-016	4 Clusters, Separation 9.00 cm	2.35	-	
271	LEU-COMP-THERM-003-017	4 Clusters, Separation 9.97 cm	2.35	-	
272	LEU-COMP-THERM-003-018	4 Clusters, Separation 11.45 cm	2.35	-	
273	LEU-COMP-THERM-003-019	4 Clusters, Separation 13.87 cm	2.35	-	
274	LEU-COMP-THERM-003-020	3 Clusters, Separation 9.88 cm	2.35	-	
275	LEU-COMP-THERM-003-021	3 Clusters, Separation 6.78 cm	2.35	-	

Case	Reference	Identification	U, wt%	Pu, wt%
276	LEU-COMP-THERM-003-023	3 Clusters, Separation 6.176 cm	2.35	-
277	LEU-COMP-THERM-004-001	1 Cluster, 225.8 Rods, Gd water impurity	4.306	-
278	LEU-COMP-THERM-004-002	1 Cluster, 216.2 Rods	4.306	-
279	LEU-COMP-THERM-004-003	1 Cluster, 216.6 Rods	4.306	-
280	LEU-COMP-THERM-004-004	1 Cluster, 218.6 Rods	4.306	-
281	LEU-COMP-THERM-004-005	1 Cluster, 167.85 Rods	4.306	-
282	LEU-COMP-THERM-004-006	1 Cluster, 203 Rods	4.306	-
283	LEU-COMP-THERM-004-007	1 Cluster, 173.5 Rods	4.306	-
284	LEU-COMP-THERM-004-008	2 Clusters, Separation 2.83 cm	4.306	-
285	LEU-COMP-THERM-004-009	3 Clusters, Separation 12.27 cm	4.306	-
286	LEU-COMP-THERM-004-011	3 Clusters, Separation 12.493 cm	4.306	-
287	LEU-COMP-THERM-004-012	4 Clusters, Separation 4.72 cm	4.306	-
288	LEU-COMP-THERM-004-013	4 Clusters, Separation 8.38 cm	4.306	-
289	LEU-COMP-THERM-004-014	4 Clusters, Separation 10.86 cm	4.306	-
290	LEU-COMP-THERM-004-015	4 Clusters, Separation 11.29 cm	4.306	-
291	LEU-COMP-THERM-004-016	4 Clusters, Separation 12.02 cm	4.306	-
292	LEU-COMP-THERM-004-017	4 Clusters, Separation 13.64 cm	4.306	-
293	LEU-COMP-THERM-004-018	4 Clusters, Separation 14.98 cm	4.306	-
294	LEU-COMP-THERM-004-019	4 Clusters, Separation 19.81 cm	4.306	-
295	LEU-COMP-THERM-004-020	4 Clusters, Separation 8.50 cm	4.306	-
296	LEU-COMP-THERM-006-001	19x19, Rod Pitch - 1.849 cm	2.596	-
297	LEU-COMP-THERM-006-002	20x20, Rod Pitch - 1.849 cm	2.596	-
298	LEU-COMP-THERM-006-003	21x21, Rod Pitch - 1.849 cm	2.596	-
299	LEU-COMP-THERM-006-004	17x17, Rod Pitch - 1.956 cm	2.596	-
300	LEU-COMP-THERM-006-005	18x18, Rod Pitch - 1.956 cm	2.596	-
301	LEU-COMP-THERM-006-006	19x19, Rod Pitch - 1.956 cm	2.596	-
302	LEU-COMP-THERM-006-007	20x20, Rod Pitch - 1.956 cm	2.596	-
303	LEU-COMP-THERM-006-008	21x21, Rod Pitch - 1.956 cm	2.596	-
304	LEU-COMP-THERM-006-009	16x16, Rod Pitch - 2.15 cm	2.596	-
305	LEU-COMP-THERM-006-010	17x17, Rod Pitch - 2.15 cm	2.596	-
306	LEU-COMP-THERM-006-011	18x18, Rod Pitch - 2.15 cm	2.596	-
307	LEU-COMP-THERM-006-012	19x19, Rod Pitch - 2.15 cm	2.596	-
308	LEU-COMP-THERM-006-013	20x20, Rod Pitch - 2.15 cm	2.596	-
309	LEU-COMP-THERM-006-014	15x15, Rod Pitch - 2.293 cm	2.596	-
310	LEU-COMP-THERM-006-015	16x16, Rod Pitch - 2.293 cm	2.596	-
311	LEU-COMP-THERM-006-016	17x17, Rod Pitch - 2.293 cm	2.596	-
312	LEU-COMP-THERM-006-017	18x18, Rod Pitch - 2.293 cm	2.596	-
313	LEU-COMP-THERM-006-018	19x19, Rod Pitch - 2.293 cm	2.596	-
314	LEU-COMP-THERM-008-001	Core XI, 1511 ppm	2.459	-
315	LEU-COMP-THERM-008-002	Core XI, 1335.5 ppm	2.459	-

Case	Reference	Identification	U, wt%	Pu, wt%	
316	LEU-COMP-THERM-008-003	Core XI, 1335.5 ppm	2.459	-	
317	LEU-COMP-THERM-008-004	Core XI, 1182 ppm, 36 Pyrex Rods	2.459	-	
318	LEU-COMP-THERM-008-005	Core XI, 1182 ppm, 36 Pyrex Rods	2.459	-	
319	LEU-COMP-THERM-008-006	Core XI, 1032.5 ppm, 72 Pyrex Rods	2.459	-	
320	LEU-COMP-THERM-008-007	Core XI, 1032.5 ppm, 72 Pyrex Rods	2.459	-	
321	LEU-COMP-THERM-008-008	Core XI, 794 ppm, 144 Pyrex Rods	2.459	-	
322	LEU-COMP-THERM-008-009	Core XI, 779 ppm, 144 Pyrex Rods	2.459	-	
323	LEU-COMP-THERM-008-010	Core XI, 1245 ppm, 72 Vicor Rods	2.459	-	
324	LEU-COMP-THERM-008-011	Core XI, 1384 ppm, 144 Al_2O_3 Rods	2.459	-	
325	LEU-COMP-THERM-008-012	Core XI, 1348 ppm, 36 Al2O3 Rods	2.459	-	
326	LEU-COMP-THERM-008-013	Core XI, 1348 ppm, 36 Al2O3 Rods	2.459	-	
327	LEU-COMP-THERM-008-014	Core XI, 1363 ppm, 72 Al2O3 Rods	2.459	-	
328	LEU-COMP-THERM-008-015	Core XI, 1362 ppm, 72 Al2O3 Rods	2.459	-	
329	LEU-COMP-THERM-008-016	Core XI, 1158 ppm	2.459	-	
330	LEU-COMP-THERM-008-017	Core XI, 921 ppm	2.459	-	
331	LEU-COMP-THERM-009-001	0% Boron Steel plates, dist. 0.245 cm	4.306	-	
332	LEU-COMP-THERM-009-002	0% Boron Steel plates, dist. 3.277 cm	4.306	-	
333	LEU-COMP-THERM-009-003	0% Boron Steel plates, dist. 0.428 cm	4.306	-	
334	LEU-COMP-THERM-009-004	0% Boron Steel plates, dist. 3.277 cm	4.306	-	
335	LEU-COMP-THERM-009-006	1.05% Boron Steel plates, dist. 3.277 cm	4.306	-	
336	LEU-COMP-THERM-009-008	1.62% Boron Steel plates, dist. 3.277 cm	4.306	-	
337	LEU-COMP-THERM-009-024	Al plates, dist. 0.105 cm	4.306	-	
338	LEU-COMP-THERM-009-025	Al plates, dist. 3.277 cm	4.306	-	
339	LEU-COMP-THERM-009-026	Zircaloy-4 plates, dist. 0.078 cm	4.306	-	
340	LEU-COMP-THERM-009-027	Zircaloy-4 plates, dist. 3.277 cm	4.306	-	
341	LEU-COMP-THERM-010-001	Lead Reflector, 0 cm separation	4.306	-	
342	LEU-COMP-THERM-010-002	Lead Reflector, 0.660 cm separation	4.306	-	
343	LEU-COMP-THERM-010-003	Lead Reflector, 1.321 cm separation	4.306	-	
344	LEU-COMP-THERM-010-004	Lead Reflector, 5.405 cm separation	4.306	-	
345	LEU-COMP-THERM-010-009	Steel Reflector, 0 cm separation	4.306	-	
346	LEU-COMP-THERM-010-010	Steel Reflector, 0.660 cm separation	4.306	-	
347	LEU-COMP-THERM-010-011	Steel Reflector, 1.321 cm separation	4.306	-	
348	LEU-COMP-THERM-010-012	Steel Reflector, 2.616 cm separation	4.306	-	
349	LEU-COMP-THERM-010-013	Steel Reflector, 5.405 cm separation	4.306	-	
350	LEU-COMP-THERM-010-014	Steel Reflector, 0 cm separation	4.306	-	
351	LEU-COMP-THERM-010-015	Steel Reflector, 0.660 cm separation	4.306	-	
352	LEU-COMP-THERM-010-017	Steel Reflector, 1.956 cm separation	4.306	-	
353	LEU-COMP-THERM-010-020	Lead Reflector, 0 cm separation	4.306	-	
354	LEU-COMP-THERM-011-003	Core IIIA	2.46	-	
355	LEU-COMP-THERM-011-005	Core IIIC	2.46	-	

Case	Reference	Identification	U, wt%	Pu, wt%	
356	LEU-COMP-THERM-011-006	Core IIID	2.46	-	
357	LEU-COMP-THERM-011-007	Core IIIE	2.46	-	
358	LEU-COMP-THERM-011-008	Core IIIF	2.46	-	
359	LEU-COMP-THERM-011-009	Core IIIG	2.46	-	
360	LEU-COMP-THERM-011-010	Core IV	2.46	-	
361	LEU-COMP-THERM-011-011	Core V	2.46	-	
362	LEU-COMP-THERM-011-012	Core VI	2.46	-	
363	LEU-COMP-THERM-011-013	Core VII	2.46	-	
364	LEU-COMP-THERM-011-014	Core VIII	2.46	-	
365	LEU-COMP-THERM-012-001	0% Boron Steel plate, Gd water impurity	2.35	-	
366	LEU-COMP-THERM-012-002	1.1% Boron Steel plate	2.35	-	
367	LEU-COMP-THERM-012-003	1.6% Boron Steel plate	2.35	-	
368	LEU-COMP-THERM-012-004	Boral B plate	2.35	-	
369	LEU-COMP-THERM-012-005	Boral C plate	2.35	-	
370	LEU-COMP-THERM-012-006	Boroflex, 1.84 cm separation	2.35	-	
371	LEU-COMP-THERM-012-007	Boroflex, 1.73 cm separation	2.35	-	
372	LEU-COMP-THERM-013-001	Steel Reflector, 0% Boron Steel plate	4.306	-	
373	LEU-COMP-THERM-013-002	Steel Reflector, 1.1% Boron Steel plate	4.306	-	
374	LEU-COMP-THERM-013-004	Steel Reflector, Boroflex, 8.37 cm separation	4.306	-	
375	LEU-COMP-THERM-014-002	Borated Water, 490 ppm	4.306	-	
376	LEU-COMP-THERM-014-006	Unborated Water	4.306	-	
377	LEU-COMP-THERM-014-007	Borated Water, 1030 ppm	4.306	-	
378	LEU-COMP-THERM-016-001	0% Boron Steel plates, dist. 0.645 cm	2.35	-	
379	LEU-COMP-THERM-016-002	0% Boron Steel plates, dist. 2.732 cm	2.35	-	
380	LEU-COMP-THERM-016-003	0% Boron Steel plates, dist. 4.042 cm	2.35	-	
381	LEU-COMP-THERM-016-004	0% Boron Steel plates, dist. 0.645 cm	2.35	-	
382	LEU-COMP-THERM-016-005	0% Boron Steel plates, dist. 4.042 cm	2.35	-	
383	LEU-COMP-THERM-016-006	0% Boron Steel plates, dist. 0.645 cm	2.35	-	
384	LEU-COMP-THERM-016-007	0% Boron Steel plates, dist. 4.042 cm	2.35	-	
385	LEU-COMP-THERM-016-008	1.05% Boron Steel plates, dist. 0.645 cm	2.35	-	
386	LEU-COMP-THERM-016-009	1.05% Boron Steel plates, dist. 4.042 cm	2.35	-	
387	LEU-COMP-THERM-016-010	1.62% Boron Steel plates, dist. 0.645 cm	2.35	-	
388	LEU-COMP-THERM-016-011	1.62% Boron Steel plates, dist. 4.042 cm	2.35	-	
389	LEU-COMP-THERM-016-012	Boral plates, dist. 0.645 cm	2.35	-	
390	LEU-COMP-THERM-016-013	Boral plates, dist. 4.442 cm	2.35	-	
391	LEU-COMP-THERM-016-014	Boral plates, dist. 0.645 cm	2.35	-	
392	LEU-COMP-THERM-016-028	Al plates, dist. 0.645 cm	2.35	-	
393	LEU-COMP-THERM-016-029	Al plates, dist. 4.042 cm	2.35	-	
394	LEU-COMP-THERM-016-030	Al plates, dist. 4.442 cm	2.35	-	
395	LEU-COMP-THERM-016-031	Zircaloy-4 plates, dist. 0.645 cm	2.35	-	

Case	Reference	Identification	U, wt%	Pu, wt%	
396	LEU-COMP-THERM-016-032	Zircaloy-4 plates, dist. 4.042 cm	2.35	-	
397	LEU-COMP-THERM-026-001	Hex, 621 Rods, Temperature 20.1C	4.92	-	
398	LEU-COMP-THERM-026-002	Hex, 889 Rods, Temperature 231.4C	4.92	-	
399	LEU-COMP-THERM-026-003	Hex, 1951 Rods, Temperature 19.3C	4.92	-	
400	LEU-COMP-THERM-026-004	Hex, 2791 Rods, Temperature 206.0C	4.92	-	
401	LEU-COMP-THERM-026-005	Hex, 325/680 Rods, Temperature 20.8C	4.92	-	
402	LEU-COMP-THERM-026-006	Hex, 325/912 Rods, Temperature 212.1C	4.92	-	
403	LEU-COMP-THERM-051-002	Core XIA	2.46	-	
404	LEU-COMP-THERM-051-004	Core XIC	2.46	-	
405	LEU-COMP-THERM-051-005	Core XID	2.46	-	
406	LEU-COMP-THERM-051-006	Core XIE	2.46	-	
407	LEU-COMP-THERM-051-007	Core XIF	2.46	-	
408	LEU-COMP-THERM-051-008	Core XIG	2.46	-	
409	LEU-COMP-THERM-051-011	Core XIIIA	2.46	-	
410	LEU-COMP-THERM-062-001	No Boron Steel plates	2.6	-	
411	LEU-COMP-THERM-062-002	0% Boron Steel plates, 3 mm, dist. 0	2.6	-	
412	LEU-COMP-THERM-062-003	0% Boron Steel plates, 6 mm, dist. 0	2.6	-	
413	LEU-COMP-THERM-062-004	0% Boron Steel plates, 6 mm, dist. 0.5	2.6	-	
414	LEU-COMP-THERM-062-005	0% Boron Steel plates, 6 mm, dist. 1	2.6	-	
415	LEU-COMP-THERM-062-006	0.67% Boron Steel plates, 3 mm, dist. 0	2.6	-	
416	LEU-COMP-THERM-062-007	0.67% Boron Steel plates, 6 mm, dist. 0	2.6	-	
417	LEU-COMP-THERM-062-008	0.67% Boron Steel plates, 3 mm, dist. 0.5	2.6	-	
418	LEU-COMP-THERM-062-009	0.67% Boron Steel plates, 6 mm, dist. 0.5	2.6	-	
419	LEU-COMP-THERM-062-010	0.67% Boron Steel plates, 3 mm, dist. 1	2.6	-	
420	LEU-COMP-THERM-062-011	0.67% Boron Steel plates, 6 mm, dist. 1	2.6	-	
421	LEU-COMP-THERM-062-012	0.98% Boron Steel plates, 3 mm, dist. 0	2.6	-	
422	LEU-COMP-THERM-062-013	0.98% Boron Steel plates, 6 mm, dist. 0	2.6	-	
423	LEU-COMP-THERM-062-014	0.98% Boron Steel plates, 6 mm, dist. 0.5	2.6	-	
424	LEU-COMP-THERM-062-015	0.98% Boron Steel plates, 6 mm, dist. 1	2.6	-	
425	LEU-COMP-THERM-065-001	No Boron Steel plates	2.6	-	
426	LEU-COMP-THERM-065-002	0% Boron Steel plates, dist. 0	2.6	-	
427	LEU-COMP-THERM-065-003	0.67% Boron Steel plates, dist. 0	2.6	-	
428	LEU-COMP-THERM-065-004	0.98% Boron Steel plates, dist. 0	2.6	-	
429	LEU-COMP-THERM-065-005	No Boron Steel plates	2.6	-	
430	LEU-COMP-THERM-065-006	0% Boron Steel plates, dist. 0	2.6	-	
431	LEU-COMP-THERM-065-007	0% Boron Steel plates, dist. 0.5	2.6	-	
432	LEU-COMP-THERM-065-008	0% Boron Steel plates, dist. 0	2.6	-	
433	LEU-COMP-THERM-065-009	0% Boron Steel plates, dist. 0.5	2.6	-	
434	LEU-COMP-THERM-065-010	0.67% Boron Steel plates, dist. 0	2.6	-	
435	LEU-COMP-THERM-065-011	0.67% Boron Steel plates, dist. 0.5	2.6	-	

Case	Reference	Identification	U, wt%	Pu, wt%
436	LEU-COMP-THERM-065-012	0.67% Boron Steel plates, dist. 0	2.6	-
437	LEU-COMP-THERM-065-013	0.67% Boron Steel plates, dist. 0.5	2.6	-
438	LEU-COMP-THERM-065-014	0.98% Boron Steel plates, dist. 0	2.6	-
439	LEU-COMP-THERM-065-015	0.98% Boron Steel plates, dist. 0.5	2.6	-
440	LEU-COMP-THERM-065-016	0.98% Boron Steel plates, dist. 0	2.6	-
441	LEU-COMP-THERM-065-017	0.98% Boron Steel plates, dist. 0.5	2.6	-
442	LEU-COMP-THERM-081-001	Otto Hahn, ZrB_2 and B_4C rods	5.423	-
443	LEU-COMP-THERM-082-001	IPEN/MB-01 (580 pins)	4.3486	-
444	LEU-COMP-THERM-082-002	IPEN/MB-01 (560 pins)	4.3486	-
445	LEU-COMP-THERM-082-003	670 pins, Al_2O_3-B_4C rods	4.3486	-
446	LEU-COMP-THERM-082-004	672 pins, Al_2O_3-B_4C rods	4.3486	-
447	LEU-COMP-THERM-082-005	668 pins, Al_2O_3-B_4C rods	4.3486	-
448	LEU-COMP-THERM-082-006	668 pins, Al_2O_3-B_4C rods	4.3486	-
449	LEU-COMP-THERM-090-001	664 pins, 16 steel rods	4.3486	-
450	LEU-COMP-THERM-090-002	662 pins, 18 steel rods	4.3486	-
451	LEU-COMP-THERM-090-003	658 pins, 14 steel rods	4.3486	-
452	LEU-COMP-THERM-090-004	660 pins, 12 steel rods	4.3486	-
453	LEU-COMP-THERM-090-005	660 pins, 12 steel rods	4.3486	-
454	LEU-COMP-THERM-090-006	661 pins, 17 steel rods	4.3486	-
455	LEU-COMP-THERM-090-007	662 pins, 16 steel rods	4.3486	-
456	LEU-COMP-THERM-090-008	634 pins, 12 steel rods	4.3486	-
457	LEU-COMP-THERM-090-009	620 pins, 26 steel rods	4.3486	-
458	LEU-COMP-THERM-091-001	668 pins, 0 steel rods, 4 Gd_2O_3 rods	4.3486	-
459	LEU-COMP-THERM-091-002	648 pins, 0 steel rods, 8 Gd_2O_3 rods	4.3486	-
460	LEU-COMP-THERM-091-003	672 pins, 0 steel rods, 4 Gd_2O_3 rods	4.3486	-
461	LEU-COMP-THERM-091-004	646 pins, 4 steel rods, 4 Gd_2O_3 rods	4.3486	-
462	LEU-COMP-THERM-091-005	656 pins, 4 steel rods, 4 Gd_2O_3 rods	4.3486	-
463	LEU-COMP-THERM-091-006	664 pins, 4 steel rods, 2 Gd_2O_3 rods	4.3486	-
464	LEU-COMP-THERM-091-007	670 pins, 2 steel rods, 2 Gd_2O_3 rods	4.3486	-
465	LEU-COMP-THERM-091-008	664 pins, 2 steel rods, 2 Gd_2O_3 rods	4.3486	-
466	LEU-COMP-THERM-091-009	656 pins, 0 steel rods, 2 Gd_2O_3 rods	4.3486	-
467	MIX-COMP-THERM-004-001	23x23, 1.825 cm pitch	0.72	3.01
468	MIX-COMP-THERM-004-002	23x23, 1.825 cm pitch	0.72	3.01
469	MIX-COMP-THERM-004-003	23x23, 1.825 cm pitch	0.72	3.01
470	MIX-COMP-THERM-004-004	21x21, 1.956 cm pitch	0.72	3.01
471	MIX-COMP-THERM-004-005	21x21, 1.956 cm pitch	0.72	3.01
472	MIX-COMP-THERM-004-006	21x21, 1.956 cm pitch	0.72	3.01
473	MIX-COMP-THERM-004-007	20x20, 2.225 cm pitch	0.72	3.01

Case	Reference	Identification	U, wt%	Pu, wt%
474	MIX-COMP-THERM-004-008	20x20, 2.225 cm pitch	0.72	3.01
475	MIX-COMP-THERM-004-009	20x20, 2.225 cm pitch	0.72	3.01
476	MIX-COMP-THERM-004-010	21x21, 2.474 cm pitch	0.72	3.01
477	MIX-COMP-THERM-004-011	21x21, 2.474 cm pitch	0.72	3.01
478	MIX-COMP-THERM-006-007	8 wt% 240Pu 1.05” pitch, Al Rods	0.72	2.0
479	MIX-COMP-THERM-006-013	8 wt% 240Pu 1.05” pitch, B4 Rods	0.72	2.0
480	MIX-COMP-THERM-006-014	8 wt% 240Pu 1.05” pitch, B3 Rods	0.72	2.0
481	MIX-COMP-THERM-006-015	8 wt% 240Pu 1.05” pitch, B2 Rods	0.72	2.0
482	MIX-COMP-THERM-006-016	8 wt% 240Pu 1.05” pitch, B1 Rods	0.72	2.0
483	MIX-COMP-THERM-006-017	8 wt% 240Pu 1.05” pitch, Al+Cd Rods	0.72	2.0
484	MIX-COMP-THERM-006-023	8 wt% 240Pu 1.05” pitch, B4+Cd Rods	0.72	2.0
485	MIX-COMP-THERM-006-024	8 wt% 240Pu 1.05” pitch, B3+Cd Rods	0.72	2.0
486	MIX-COMP-THERM-006-025	8 wt% 240Pu 1.05” pitch, B2+Cd Rods	0.72	2.0
487	MIX-COMP-THERM-006-026	8 wt% 240Pu 1.05” pitch, B1+Cd Rods	0.72	2.0
488	MIX-COMP-THERM-006-027	8 wt% 240Pu 1.05” pitch, Air+Cd Rods	0.72	2.0
489	MIX-COMP-THERM-006-028	8 wt% 240Pu 1.05” pitch, H2O+Cd Rods	0.72	2.0
490	MIX-COMP-THERM-006-029	8 wt% 240Pu 1.32” pitch, Al Rods	0.72	2.0
491	MIX-COMP-THERM-006-035	8 wt% 240Pu 1.32” pitch, B4 Rods	0.72	2.0
492	MIX-COMP-THERM-006-036	8 wt% 240Pu 1.32” pitch, B3 Rods	0.72	2.0
493	MIX-COMP-THERM-006-037	8 wt% 240Pu 1.32” pitch, B2 Rods	0.72	2.0
494	MIX-COMP-THERM-006-038	8 wt% 240Pu 1.32” pitch, B1 Rods	0.72	2.0
495	MIX-COMP-THERM-006-039	8 wt% 240Pu 1.32” pitch, Al+Cd Rods	0.72	2.0
496	MIX-COMP-THERM-006-045	8 wt% 240Pu 1.32” pitch, B4+Cd Rods	0.72	2.0
497	MIX-COMP-THERM-006-046	8 wt% 240Pu 1.32” pitch, B3+Cd Rods	0.72	2.0
498	MIX-COMP-THERM-006-047	8 wt% 240Pu 1.32” pitch, B2+Cd Rods	0.72	2.0
499	MIX-COMP-THERM-006-048	8 wt% 240Pu 1.32” pitch, B1+Cd Rods	0.72	2.0
500	MIX-COMP-THERM-006-049	8 wt% 240Pu 1.32” pitch, Air+Cd Rods	0.72	2.0
501	MIX-COMP-THERM-006-050	8 wt% 240Pu 1.32” pitch, H2O+Cd Rods	0.72	2.0
502	MIX-COMP-THERM-007-005	16 wt% 240Pu 1.386” pitch	0.72	2.0
503	MIX-COMP-THERM-007-006	16 wt% 240Pu 1.05” pitch, Al Rods	0.72	2.0
504	MIX-COMP-THERM-007-012	16 wt% 240Pu 1.05” pitch, B4 Rods	0.72	2.0
505	MIX-COMP-THERM-007-013	16 wt% 240Pu 1.05” pitch, B3 Rods	0.72	2.0
506	MIX-COMP-THERM-007-014	16 wt% 240Pu 1.05” pitch, B2 Rods	0.72	2.0
507	MIX-COMP-THERM-007-015	16 wt% 240Pu 1.05” pitch, B1 Rods	0.72	2.0
508	MIX-COMP-THERM-007-016	16 wt% 240Pu 1.05” pitch, Al+Cd Rods	0.72	2.0
509	MIX-COMP-THERM-007-022	16 wt% 240Pu 1.05” pitch, B4+Cd Rods	0.72	2.0
510	MIX-COMP-THERM-007-023	16 wt% 240Pu 1.05” pitch, B3+Cd Rods	0.72	2.0
511	MIX-COMP-THERM-007-024	16 wt% 240Pu 1.05” pitch, B2+Cd Rods	0.72	2.0
512	MIX-COMP-THERM-007-025	16 wt% 240Pu 1.05” pitch, B1+Cd Rods	0.72	2.0
513	MIX-COMP-THERM-007-026	16 wt% 240Pu 1.05” pitch, Air+Cd Rods	0.72	2.0

Case	Reference	Identification	U, wt%	Pu, wt%
514	MIX-COMP-THERM-007-027	16 wt% 240Pu 1.05” pitch, H2O+Cd Rods	0.72	2.0
515	MIX-COMP-THERM-008-007	24 wt% 240Pu 1.05” pitch, Al Rods	0.72	2.0
516	MIX-COMP-THERM-008-013	24 wt% 240Pu 1.05” pitch, B4 Rods	0.72	2.0
517	MIX-COMP-THERM-008-014	24 wt% 240Pu 1.05” pitch, B3 Rods	0.72	2.0
518	MIX-COMP-THERM-008-015	24 wt% 240Pu 1.05” pitch, B2 Rods	0.72	2.0
519	MIX-COMP-THERM-008-016	24 wt% 240Pu 1.05” pitch, B1 Rods	0.72	2.0
520	MIX-COMP-THERM-008-017	24 wt% 240Pu 1.05” pitch, Al+Cd Rods	0.72	2.0
521	MIX-COMP-THERM-008-023	24 wt% 240Pu 1.05” pitch, B4+Cd Rods	0.72	2.0
522	MIX-COMP-THERM-008-024	24 wt% 240Pu 1.05” pitch, B3+Cd Rods	0.72	2.0
523	MIX-COMP-THERM-008-025	24 wt% 240Pu 1.05” pitch, B2+Cd Rods	0.72	2.0
524	MIX-COMP-THERM-008-026	24 wt% 240Pu 1.05” pitch, B1+Cd Rods	0.72	2.0
525	MIX-COMP-THERM-008-027	24 wt% 240Pu 1.05” pitch, Air+Cd Rods	0.72	2.0
526	MIX-COMP-THERM-008-028	24 wt% 240Pu 1.05” pitch, H2O+Cd Rods	0.72	2.0
527	MIX-COMP-THERM-009-001	8 wt% 240Pu 0.55” pitch	0.16	1.5
528	MIX-COMP-THERM-009-002	8 wt% 240Pu 0.60” pitch	0.16	1.5
529	MIX-COMP-THERM-009-003	8 wt% 240Pu 0.71” pitch	0.16	1.5
530	MIX-COMP-THERM-009-004	8 wt% 240Pu 0.80” pitch	0.16	1.5
531	MIX-COMP-THERM-009-005	8 wt% 240Pu 0.90” pitch	0.16	1.5
532	MIX-COMP-THERM-009-006	8 wt% 240Pu 0.93” pitch	0.16	1.5

Appendix C

Benchmark of MCNP5-1.51 with ENDF/B-V

(total number of pages: 27 including this page)

C.1 Introduction

This Appendix presents the analysis of the validation results for MCNP5-1.51 code and includes the results of the calculations, normality test, the detailed statistical trending analysis, calculation bias and bias uncertainty for each distinct area of applicability of the parameters of interest.

C.2 Computer Code Parameter Data

The computer code MCNP5-1.51 [C.1] is the continuous energy Monte Carlo codes and treats an arbitrary three-dimensional configuration of materials in geometric cells bounded by first- and second-degree surfaces and fourth-degree elliptical tori. Thermal neutrons are described by both the free gas and S(α,β) models. All calculations were performed using the default data libraries provided with the code: the default continuous energy neutron transport data predominantly based on ENDF/B-V. The list of ZAIDs that were used in the analysis is presented in Table C.2-1. The criticality source card was set to accumulate a total of 1.8 million neutron histories for every individual run. The neutrons start from an arbitrary distribution, causing a generally very large variance of results from the first cycles in comparison with the following cycles. Therefore, the results from the first 50 cycles were skipped when calculating the average k_{eff}. The calculated k_{eff} values have associated uncertainties due to the statistical nature of the Monte Carlo codes.

C.3 Analysis of MCNP5-1.51 Validation Results

C.3.1. Calculational Results

The calculation results for the 156 HTC critical experiments and for the 135 selected critical experiments described in Appendix B are presented and discussed in this section. The calculation results are summarized by grouping the experiments in terms of the categories as set forth in Appendix B. Calculation results, including $k_{eff\text{-}I}$, $\sigma_{calc\text{-}i}$ and EALF, measurement uncertainties (σ_{exp}) and the calculation and measurement combined uncertainty (σ_i) are shown in Table C.3-1 through Table C.3-5.

Figure C.3-1 and C.3-2 are histograms showing the frequency of calculated k_{eff} and EALF for all 291 benchmarks. The nominal calculated k_{eff} values range from [redacted]. The EALF results values show a range between [redacted].

Descriptive statistics for the different group of experiments is summarized in Table C.3-6.

C.3.2. Normality Test

In order to assess the normality assumption, Shapiro and Wilk [5] test has been used for groups with fewer than 50 samples while the Pearson's chi-square (χ^2) test [4] has been used for samples larger than 20 samples. The tests are applied to the group of experiments in terms of the categories as set forth in Appendix B.

For the Shapiro and Wilk test, Table C.3-7 shows the computed *Wtest* value, and *W* value that can be obtained for the number of experiments from [5] to accept the normality hypothesis. If W

is less than the test statistic, *Wtest*, then the data is considered normally distributed. For the χ^2 test, it is concluded normal for $\chi^2 \leq n$, where n is a number of bins for the group of experiments. The probability $P_d(\tilde{\chi}^2 \geq \tilde{\chi}_0{}^2)$ of obtaining a value of $\tilde{\chi}^2 \geq \tilde{\chi}_0{}^2$ in an experiment with d degrees of freedom to confirm quantitatively that the agreement is satisfactory was taken or interpolated, if necessary, from Appendix D in Reference [4]. Thus, if $P_d(\tilde{\chi}^2 \geq \tilde{\chi}_0{}^2)$ is large, the obtained and expected distributions are consistent; if it is small, they probably disagree. In particular, if $P_d(\tilde{\chi}^2 \geq \tilde{\chi}_0{}^2)$ is less than 5%, we say that the disagreement is significant and reject the assumed distributions at the 5% level. If it is less than 1%, the disagreement is called highly significant, and we reject the assumed distributions at the 1% level.

As it is shown in Table C.3-7, all cases except Phase 1 test normal. Nevertheless, the group with all 291 experiments shows an agreement with the assumed normal distribution with the probability P_d = 7.36%.

C.3.3. Trending Analysis

Trends are determined through the use of regression fits to the calculated results. The equations used to identify trends are given below:

$$Y(x) = a + bx \tag{7-1}$$

$$a = \frac{1}{\Delta}\left(\sum \frac{x_i^2}{\sigma_i^2}\sum \frac{y_i}{\sigma_i^2} - \sum \frac{x_i}{\sigma_i^2}\sum \frac{x_i y_i}{\sigma_i^2}\right) \tag{7-2}$$

$$b = \frac{1}{\Delta}\left(\sum \frac{1}{\sigma_i^2}\sum \frac{x_i y_i}{\sigma_i^2} - \sum \frac{x_i}{\sigma_i^2}\sum \frac{y_i}{\sigma_i^2}\right) \tag{7-3}$$

$$\Delta = \sum \frac{1}{\sigma_i^2}\sum \frac{x_i^2}{\sigma_i^2} - \left(\sum \frac{x_i}{\sigma_i^2}\right)^2 \tag{7-4}$$

The squared term of the linear correlation factor r defined below (from Reference [5]) is used to quantitatively measure the degree to which a linear relationship exist between two variables.

$$r = \frac{\sum \frac{1}{\sigma_i^2}(x_i - \bar{x})(y_i - \bar{y})}{\sqrt{\left[\sum \frac{1}{\sigma_i^2}(x_i - \bar{x})^2\right]\left[\sum \frac{1}{\sigma_i^2}(y_i - \bar{y})^2\right]}} \tag{7-5}$$

The closer r^2 approaches the value of 1, the better the fit of the data to the linear equation. A more quantitative measure of the fit can be found by using Appendix C in Reference [4]. The interpolation was applied, if necessary. For any given observed value r_0, $P_N(|r| \geq |r_0|)$ is the probability that N measurements of two uncorrelated variables would give a coefficient r as large as r_0. Thus, if we obtain a coefficient r_0 for which $P_N(|r| \geq |r_0|)$ is small, it is correspondingly unlikely that our variables are uncorrelated; that is, a correlation indicated. In particular, if

$P_N(|r| \geq |r_0|) \leq 5\%$, the correlation is called significant; if it is less than 1%, the correlation is called highly significant.

The validation results are analyzed by grouping the experiments in terms of the categories as set forth in Appendix B. Independent variables used in the trending analysis by group, correlation coefficients and trending analysis results are summarized in Table C.3-8. The linear regression equations for the independent parameter with the significant correlation of k_{eff} were presented in Table C.3-8.

C.3.4. Bias and Bias Uncertainty

In this section, benchmark results are analyzed using the statistical method described in section 2.2.

The first step is to evaluate whether the four HTC phases and selected experiments, should be reduced to a single set. The mean k_{eff} of the Phase 1 data set is [redacted], the mean k_{eff} of the Phase 2 data set is [redacted], the mean k_{eff} of the Phase 3 data set is [redacted], the mean k_{eff} of the Phase 4 data set is [redacted] and the mean k_{eff} of the selected experiments data is [redacted]. The maximum difference between the means is just [redacted] which is less than the uncertainty. These sets are water moderated uranium or mixed plutonium-uranium dioxide lattices. The addition of a absorber rods, separator plates or reflector plates is not introducing a significant increase in the ability to calculate k_{eff}. The Phase 1 through Phase 4 sets and the selected experiments are considered one large set of 291 experiments from now on.

The analysis of the correlation coefficient in Table C.3-8 (combined set) and the plot of data trend (Figure C.3-3) show that there is a significant trend a function of the rod pitch. This is discussed in the Section C.3.5.2.

The total bias (systematic error or mean of the deviation from a keff of exactly 1.000) of the MCNP5-1.51 code is shown in the table below

Calculational Bias of the MCNP5-1.51 code		
Description	Total Bias	Bias Uncertainty
HTC and Selected Experiments	[redacted]	[redacted]

C.3.5. Applicability of MCNP5-1.51 Validation Results

This subsection contains a more detailed evaluation of the set of critical experiments. Regarding the selected experiments, the following subjects are discussed:

- Neutron absorber and neutron reflector materials
- Fuel rod pitch trend
- Neutron absorber geometry

- Fuel burnup
- Unborated and borated water.

The general focus is to justify that using the full set of critical experiments is appropriate. In some cases, subsets of full set of experiments are established. For those subsets, statistical evaluations are performed to determine bias, bias uncertainty, normality and trends. Trends are evaluated for fuel rod outer diameter, fuel rod pitch, fuel density, and EALF.

C.3.5.1. Neutron Absorber and Neutron Reflector Materials

The HTC and Selected Experiments consider the following neutron absorbers and reflectors:

- Absorbers
    - Boron, in the form of soluble boron in the water, boron in solid form (B_4C), and boron in borated steel
    - Soluble gadolinium in water
    - Cadmium
- Reflectors
    - Steel
    - Lead
    - Water

Some typical configurations do not contain gadolinium or cadmium neutron absorbers or lead reflectors. To verify that including those materials does not have a significant effect on the results of the benchmarking analyses, a subset without those experiments containing those materials was analyzed. The comparison with the full set is presented in Table C.3-9 and shows no significant differences when those materials are excluded. However, in both cases, a significant trend is observed, as a function of the rod pitch in the experiment. This is discussed in the next section.

C.3.5.2. Fuel Rod Pitch Trend

To better understand the observed rod pitch trend, the results for all 291 experiments are shown in Figure C.3-4 as a function of rod pitch. It appears that the trend is due to the experiments at higher rod pitch value (> 2 cm), which consistently show k_{eff} values well above 1.0. To evaluate the impact of those experiments at larger rod pitches, the Table C.3-10 shows a comparison of results with and without those experiments. When results above 2 cm rod pitch are excluded, a slightly higher absolute bias is observed, in this case with a lower uncertainty, and no significant rod pitch trend. Based on those results it could be concluded that the trend is only caused by the experiments at higher rod pitch values. To ensure that a potential trend would not be ignored, all following evaluations are performed for the two conditions used above, i.e. for all rod pitch values, and for experiments with rod pitch values limited to no more than 2 cm.

C.3.5.3. Absorber Geometry

The criticality experiments analyzed in this report include experiments with Boron in the form of plates, absorber rods and soluble boron in water. No trend relating to these experiments is observed.

C.3.5.4. Fuel Burnup

The full set of critical experiments contains experiments with fresh UO_2 fuel, with simulated spent fuel (37.5 GWd/MTU), and MOX fuel with Pu content between 2 and 20%, which is even higher than typically found in spent fuel. The experiments are therefore reasonably representative of burned fuel at different burnup levels. To verify that the experiments cover the burnup range sufficiently, the experiments are subdivided into fresh UO_2 fuel, HTC experiments and MOX experiments, and compared to the results of the entire set. The comparison is shown in Table C.3-11. The comparison shows no significant differences between the entire set and the UO_2 and HTC subsets, but for MOX the bias is now positive (i.e. truncated bias of 0.0), with a larger uncertainty, and some trends. However, this is based on relatively small sets of experiments. Bias values are comparable between sets with and without rod pitch values above 2 cm, with a maximum absolute value of [redacted].

C.3.5.5. Unborated and Borated Water

The full set of critical experiments contains both experiments with and without soluble boron. The entire set of analyses shows no significant trend when analyzed as a function of the soluble boron level. Nevertheless, sets with and without soluble boron are analyzed and compared to the full set that contains all experiments. The results are shown in Table C.3-12. Similar to the previous subsection, the comparison shows no significant differences between those subsets. Bias values are comparable between sets with and without rod pitch values above 2 cm, with a maximum absolute value of [redacted].

C.4 Summary

A set of 291 critical experiments has been selected and has been used for the validation of the Holtec International criticality safety methodology. The similarity between the chosen experiments and the actual systems has been based on a set of screening criteria as is stated in the NUREG/CR-6698 [5]. Experiments have been categorized by common features as Phase 1 through Phase 4 and selected experiments and parameterized by key variables such as lattice pitch / assembly pitch, absorber solution concentration, number of fuel rods, rod outer diameter, fuel density, screen array distance, fuel enrichment and EALF. Benchmark calculations have been performed using the Monte Carlo code MCNP5-1.51. It was determined that Phase 1 through Phase 4 and selected experiments are in sufficient agreement that this sets are lumped together as a single set of 291 experiments. The bias and bias uncertainty are presented in section C.3.4. The applicability of validation results is considered in section C.3.5.

The range of key parameters for the design application, benchmarks and validated AOA are summarized in Table C.3-13. A point by point comparison between design application and benchmarks shows that the experimental range covers all the parameters. The soluble boron

concentration is extrapolated generously since ^{10}B is a 1/v absorber (as permitted on Table 2.3 of [5]).

As for the fuel density, Table 2.3 of Reference [5] states there is "no requirement" and that "experiments should be as close to the desired concentration as possible". Since the experiment fuel density is 9.2 – 10.4 g/cm^3 and the design application one is around 10.0 – 10.7 g/cm^3, it is considered that the values are very close so the validated AOA covers the design application range.

The fuel enrichment can be up to 5%. The experiments used go up to 5.74 wt% ^{235}U. Therefore, it is considered that the validated AOA covers the design application range.

C.5 References

[C.1] "MCNP - A General Monte Carlo N-Particle Transport Code, Version 5"; Los Alamos National Laboratory, LA-UR-03-1987 (Revised 2/1/2008).

Table C.2-1 MCNP5-1.51 ZAIDs Used for Each Nuclide

Nuclide	ZAID
^{1}H	1001.50c
^{10}B	5010.50c
^{11}B	5011.55c
C	6000.50c
^{14}N	7014.50c
^{16}O	8016.50c
^{23}Na	11023.51c
Mg	12000.50c
^{27}Al	13027.50c
Si	14000.51c
^{31}P	15031.50c
^{32}S	16032.51c
Ca	20000.51c
Ti	22000.50c
Cr	24000.50c
^{55}Mn	25055.51c
Fe	26000.55c
^{59}Co	27059.50c
Ni	28000.50c
Cu	29000.50c
Zn	30000.40c
Zr	40000.56c
Mo	42000.50c
Cd	48000.50c
Sn	50000.40c
Gd	64000.35c
Pb	82000.50c
^{234}U	92234.50c
^{235}U	92235.50c
^{236}U	92236.50c
^{238}U	92238.50c
^{238}Pu	94238.50c
^{239}Pu	94239.50c
^{240}Pu	94240.50c
^{241}Pu	94241.50c
^{242}Pu	94242.50c
^{241}Am	95241.50c

Table C.3-1 The MCNP5-1.51 Calculational Results and Measurements Uncertainties for Phase 1 Critical Experiments: Water-Moderated and Reflected Arrays

Case	Evaluation Identification	File-name	k_{eff-i}	$\pm \sigma_{calc-i}$	$\pm \sigma_{exp}$	$\pm \sigma_i$	EALF (eV)
1	MIX-COMP-THERM-HTC-001	[redacted]	[redacted]	[redacted]	[redacted]	[redacted]	[redacted]
2	MIX-COMP-THERM-HTC-002	[redacted]	[redacted]	[redacted]	[redacted]	[redacted]	[redacted]
3	MIX-COMP-THERM-HTC-003	[redacted]	[redacted]	[redacted]	[redacted]	[redacted]	[redacted]
4	MIX-COMP-THERM-HTC-004	[redacted]	[redacted]	[redacted]	[redacted]	[redacted]	[redacted]
5	MIX-COMP-THERM-HTC-005	[redacted]	[redacted]	[redacted]	[redacted]	[redacted]	[redacted]
6	MIX-COMP-THERM-HTC-006	[redacted]	[redacted]	[redacted]	[redacted]	[redacted]	[redacted]
7	MIX-COMP-THERM-HTC-007	[redacted]	[redacted]	[redacted]	[redacted]	[redacted]	[redacted]
8	MIX-COMP-THERM-HTC-008	[redacted]	[redacted]	[redacted]	[redacted]	[redacted]	[redacted]
9	MIX-COMP-THERM-HTC-009	[redacted]	[redacted]	[redacted]	[redacted]	[redacted]	[redacted]
10	MIX-COMP-THERM-HTC-010	[redacted]	[redacted]	[redacted]	[redacted]	[redacted]	[redacted]
11	MIX-COMP-THERM-HTC-011	[redacted]	[redacted]	[redacted]	[redacted]	[redacted]	[redacted]
12	MIX-COMP-THERM-HTC-012	[redacted]	[redacted]	[redacted]	[redacted]	[redacted]	[redacted]
13	MIX-COMP-THERM-HTC-013	[redacted]	[redacted]	[redacted]	[redacted]	[redacted]	[redacted]
14	MIX-COMP-THERM-HTC-014	[redacted]	[redacted]	[redacted]	[redacted]	[redacted]	[redacted]
15	MIX-COMP-THERM-HTC-015	[redacted]	[redacted]	[redacted]	[redacted]	[redacted]	[redacted]
16	MIX-COMP-THERM-HTC-016	[redacted]	[redacted]	[redacted]	[redacted]	[redacted]	[redacted]
17	MIX-COMP-THERM-HTC-017	[redacted]	[redacted]	[redacted]	[redacted]	[redacted]	[redacted]
18	MIX-COMP-THERM-HTC-018	[redacted]	[redacted]	[redacted]	[redacted]	[redacted]	[redacted]

Table C.3-2 The MCNP5-1.51 Calculational Results and Measurements Uncertainties for Phase 2 Critical Experiments: Reflected Simple Arrays Moderated by Poisoned Water with Gadolinium or Boron

Case	Evaluation Identification	File-name	k_{eff-i}	$\pm \sigma_{calc-i}$	$\pm \sigma_{exp}$	$\pm \sigma_i$	EALF (eV)
19	MIX-COMP-THERM-HTC-019	[redacted]	[redacted]	[redacted]	[redacted]	[redacted]	[redacted]
20	MIX-COMP-THERM-HTC-020	[redacted]	[redacted]	[redacted]	[redacted]	[redacted]	[redacted]
21	MIX-COMP-THERM-HTC-021	[redacted]	[redacted]	[redacted]	[redacted]	[redacted]	[redacted]
22	MIX-COMP-THERM-HTC-022	[redacted]	[redacted]	[redacted]	[redacted]	[redacted]	[redacted]
23	MIX-COMP-THERM-HTC-023	[redacted]	[redacted]	[redacted]	[redacted]	[redacted]	[redacted]
24	MIX-COMP-THERM-HTC-024	[redacted]	[redacted]	[redacted]	[redacted]	[redacted]	[redacted]
25	MIX-COMP-THERM-HTC-025	[redacted]	[redacted]	[redacted]	[redacted]	[redacted]	[redacted]
26	MIX-COMP-THERM-HTC-026	[redacted]	[redacted]	[redacted]	[redacted]	[redacted]	[redacted]
27	MIX-COMP-THERM-HTC-027	[redacted]	[redacted]	[redacted]	[redacted]	[redacted]	[redacted]
28	MIX-COMP-THERM-HTC-028	[redacted]	[redacted]	[redacted]	[redacted]	[redacted]	[redacted]
29	MIX-COMP-THERM-HTC-029	[redacted]	[redacted]	[redacted]	[redacted]	[redacted]	[redacted]
30	MIX-COMP-THERM-HTC-030	[redacted]	[redacted]	[redacted]	[redacted]	[redacted]	[redacted]
31	MIX-COMP-THERM-HTC-031	[redacted]	[redacted]	[redacted]	[redacted]	[redacted]	[redacted]
32	MIX-COMP-THERM-HTC-032	[redacted]	[redacted]	[redacted]	[redacted]	[redacted]	[redacted]
33	MIX-COMP-THERM-HTC-033	[redacted]	[redacted]	[redacted]	[redacted]	[redacted]	[redacted]
34	MIX-COMP-THERM-HTC-034	[redacted]	[redacted]	[redacted]	[redacted]	[redacted]	[redacted]
35	MIX-COMP-THERM-HTC-035	[redacted]	[redacted]	[redacted]	[redacted]	[redacted]	[redacted]
36	MIX-COMP-THERM-HTC-036	[redacted]	[redacted]	[redacted]	[redacted]	[redacted]	[redacted]
37	MIX-COMP-THERM-HTC-037	[redacted]	[redacted]	[redacted]	[redacted]	[redacted]	[redacted]
38	MIX-COMP-THERM-HTC-038	[redacted]	[redacted]	[redacted]	[redacted]	[redacted]	[redacted]
39	MIX-COMP-THERM-HTC-039	[redacted]	[redacted]	[redacted]	[redacted]	[redacted]	[redacted]
40	MIX-COMP-THERM-HTC-040	[redacted]	[redacted]	[redacted]	[redacted]	[redacted]	[redacted]
41	MIX-COMP-THERM-HTC-041	[redacted]	[redacted]	[redacted]	[redacted]	[redacted]	[redacted]
42	MIX-COMP-THERM-HTC-042	[redacted]	[redacted]	[redacted]	[redacted]	[redacted]	[redacted]
43	MIX-COMP-THERM-HTC-043	[redacted]	[redacted]	[redacted]	[redacted]	[redacted]	[redacted]
44	MIX-COMP-THERM-HTC-044	[redacted]	[redacted]	[redacted]	[redacted]	[redacted]	[redacted]
45	MIX-COMP-THERM-HTC-045	[redacted]	[redacted]	[redacted]	[redacted]	[redacted]	[redacted]
46	MIX-COMP-THERM-HTC-046	[redacted]	[redacted]	[redacted]	[redacted]	[redacted]	[redacted]
47	MIX-COMP-THERM-HTC-047	[redacted]	[redacted]	[redacted]	[redacted]	[redacted]	[redacted]
48	MIX-COMP-THERM-HTC-048	[redacted]	[redacted]	[redacted]	[redacted]	[redacted]	[redacted]
49	MIX-COMP-THERM-HTC-049	[redacted]	[redacted]	[redacted]	[redacted]	[redacted]	[redacted]
50	MIX-COMP-THERM-HTC-050	[redacted]	[redacted]	[redacted]	[redacted]	[redacted]	[redacted]
51	MIX-COMP-THERM-HTC-051	[redacted]	[redacted]	[redacted]	[redacted]	[redacted]	[redacted]
52	MIX-COMP-THERM-HTC-052	[redacted]	[redacted]	[redacted]	[redacted]	[redacted]	[redacted]
53	MIX-COMP-THERM-HTC-053	[redacted]	[redacted]	[redacted]	[redacted]	[redacted]	[redacted]
54	MIX-COMP-THERM-HTC-054	[redacted]	[redacted]	[redacted]	[redacted]	[redacted]	[redacted]
55	MIX-COMP-THERM-HTC-055	[redacted]	[redacted]	[redacted]	[redacted]	[redacted]	[redacted]

Case	Evaluation Identification	File-name	k_{eff-i}	$\pm \sigma_{calc-i}$	$\pm \sigma_{exp}$	$\pm \sigma_i$	EALF (eV)
56	MIX-COMP-THERM-HTC-056	[redacted]	[redacted]	[redacted]	[redacted]	[redacted]	[redacted]
57	MIX-COMP-THERM-HTC-057	[redacted]	[redacted]	[redacted]	[redacted]	[redacted]	[redacted]
58	MIX-COMP-THERM-HTC-058	[redacted]	[redacted]	[redacted]	[redacted]	[redacted]	[redacted]
59	MIX-COMP-THERM-HTC-059	[redacted]	[redacted]	[redacted]	[redacted]	[redacted]	[redacted]

Table C.3-3 The MCNP5-1.51 Calculational Results and Measurements Uncertainties for Phase 3 Critical Experiments: Pool Storage

Case	Evaluation Identification	File-name	k_{eff-i}	$\pm \sigma_{calc-i}$	$\pm \sigma_{exp}$	$\pm \sigma_i$	EALF (eV)
60	MIX-COMP-THERM-HTC-060	[redacted]	[redacted]	[redacted]	[redacted]	[redacted]	[redacted]
61	MIX-COMP-THERM-HTC-061	[redacted]	[redacted]	[redacted]	[redacted]	[redacted]	[redacted]
62	MIX-COMP-THERM-HTC-062	[redacted]	[redacted]	[redacted]	[redacted]	[redacted]	[redacted]
63	MIX-COMP-THERM-HTC-063	[redacted]	[redacted]	[redacted]	[redacted]	[redacted]	[redacted]
64	MIX-COMP-THERM-HTC-064	[redacted]	[redacted]	[redacted]	[redacted]	[redacted]	[redacted]
65	MIX-COMP-THERM-HTC-065	[redacted]	[redacted]	[redacted]	[redacted]	[redacted]	[redacted]
66	MIX-COMP-THERM-HTC-066	[redacted]	[redacted]	[redacted]	[redacted]	[redacted]	[redacted]
67	MIX-COMP-THERM-HTC-067	[redacted]	[redacted]	[redacted]	[redacted]	[redacted]	[redacted]
68	MIX-COMP-THERM-HTC-068	[redacted]	[redacted]	[redacted]	[redacted]	[redacted]	[redacted]
69	MIX-COMP-THERM-HTC-069	[redacted]	[redacted]	[redacted]	[redacted]	[redacted]	[redacted]
70	MIX-COMP-THERM-HTC-070	[redacted]	[redacted]	[redacted]	[redacted]	[redacted]	[redacted]
71	MIX-COMP-THERM-HTC-071	[redacted]	[redacted]	[redacted]	[redacted]	[redacted]	[redacted]
72	MIX-COMP-THERM-HTC-072	[redacted]	[redacted]	[redacted]	[redacted]	[redacted]	[redacted]
73	MIX-COMP-THERM-HTC-073	[redacted]	[redacted]	[redacted]	[redacted]	[redacted]	[redacted]
74	MIX-COMP-THERM-HTC-074	[redacted]	[redacted]	[redacted]	[redacted]	[redacted]	[redacted]
75	MIX-COMP-THERM-HTC-075	[redacted]	[redacted]	[redacted]	[redacted]	[redacted]	[redacted]
76	MIX-COMP-THERM-HTC-076	[redacted]	[redacted]	[redacted]	[redacted]	[redacted]	[redacted]
77	MIX-COMP-THERM-HTC-077	[redacted]	[redacted]	[redacted]	[redacted]	[redacted]	[redacted]
78	MIX-COMP-THERM-HTC-078	[redacted]	[redacted]	[redacted]	[redacted]	[redacted]	[redacted]
79	MIX-COMP-THERM-HTC-079	[redacted]	[redacted]	[redacted]	[redacted]	[redacted]	[redacted]
80	MIX-COMP-THERM-HTC-080	[redacted]	[redacted]	[redacted]	[redacted]	[redacted]	[redacted]
81	MIX-COMP-THERM-HTC-081	[redacted]	[redacted]	[redacted]	[redacted]	[redacted]	[redacted]
82	MIX-COMP-THERM-HTC-082	[redacted]	[redacted]	[redacted]	[redacted]	[redacted]	[redacted]
83	MIX-COMP-THERM-HTC-083	[redacted]	[redacted]	[redacted]	[redacted]	[redacted]	[redacted]
84	MIX-COMP-THERM-HTC-084	[redacted]	[redacted]	[redacted]	[redacted]	[redacted]	[redacted]
85	MIX-COMP-THERM-HTC-085	[redacted]	[redacted]	[redacted]	[redacted]	[redacted]	[redacted]

Table C.3-4 The MCNP5-1.51 Calculational Results and Measurements Uncertainties for Phase 4 Critical Experiments: Shipping Cask

Case	Evaluation Identification	File-name	k_{eff-i}	$\pm \sigma_{calc-i}$	$\pm \sigma_{exp}$	$\pm \sigma_i$	EALF (eV)
86	MIX-COMP-THERM-HTC-086	[redacted]	[redacted]	[redacted]	[redacted]	[redacted]	[redacted]
87	MIX-COMP-THERM-HTC-087	[redacted]	[redacted]	[redacted]	[redacted]	[redacted]	[redacted]
88	MIX-COMP-THERM-HTC-088	[redacted]	[redacted]	[redacted]	[redacted]	[redacted]	[redacted]
89	MIX-COMP-THERM-HTC-089	[redacted]	[redacted]	[redacted]	[redacted]	[redacted]	[redacted]
90	MIX-COMP-THERM-HTC-090	[redacted]	[redacted]	[redacted]	[redacted]	[redacted]	[redacted]
91	MIX-COMP-THERM-HTC-091	[redacted]	[redacted]	[redacted]	[redacted]	[redacted]	[redacted]
92	MIX-COMP-THERM-HTC-092	[redacted]	[redacted]	[redacted]	[redacted]	[redacted]	[redacted]
93	MIX-COMP-THERM-HTC-093	[redacted]	[redacted]	[redacted]	[redacted]	[redacted]	[redacted]
94	MIX-COMP-THERM-HTC-094	[redacted]	[redacted]	[redacted]	[redacted]	[redacted]	[redacted]
95	MIX-COMP-THERM-HTC-095	[redacted]	[redacted]	[redacted]	[redacted]	[redacted]	[redacted]
96	MIX-COMP-THERM-HTC-096	[redacted]	[redacted]	[redacted]	[redacted]	[redacted]	[redacted]
97	MIX-COMP-THERM-HTC-097	[redacted]	[redacted]	[redacted]	[redacted]	[redacted]	[redacted]
98	MIX-COMP-THERM-HTC-098	[redacted]	[redacted]	[redacted]	[redacted]	[redacted]	[redacted]
99	MIX-COMP-THERM-HTC-099	[redacted]	[redacted]	[redacted]	[redacted]	[redacted]	[redacted]
100	MIX-COMP-THERM-HTC-100	[redacted]	[redacted]	[redacted]	[redacted]	[redacted]	[redacted]
101	MIX-COMP-THERM-HTC-101	[redacted]	[redacted]	[redacted]	[redacted]	[redacted]	[redacted]
102	MIX-COMP-THERM-HTC-102	[redacted]	[redacted]	[redacted]	[redacted]	[redacted]	[redacted]
103	MIX-COMP-THERM-HTC-103	[redacted]	[redacted]	[redacted]	[redacted]	[redacted]	[redacted]
104	MIX-COMP-THERM-HTC-104	[redacted]	[redacted]	[redacted]	[redacted]	[redacted]	[redacted]
105	MIX-COMP-THERM-HTC-105	[redacted]	[redacted]	[redacted]	[redacted]	[redacted]	[redacted]
106	MIX-COMP-THERM-HTC-106	[redacted]	[redacted]	[redacted]	[redacted]	[redacted]	[redacted]
107	MIX-COMP-THERM-HTC-107	[redacted]	[redacted]	[redacted]	[redacted]	[redacted]	[redacted]
108	MIX-COMP-THERM-HTC-108	[redacted]	[redacted]	[redacted]	[redacted]	[redacted]	[redacted]
109	MIX-COMP-THERM-HTC-109	[redacted]	[redacted]	[redacted]	[redacted]	[redacted]	[redacted]
110	MIX-COMP-THERM-HTC-110	[redacted]	[redacted]	[redacted]	[redacted]	[redacted]	[redacted]
111	MIX-COMP-THERM-HTC-111	[redacted]	[redacted]	[redacted]	[redacted]	[redacted]	[redacted]
112	MIX-COMP-THERM-HTC-112	[redacted]	[redacted]	[redacted]	[redacted]	[redacted]	[redacted]
113	MIX-COMP-THERM-HTC-113	[redacted]	[redacted]	[redacted]	[redacted]	[redacted]	[redacted]
114	MIX-COMP-THERM-HTC-114	[redacted]	[redacted]	[redacted]	[redacted]	[redacted]	[redacted]
115	MIX-COMP-THERM-HTC-115	[redacted]	[redacted]	[redacted]	[redacted]	[redacted]	[redacted]
116	MIX-COMP-THERM-HTC-116	[redacted]	[redacted]	[redacted]	[redacted]	[redacted]	[redacted]
117	MIX-COMP-THERM-HTC-117	[redacted]	[redacted]	[redacted]	[redacted]	[redacted]	[redacted]
118	MIX-COMP-THERM-HTC-118	[redacted]	[redacted]	[redacted]	[redacted]	[redacted]	[redacted]
119	MIX-COMP-THERM-HTC-119	[redacted]	[redacted]	[redacted]	[redacted]	[redacted]	[redacted]
120	MIX-COMP-THERM-HTC-120	[redacted]	[redacted]	[redacted]	[redacted]	[redacted]	[redacted]
121	MIX-COMP-THERM-HTC-121	[redacted]	[redacted]	[redacted]	[redacted]	[redacted]	[redacted]
122	MIX-COMP-THERM-HTC-122	[redacted]	[redacted]	[redacted]	[redacted]	[redacted]	[redacted]
123	MIX-COMP-THERM-HTC-123	[redacted]	[redacted]	[redacted]	[redacted]	[redacted]	[redacted]

Case	Evaluation Identification	File-name	k_{eff-i}	$\pm \sigma_{calc-i}$	$\pm \sigma_{exp}$	$\pm \sigma_i$	EALF (eV)
124	MIX-COMP-THERM-HTC-124	[redacted]	[redacted]	[redacted]	[redacted]	[redacted]	[redacted]
125	MIX-COMP-THERM-HTC-125	[redacted]	[redacted]	[redacted]	[redacted]	[redacted]	[redacted]
126	MIX-COMP-THERM-HTC-126	[redacted]	[redacted]	[redacted]	[redacted]	[redacted]	[redacted]
127	MIX-COMP-THERM-HTC-127	[redacted]	[redacted]	[redacted]	[redacted]	[redacted]	[redacted]
128	MIX-COMP-THERM-HTC-128	[redacted]	[redacted]	[redacted]	[redacted]	[redacted]	[redacted]
129	MIX-COMP-THERM-HTC-129	[redacted]	[redacted]	[redacted]	[redacted]	[redacted]	[redacted]
130	MIX-COMP-THERM-HTC-130	[redacted]	[redacted]	[redacted]	[redacted]	[redacted]	[redacted]
131	MIX-COMP-THERM-HTC-131	[redacted]	[redacted]	[redacted]	[redacted]	[redacted]	[redacted]
132	MIX-COMP-THERM-HTC-132	[redacted]	[redacted]	[redacted]	[redacted]	[redacted]	[redacted]
133	MIX-COMP-THERM-HTC-133	[redacted]	[redacted]	[redacted]	[redacted]	[redacted]	[redacted]
134	MIX-COMP-THERM-HTC-134	[redacted]	[redacted]	[redacted]	[redacted]	[redacted]	[redacted]
135	MIX-COMP-THERM-HTC-135	[redacted]	[redacted]	[redacted]	[redacted]	[redacted]	[redacted]
136	MIX-COMP-THERM-HTC-136	[redacted]	[redacted]	[redacted]	[redacted]	[redacted]	[redacted]
137	MIX-COMP-THERM-HTC-137	[redacted]	[redacted]	[redacted]	[redacted]	[redacted]	[redacted]
138	MIX-COMP-THERM-HTC-138	[redacted]	[redacted]	[redacted]	[redacted]	[redacted]	[redacted]
139	MIX-COMP-THERM-HTC-139	[redacted]	[redacted]	[redacted]	[redacted]	[redacted]	[redacted]
140	MIX-COMP-THERM-HTC-140	[redacted]	[redacted]	[redacted]	[redacted]	[redacted]	[redacted]
141	MIX-COMP-THERM-HTC-141	[redacted]	[redacted]	[redacted]	[redacted]	[redacted]	[redacted]
142	MIX-COMP-THERM-HTC-142	[redacted]	[redacted]	[redacted]	[redacted]	[redacted]	[redacted]
143	MIX-COMP-THERM-HTC-143	[redacted]	[redacted]	[redacted]	[redacted]	[redacted]	[redacted]
144	MIX-COMP-THERM-HTC-144	[redacted]	[redacted]	[redacted]	[redacted]	[redacted]	[redacted]
145	MIX-COMP-THERM-HTC-145	[redacted]	[redacted]	[redacted]	[redacted]	[redacted]	[redacted]
146	MIX-COMP-THERM-HTC-146	[redacted]	[redacted]	[redacted]	[redacted]	[redacted]	[redacted]
147	MIX-COMP-THERM-HTC-147	[redacted]	[redacted]	[redacted]	[redacted]	[redacted]	[redacted]
148	MIX-COMP-THERM-HTC-148	[redacted]	[redacted]	[redacted]	[redacted]	[redacted]	[redacted]
149	MIX-COMP-THERM-HTC-149	[redacted]	[redacted]	[redacted]	[redacted]	[redacted]	[redacted]
150	MIX-COMP-THERM-HTC-150	[redacted]	[redacted]	[redacted]	[redacted]	[redacted]	[redacted]
151	MIX-COMP-THERM-HTC-151	[redacted]	[redacted]	[redacted]	[redacted]	[redacted]	[redacted]
152	MIX-COMP-THERM-HTC-152	[redacted]	[redacted]	[redacted]	[redacted]	[redacted]	[redacted]
153	MIX-COMP-THERM-HTC-153	[redacted]	[redacted]	[redacted]	[redacted]	[redacted]	[redacted]
154	MIX-COMP-THERM-HTC-154	[redacted]	[redacted]	[redacted]	[redacted]	[redacted]	[redacted]
155	MIX-COMP-THERM-HTC-155	[redacted]	[redacted]	[redacted]	[redacted]	[redacted]	[redacted]
156	MIX-COMP-THERM-HTC-156	[redacted]	[redacted]	[redacted]	[redacted]	[redacted]	[redacted]

Table C.3-5 The MCNP5-1.51 Calculational Results and Measurements Uncertainties for Selected Critical Experiments

Case	Evaluation Identification	File-name	k_{eff-i}	$\pm \sigma_{calc-i}$	$\pm \sigma_{exp}$	$\pm \sigma_i$	EALF (eV)
157	Core I	[redacted]	[redacted]	[redacted]	[redacted]	[redacted]	[redacted]
158	Core II	[redacted]	[redacted]	[redacted]	[redacted]	[redacted]	[redacted]
159	Core III	[redacted]	[redacted]	[redacted]	[redacted]	[redacted]	[redacted]
160	Core IX	[redacted]	[redacted]	[redacted]	[redacted]	[redacted]	[redacted]
161	Core X	[redacted]	[redacted]	[redacted]	[redacted]	[redacted]	[redacted]
162	Core XI	[redacted]	[redacted]	[redacted]	[redacted]	[redacted]	[redacted]
163	Core XII	[redacted]	[redacted]	[redacted]	[redacted]	[redacted]	[redacted]
164	Core XIII	[redacted]	[redacted]	[redacted]	[redacted]	[redacted]	[redacted]
165	Core XIV	[redacted]	[redacted]	[redacted]	[redacted]	[redacted]	[redacted]
166	Core XV	[redacted]	[redacted]	[redacted]	[redacted]	[redacted]	[redacted]
167	Core XVI	[redacted]	[redacted]	[redacted]	[redacted]	[redacted]	[redacted]
168	Core XVII	[redacted]	[redacted]	[redacted]	[redacted]	[redacted]	[redacted]
169	Core XVIII	[redacted]	[redacted]	[redacted]	[redacted]	[redacted]	[redacted]
170	Core XIX	[redacted]	[redacted]	[redacted]	[redacted]	[redacted]	[redacted]
171	Core XX	[redacted]	[redacted]	[redacted]	[redacted]	[redacted]	[redacted]
172	Core XXI	[redacted]	[redacted]	[redacted]	[redacted]	[redacted]	[redacted]
173	S-type Fuel, w/886 ppm B	[redacted]	[redacted]	[redacted]	[redacted]	[redacted]	[redacted]
174	S-type Fuel, w/746 ppm B	[redacted]	[redacted]	[redacted]	[redacted]	[redacted]	[redacted]
175	SO-type Fuel, w/1156 ppm B	[redacted]	[redacted]	[redacted]	[redacted]	[redacted]	[redacted]
176	Case 1 1337 ppm B	[redacted]	[redacted]	[redacted]	[redacted]	[redacted]	[redacted]
177	Case 12 1899 ppm B	[redacted]	[redacted]	[redacted]	[redacted]	[redacted]	[redacted]
178	Water Moderator 0 gap	[redacted]	[redacted]	[redacted]	[redacted]	[redacted]	[redacted]
179	Water Moderator 2.5 cm gap	[redacted]	[redacted]	[redacted]	[redacted]	[redacted]	[redacted]
180	Water Moderator 5 cm gap	[redacted]	[redacted]	[redacted]	[redacted]	[redacted]	[redacted]
181	Water Moderator 10 cm gap	[redacted]	[redacted]	[redacted]	[redacted]	[redacted]	[redacted]
182	Steel Reflector, 1.321 cm separation	[redacted]	[redacted]	[redacted]	[redacted]	[redacted]	[redacted]
183	Steel Reflector, 2.616 cm separation	[redacted]	[redacted]	[redacted]	[redacted]	[redacted]	[redacted]
184	Steel Reflector, 3.912 cm separation	[redacted]	[redacted]	[redacted]	[redacted]	[redacted]	[redacted]
185	Steel Reflector, Infinite separation	[redacted]	[redacted]	[redacted]	[redacted]	[redacted]	[redacted]
186	Steel Reflector, 1.321 cm separation	[redacted]	[redacted]	[redacted]	[redacted]	[redacted]	[redacted]
187	Steel Reflector, 2.616 cm separation	[redacted]	[redacted]	[redacted]	[redacted]	[redacted]	[redacted]
188	Steel Reflector, 5.405 cm separation	[redacted]	[redacted]	[redacted]	[redacted]	[redacted]	[redacted]
189	Steel Reflector, Infinite separation	[redacted]	[redacted]	[redacted]	[redacted]	[redacted]	[redacted]
190	Steel Reflector, with Boral Sheets	[redacted]	[redacted]	[redacted]	[redacted]	[redacted]	[redacted]
191	Lead Reflector, 0.55 cm sepn.	[redacted]	[redacted]	[redacted]	[redacted]	[redacted]	[redacted]
192	Lead Reflector, 1.956 cm sepn.	[redacted]	[redacted]	[redacted]	[redacted]	[redacted]	[redacted]
193	Lead Reflector, 5.405 cm sepn.	[redacted]	[redacted]	[redacted]	[redacted]	[redacted]	[redacted]
194	Experiment 004/032 – no absorber	[redacted]	[redacted]	[redacted]	[redacted]	[redacted]	[redacted]

Case	Evaluation Identification	File-name	k_{eff-i}	$\pm \sigma_{calc-i}$	$\pm \sigma_{exp}$	$\pm \sigma_i$	EALF (eV)
195	Exp. 009 1.05% Boron Steel plates						
196	Exp. 009 1.62% Boron Steel plates						
197	Exp. 031 – Boral plates						
198	Experiment 214R – with flux traps						
199	Experiment 214V3 –with flux trap						
200	Case 173 – 0 ppm B						
201	Case 177 – 2550 ppm B						
202	MOX Fuel – Type 3.2 Exp. 21						
203	MOX Fuel – Type 3.2 Exp. 43						
204	MOX Fuel – Type 3.2 Exp. 13						
205	MOX Fuel – Type 3.2 Exp. 32						
206	Saxton Case 52 PuO2 0.52” pitch						
207	Saxton Case 52 U 0.52” pitch						
208	Saxton Case 56 PuO2 0.56” pitch						
209	Saxton Case 56 borated PuO2						
210	Saxton Case 56 U 0.56” pitch						
211	Saxton Case 79 PuO2 0.79” pitch						
212	Saxton Case 79 U 0.79” pitch						
213	0.700-in. pitch 0 ppm B						
214	0.700-in. pitch 688 ppm B						
215	0.870-in. pitch 0 ppm B						
216	0.870-in. pitch 1090 ppm B						
217	0.990-in. pitch 0 ppm B						
218	0.990-in. pitch 767 ppm B						
219	Saxton Case PuO2 0.735” pitch						
220	Saxton Case PuO2 1.04” pitch						
221	8 wt% 240Pu 0.80” pitch						
222	8 wt% 240Pu 0.93” pitch						
223	8 wt% 240Pu 1.05” pitch						
224	8 wt% 240Pu 1.143” pitch						
225	8 wt% 240Pu 1.32” pitch						
226	8 wt% 240Pu 1.386” pitch						
227	16 wt% 240Pu 0.93” pitch						
228	16 wt% 240Pu 1.05” pitch						
229	16 wt% 240Pu 1.143” pitch						
230	16 wt% 240Pu 1.32” pitch						
231	24 wt% 240Pu 0.80” pitch						
232	24 wt% 240Pu 0.93” pitch						
233	24 wt% 240Pu 1.05” pitch						
234	24 wt% 240Pu 1.143” pitch						

Case	Evaluation Identification	File-name	k_{eff-i}	$\pm \sigma_{calc-i}$	$\pm \sigma_{exp}$	$\pm \sigma_i$	EALF (eV)
235	24 wt% 240Pu 1.32” pitch						
236	24 wt% 240Pu 1.386” pitch						
237	18 wt% 240Pu 0.85” pitch						
238	18 wt% 240Pu 0.93” pitch						
239	18 wt% 240Pu 1.05” pitch						
240	18 wt% 240Pu 1.143” pitch						
241	18 wt% 240Pu 1.386” pitch						
242	18 wt% 240Pu 1.60” pitch						
243	18 wt% 240Pu 1.70” pitch						
317	Core XI, 1182 ppm, 36 Pyrex Rods						
318	Core XI, 1182 ppm, 36 Pyrex Rods						
319	Core XI, 1032.5 ppm, 72 Pyrex Rods						
320	Core XI, 1032.5 ppm, 72 Pyrex Rods						
321	Core XI, 794 ppm, 144 Pyrex Rods						
322	Core XI, 779 ppm, 144 Pyrex Rods						
323	Core XI, 1245 ppm, 72 Vicor Rods						
360	Core IV						
361	Core V						
362	Core VI						
363	Core VII						
364	Core VIII						
445	670 pins, Al2O3-B4C rods						
446	672 pins, Al2O3-B4C rods						
447	668 pins, Al2O3-B4C rods						
448	668 pins, Al2O3-B4C rods						
479	8 wt% 240Pu 1.05” pitch, B4 Rods						
480	8 wt% 240Pu 1.05” pitch, B3 Rods						
481	8 wt% 240Pu 1.05” pitch, B2 Rods						
482	8 wt% 240Pu 1.05” pitch, B1 Rods						
484	8 wt% 240Pu 1.05” pitch, B4+Cd Rods						
485	8 wt% 240Pu 1.05” pitch, B3+Cd Rods						
486	8 wt% 240Pu 1.05” pitch, B2+Cd Rods						
487	8 wt% 240Pu 1.05” pitch, B1+Cd Rods						
491	8 wt% 240Pu 1.32” pitch, B4 Rods						
492	8 wt% 240Pu 1.32” pitch, B3 Rods						
493	8 wt% 240Pu 1.32” pitch, B2 Rods						
494	8 wt% 240Pu 1.32” pitch, B1 Rods						

Case	Evaluation Identification	File-name	k_{eff-i}	$\pm \sigma_{calc-i}$	$\pm \sigma_{exp}$	$\pm \sigma_i$	EALF (eV)
496	8 wt% 240Pu 1.32” pitch, B4+Cd Rods	[redacted]	[redacted]	[redacted]	[redacted]	[redacted]	[redacted]
497	8 wt% 240Pu 1.32” pitch, B3+Cd Rods	[redacted]	[redacted]	[redacted]	[redacted]	[redacted]	[redacted]
498	8 wt% 240Pu 1.32” pitch, B2+Cd Rods	[redacted]	[redacted]	[redacted]	[redacted]	[redacted]	[redacted]
499	8 wt% 240Pu 1.32” pitch, B1+Cd Rods	[redacted]	[redacted]	[redacted]	[redacted]	[redacted]	[redacted]
504	16 wt% 240Pu 1.05” pitch, B4 Rods	[redacted]	[redacted]	[redacted]	[redacted]	[redacted]	[redacted]
505	16 wt% 240Pu 1.05” pitch, B3 Rods	[redacted]	[redacted]	[redacted]	[redacted]	[redacted]	[redacted]
506	16 wt% 240Pu 1.05” pitch, B2 Rods	[redacted]	[redacted]	[redacted]	[redacted]	[redacted]	[redacted]
507	16 wt% 240Pu 1.05” pitch, B1 Rods	[redacted]	[redacted]	[redacted]	[redacted]	[redacted]	[redacted]
509	16 wt% 240Pu 1.05” pitch, B4+Cd Rods	[redacted]	[redacted]	[redacted]	[redacted]	[redacted]	[redacted]
510	16 wt% 240Pu 1.05” pitch, B3+Cd Rods	[redacted]	[redacted]	[redacted]	[redacted]	[redacted]	[redacted]
511	16 wt% 240Pu 1.05” pitch, B2+Cd Rods	[redacted]	[redacted]	[redacted]	[redacted]	[redacted]	[redacted]
512	16 wt% 240Pu 1.05” pitch, B1+Cd Rods	[redacted]	[redacted]	[redacted]	[redacted]	[redacted]	[redacted]
516	24 wt% 240Pu 1.05” pitch, B4 Rods	[redacted]	[redacted]	[redacted]	[redacted]	[redacted]	[redacted]
517	24 wt% 240Pu 1.05” pitch, B3 Rods	[redacted]	[redacted]	[redacted]	[redacted]	[redacted]	[redacted]
518	24 wt% 240Pu 1.05” pitch, B2 Rods	[redacted]	[redacted]	[redacted]	[redacted]	[redacted]	[redacted]
519	24 wt% 240Pu 1.05” pitch, B1 Rods	[redacted]	[redacted]	[redacted]	[redacted]	[redacted]	[redacted]
521	24 wt% 240Pu 1.05” pitch, B4+Cd Rods	[redacted]	[redacted]	[redacted]	[redacted]	[redacted]	[redacted]
522	24 wt% 240Pu 1.05” pitch, B3+Cd Rods	[redacted]	[redacted]	[redacted]	[redacted]	[redacted]	[redacted]
523	24 wt% 240Pu 1.05” pitch, B2+Cd Rods	[redacted]	[redacted]	[redacted]	[redacted]	[redacted]	[redacted]
524	24 wt% 240Pu 1.05” pitch, B1+Cd Rods	[redacted]	[redacted]	[redacted]	[redacted]	[redacted]	[redacted]

Table C.3-6 Descriptive Statistics of the MCNP5-1.51 Calculational Results

Experiment Description	No. of exp.	k_{eff} range	EALF (eV) range
Phase 1	18	[redacted]	[redacted]
Phase 2	41	[redacted]	[redacted]
Phase 3	26	[redacted]	[redacted]
Phase 4	71	[redacted]	[redacted]
Selected Experiments	135	[redacted]	[redacted]
All experiments	291	[redacted]	[redacted]

Table C.3-7 Normality Test Results for the MCNP5-1.51 calculations

Experiment Description	No. of exp.	Shapiro-Wilk		Pearson's chi-square (χ^2)			
		Wtest	W	χ^2	n	$P_d(\chi^2;d)$	Normal
Phase 1	18	[redacted]	[redacted]	[redacted]	[redacted]	[redacted]	[redacted]
Phase 2	41	[redacted]	[redacted]	[redacted]	[redacted]	[redacted]	[redacted]
Phase 3	26	[redacted]	[redacted]	[redacted]	[redacted]	[redacted]	[redacted]
Phase 4	71	[redacted]	[redacted]	[redacted]	[redacted]	[redacted]	[redacted]
HTC Experiments	156	[redacted]	[redacted]	[redacted]	[redacted]	[redacted]	[redacted]
Selected Experiments	135	[redacted]	[redacted]	[redacted]	[redacted]	[redacted]	[redacted]
All experiments	291	[redacted]	[redacted]	[redacted]	[redacted]	[redacted]	[redacted]

Table C.3-8 Trending Analysis Results for the MCNP5-1.51 calculations

Experiment Description	No. of exp.	Correlated Parameter, *x*	Correlation Coefficient, r^2	Probability, Pd(N;r)	Correlation	Regression Equation, k(*x*)
Phase 1	18	EALF	[redacted]	[redacted]	[redacted]	[redacted]
		Pitch	[redacted]	[redacted]	[redacted]	[redacted]
		Number of Rods	[redacted]	[redacted]	[redacted]	[redacted]
Phase 2	41	EALF	[redacted]	[redacted]	[redacted]	[redacted]
		Pitch	[redacted]	[redacted]	[redacted]	[redacted]
		Number of Rods	[redacted]	[redacted]	[redacted]	[redacted]
		Gadolinium Conc.	[redacted]	[redacted]	[redacted]	[redacted]
		Boron Conc.	[redacted]	[redacted]	[redacted]	[redacted]
Phase 3	26	EALF	[redacted]	[redacted]	[redacted]	[redacted]
		Water Gap	[redacted]	[redacted]	[redacted]	[redacted]
		Number of Rods	[redacted]	[redacted]	[redacted]	[redacted]
Phase 4	71	EALF	[redacted]	[redacted]	[redacted]	[redacted]
		Water Gap	[redacted]	[redacted]	[redacted]	[redacted]
		Screen Array Distance	[redacted]	[redacted]	[redacted]	[redacted]
Selected Experiments	135	EALF	[redacted]	[redacted]	[redacted]	[redacted]
		Pitch	[redacted]	[redacted]	[redacted]	[redacted]
		Rod OD	[redacted]	[redacted]	[redacted]	[redacted]
		Fuel Density	[redacted]	[redacted]	[redacted]	[redacted]
		U Enrichment	[redacted]	[redacted]	[redacted]	[redacted]
		Pu Enrichment	[redacted]	[redacted]	[redacted]	[redacted]
All experiments	291	EALF	[redacted]	[redacted]	[redacted]	[redacted]
		Pitch	[redacted]	[redacted]	[redacted]	[redacted]
		Rod OD	[redacted]	[redacted]	[redacted]	[redacted]
		Fuel Density	[redacted]	[redacted]	[redacted]	[redacted]

Table C.3-9 Analysis of Neutron Absorbers and Reflector Materials for the MCNP5-1. 51 calculations

Experiment Description	No. of exp.	Bias	Bias Uncertainty	Normality χ^2 ($P_d(\chi^2;d)$)	Significant Trends
All experiments	291				
All except those with Gadolinium, Cadmium and Lead	201				

Table C.3-10 Analysis of Fuel Rod Pitch Trend for the MCNP5-1. 51 calculations

Experiment Description	Rod Pitch	Bias	Bias Uncertainty	Normality χ^2 ($P_d(\chi^2;d)$)	Significant Trends
All experiments	All (291 total)				
	<=2 cm (218 total)				
All except those with Gadolinium, Cadmium and Lead	All (201 total)				
	<=2 cm (144 total)				

Table C.3-11 Analysis of Fuel Burnup for the MCNP5-1. 51 calculations

Experiment Description	Rod Pitch	Bias	Bias Uncertainty	Normality χ^2 ($P_d(\chi^2;d)$)	Significant Trends
All except those with Gadolinium, Cadmium and Lead†	All (201 total)				
	<=2 cm (144 total)				
Fresh UO_2 Fuel	All (61 total)				
	<=2 cm (52 total)				
HTC Experiments	All (85 total)				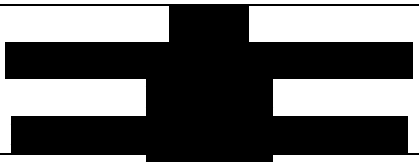
	<=2 cm (82 total)				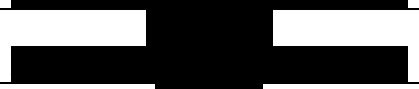
MOX Experiments	All (55 total)				
	<=2 cm (10 total)				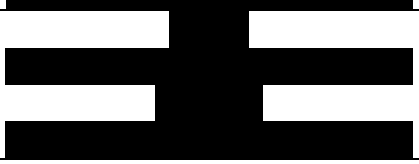

†Note: Critical experiments with Gadolinium, Cadmium and Lead were excluded from all subsequent subsets.

Table C.3-12 Analysis of the Unborated and Borated Water for the MCNP5-1.51 calculations

Experiment Description	Rod Pitch	Bias	Bias Uncertainty	Normality χ^2 ($P_d(\chi^2;d)$)	Significant Trends
All except those with Gadolinium, Cadmium and Lead†	All (201 total)				
	<=2 cm (144 total)				
All with Fresh Water	All (149 total)				
	<=2 cm (94 total)				
All with Borated Water	All (52 total)				
	<=2 cm (50 total)				

†Note: Critical experiments with Gadolinium, Cadmium and Lead were excluded from all subsequent subsets.

Table C.3-13 Comparison of Key Parameters and Definition of Validated AOA

Parameter	Design Application	Benchmarks	Validated
Fissionable Material	^{235}U, ^{239}Pu, ^{241}Pu	^{235}U, ^{239}Pu, ^{241}Pu	^{235}U, ^{239}Pu, ^{241}Pu
Isotopic Composition			
$^{235}U/Ut$	< 5.0wt%	1.57 – 5.74%	< 5wt%
Pu/(U+Pu)	< 20wt%	1.104 - 20 %	< 20wt%
Physical Form	UO_2, MOX	UO_2, MOX	UO_2, MOX
Fuel Density (g/cm^3)	10.0 – 10.7	9.2 – 10.4	9.2 – 10.7
Moderator Material (coolant)	H	H	H
Physical Form	H_20	H_20	H_20
Density (g/cm^3)	around 1.0 g/cm^3	around 1.0 g/cm^3	around 1.0 g/cm^3
Reflector Material	H	H	H
Physical Form	H_20	H_20	H_20
Density (g/cm^3)	around 1.0 g/cm^3	around 1.0 g/cm^3	around 1.0 g/cm^3
Interstitial Reflector Material			
Plate	Steel or Lead	Steel or Lead	Steel or Lead
Absorber Material			
Soluble	None, Boron or Gadolinium	None, Boron (89 - 595 ppm) or Gadolinium (49.2 – 199.7 ppm)	None, Boron (0 - 1000 ppm) or Gadolinium (0 to 1000 ppm)
Rods	Boron	Pyrex®, Vicor® or B-Al	Boron
Separating Material			
Plate	Water, B-SS, Boral or Cadmium	Water, B-SS, Boral or Cadmium	Water, B-SS, Boral or Cadmium
Geometry			
Lattice type	Square	Square, Triangle	Square, Triangle
Lattice Pitch (cm)	1.26 – 1.47 (PWR) 1.24 – 1.88 (BWR)	0.968 to 4.318	0.968 to 4.318
Neutron Energy	Thermal spectrum	Thermal spectrum	Thermal spectrum

Figure Proprietary

Figure C.3-1 Frequency Chart for Calculated k_{eff} of the Selected 243 Benchmarks for the MCNP5-1.51 code

Figure Proprietary

Figure C.3-2 Frequency Chart for Calculated EALF (eV) of the Selected 243 Benchmarks for the MCNP5-1.51 code

Figure Proprietary

Figure C.3-3 MCNP5-1.51 Calculated k_{eff} Values for Various Values of the Spectral Index (All Experiments)

Figure Proprietary

Figure C.3-4 MCNP5-1.51 Calculated k_{eff} Values as a Function of Rod Pitch (All Experiments)

Appendix D

Benchmark of MCNP5-1.51 with ENDF/B-VII

(total number of pages: 51 including this page)

D.1 Introduction

This Appendix presents the analysis of the validation results for MCNP5-1.51 code and includes the results of the calculations, normality test, the detailed statistical trending analysis, calculation bias and bias uncertainty for each distinct area of applicability of the parameters of interest.

D.2 Computer Code Parameter Data

The computer code MCNP5-1.51 [D.1] is the continuous energy Monte Carlo codes and treats an arbitrary three-dimensional configuration of materials in geometric cells bounded by first- and second-degree surfaces and fourth-degree elliptical tori. Thermal neutrons are described by both the free gas and S(α,β) models. All calculations were performed using the default data libraries provided with the code: the default continuous energy neutron transport data based on ENDF/B-VII. The list of ZAIDs that were used in the analysis is presented in Table D.2-1. The neutrons start from an arbitrary distribution, causing a generally very large variance of results from the first cycles in comparison with the following cycles. Therefore, all MCNP5-1.51 calculations are performed with 12,000 histories per cycle, 50 skipped cycles before averaging, and 100 cycles that are accumulated. The calculated k_{eff} values have associated uncertainties due to the statistical nature of the Monte Carlo codes.

D.3 Analysis of MCNP5-1.51 Validation Results

D.3.1. Calculational Results

The calculation results for the 156 HTC critical experiments and for the 376 selected critical experiments described in Appendix B are presented and discussed in this section. The calculation results are summarized by grouping the experiments in terms of the categories as set forth in Appendix B. Calculation results, including $k_{eff\text{-}I}$, $\sigma_{calc\text{-}i}$ and EALF, measurement uncertainties (σ_{exp}) and the calculation and measurement combined uncertainty (σ_i) are shown in Table D.3-1 through Table D.3-5.

Figure D.3-1 and D.3-2 are histograms showing the frequency of calculated k_{eff} and EALF for all 532 benchmarks. The nominal calculated k_{eff} values range from 0[redacted]. The EALF results values show a range between [redacted].

Descriptive statistics for the different group of experiments is summarized in Table D.3-6.

D.3.2. Normality Test

In order to assess the normality assumption, Shapiro and Wilk [5] test has been used for groups with fewer than 50 samples while the Pearson's chi-square (χ^2) test [4] has been used for samples larger than 20 samples. The tests are applied to the group of experiments in terms of the categories as set forth in Appendix B.

For the Shapiro and Wilk test, Table D.3-7 shows the computed *Wtest* value, and *W* value that can be obtained for the number of experiments from [5] to accept the normality hypothesis. If W

is less than the test statistic, *Wtest*, then the data is considered normally distributed. For the χ^2 test, it is concluded normal for $\chi^2 \leq n$, where n is a number of bins for the group of experiments. The probability $P_d(\tilde{\chi}^2 \geq \tilde{\chi}_0{}^2)$ of obtaining a value of $\tilde{\chi}^2 \geq \tilde{\chi}_0{}^2$ in an experiment with d degrees of freedom to confirm quantitatively that the agreement is satisfactory was taken or interpolated, if necessary, from Appendix D in Reference [4]. Thus, if $P_d(\tilde{\chi}^2 \geq \tilde{\chi}_0{}^2)$ is large, the obtained and expected distributions are consistent; if it is small, they probably disagree. In particular, if $P_d(\tilde{\chi}^2 \geq \tilde{\chi}_0{}^2)$ is less than 5%, we say that the disagreement is significant and reject the assumed distributions at the 5% level. If it is less than 1%, the disagreement is called highly significant, and we reject the assumed distributions at the 1% level.

D.3.3. Trending Analysis

Trends are determined through the use of regression fits to the calculated results. The equations used to identify trends are given below:

$$Y(x) = a + bx \tag{7-1}$$

$$a = \frac{1}{\Delta}\left(\sum \frac{x_i^2}{\sigma_i^2}\sum \frac{y_i}{\sigma_i^2} - \sum \frac{x_i}{\sigma_i^2}\sum \frac{x_i y_i}{\sigma_i^2}\right) \tag{7-2}$$

$$b = \frac{1}{\Delta}\left(\sum \frac{1}{\sigma_i^2}\sum \frac{x_i y_i}{\sigma_i^2} - \sum \frac{x_i}{\sigma_i^2}\sum \frac{y_i}{\sigma_i^2}\right) \tag{7-3}$$

$$\Delta = \sum \frac{1}{\sigma_i^2}\sum \frac{x_i^2}{\sigma_i^2} - \left(\sum \frac{x_i}{\sigma_i^2}\right)^2 \tag{7-4}$$

The squared term of the linear correlation factor r defined below (from Reference [5]) is used to quantitatively measure the degree to which a linear relationship exist between two variables.

$$r = \frac{\sum \frac{1}{\sigma_i^2}(x_i - \bar{x})(y_i - \bar{y})}{\sqrt{\left[\sum \frac{1}{\sigma_i^2}(x_i - \bar{x})^2\right]\left[\sum \frac{1}{\sigma_i^2}(y_i - \bar{y})^2\right]}} \tag{7-5}$$

The closer r^2 approaches the value of 1, the better the fit of the data to the linear equation. A more quantitative measure of the fit can be found by using Appendix C in Reference [4]. The interpolation was applied, if necessary. For any given observed value r_0, $P_N(|r| \geq |r_0|)$ is the probability that N measurements of two uncorrelated variables would give a coefficient r as large as r_0. Thus, if we obtain a coefficient r_0 for which $P_N(|r| \geq |r_0|)$ is small, it is correspondingly unlikely that our variables are uncorrelated; that is, a correlation indicated. In particular, if $P_N(|r| \geq |r_0|) \leq 5\%$, the correlation is called significant; if it is less than 1%, the correlation is called highly significant.

The validation results are analyzed for the group of all experiments. Independent variables used in the trending analysis, correlation coefficients and trending analysis results are summarized in Table D.3-8.

D.3.4. Bias and Bias Uncertainty

In this section, benchmark results are analyzed using the statistical method described in section 2.2.

The first step is to evaluate whether the HTC experiments and selected experiments, should be reduced to a single set. The mean k_{eff} of the HTC data set is [redacted] and the mean k_{eff} of the selected experiments data is [redacted]. The difference between the means is just 0.0010 which is less than the uncertainty. These sets are water moderated uranium or mixed plutonium-uranium dioxide lattices. The HTC sets of experiments and the selected experiments are considered one large set of 532 experiments from now on.

The normality test in Table D.3-7 and in Figure D.3-1 shows that the data is not normally distributed. Therefore, the distribution free approach [6] is used for all subsets with the rejected normality distribution. The lower tolerance limit with 95% probability and 95% confidence level is determined for order data [6] and the difference between weighted average k_{eff} and this lower tolerance limit is used to determine the bias uncertainty. This is conservative since the data is close to the normal distribution. The distribution free bias uncertainty is also provided in all subsequent tables for the subsets with the rejected normality assumption.

The analysis of the correlation coefficient in Table D.3-8 and the plot of data trend (Figure D.3-3) show that there is not a clear trend in the data.

The total bias (systematic error or mean of the deviation from a keff of exactly 1.000) of the MCNP5-1.51 code is shown in the table below

Calculational Bias of the MCNP5-1.51 code		
Description	Total Bias	Bias Uncertainty
HTC and Selected Experiments	[redacted]	[redacted]

D.3.5. Applicability of MCNP5-1.51 Validation Results

This subsection contains a more detailed evaluation of the set of critical experiments. Regarding the selected experiments, the following subjects are discussed:

- Neutron absorber and neutron reflector materials
- Neutron absorber geometry
- Fuel burnup
- Unborated and borated water

- Various Combinations of Fuel Burnup and Unborated/Borated Water.

The general focus is to justify that using the full set of critical experiments is appropriate. In some cases, subsets of full set of experiments are established. For those subsets, statistical evaluations are performed to determine bias, bias uncertainty, normality and trends. Trends are evaluated for fuel rod outer diameter, fuel rod pitch, fuel density, boron content, U or Pu enrichment and EALF. To estimate a significance of observed trend, the residuals from the trend equation were tested for a normal distribution [D.2]. If residuals are normally distributed then there is a significant trend, otherwise there is no linear trend as this violets the basic assumptions of linear regression. For each significant linear correlation, the bias and bias uncertainty were calculated as a function of the independent parameter.

D.3.5.1. Neutron Absorber and Neutron Reflector Materials

The HTC and Selected Experiments consider the following neutron absorbers and reflectors:

- Absorbers
  - Boron, in the form of soluble boron in the water, boron in solid form (B_4C), and boron in borated steel, Pyrex, Boroflex and borated aluminum
  - Soluble gadolinium in water and Gd_2O_3 rods
  - Cadmium
- Reflectors
  - Steel
  - Lead
  - Water

Some typical configurations do not contain gadolinium or cadmium neutron absorbers or lead reflectors. To verify that including those materials does not have a significant effect on the results of the benchmarking analyses, a subset without those experiments containing those materials was analyzed. In addition, according to recommendations of NUREG-6979 [B.13], the following HTC experiments were also excluded: 61, 65, 67, 86, 97, 98, 99, 102, 124, 135, and 137. The comparison with the full set is presented in Table D.3-9 and shows no significant differences when those materials are excluded. However, a significant correlation as a function of EALF was determined by the residuals normality test. This correlation is presented in the Figure D.3-4. The bias and bias uncertainty as a function of the EALF were calculated for this trend and shown in Table D.3-10, with a maximum absolute value of [redacted].

D.3.5.2. Absorber Geometry

The criticality experiments analyzed in this report include experiments with Boron in the form of plates, absorber rods and soluble boron in water. No trend relating to these experiments is observed.

D.3.5.3. Fuel Burnup

The full set of critical experiments contains experiments with fresh UO_2 fuel, with simulated spent fuel (37.5 GWd/MTU), and MOX fuel with Pu content between 1.5 and 20%, which is

even higher than typically found in spent fuel. The experiments are therefore reasonably representative of burned fuel at different burnup levels. To verify that the experiments cover the burnup range sufficiently, the experiments are subdivided into fresh UO_2 fuel and spent fuel with HTC and MOX experiments, and compared to the results of the entire set. The comparison is shown in Table D.3-11. The comparison shows no significant differences between the entire set and the fresh and spent fuel subsets. However, in some cases, the correlations are observed. The significant trends as a function of EALF and Pu enrichment were determined in the spent fuel subset by the residuals normality test. These correlations are presented in the Figure D.3-5 and Figure D.3-6. The bias and bias uncertainty as a function of the EALF and Pu enrichment were calculated for these trends and shown in Table D.3-12, with a maximum absolute value of -[redacted].

D.3.5.4. Unborated and Borated Water

The full set of critical experiments contains both experiments with and without soluble boron. The entire set of analyses shows no significant trend when analyzed as a function of the soluble boron level. Nevertheless, sets with and without soluble boron are analyzed and compared to the full set that contains all experiments. The results are shown in Table D.3-13. Similar to the previous subsection, the comparison shows no significant differences between those subsets. However, there are significant trends in the fresh water subset as a function of EALF and U enrichment and in the borated water subset as a function of fuel density that were determined by the residuals normality test. These correlations are presented in the Figure D.3-7 through Figure D.3-9. The bias and bias uncertainty as a function of the EALF, U enrichment and fuel density were calculated for these trends and shown in Table D.3-14, with a maximum absolute value of -[redacted].

D.3.5.5. Various Combinations of Fuel Burnup and Unborated/Borated Water

To perform more detailed evaluation of the set of critical experiments, the additional four subsets with different combinations of fuel burnup and unborated/borated water were analyzed. The results are shown in Table D.3-15. There are significant EALF trend in the subset of fresh UO_2 fuel with fresh water, significant trends in the subset of spent fuel with fresh water as a function of EALF and Pu enrichment and significant trends in the subset of spent fuel with borated water as a function of rod OD and fuel density, that were determined by the residuals normality test. These correlations are presented in the Figure D.3-10 through Figure D.3-14.The bias and bias uncertainty as a function of the EALF, Pu enrichment, rod OD and fuel density were calculated for these trends and shown in Table D.3-16, with a maximum absolute value of [redacted].

D.4 Summary

A set of 532 critical experiments has been selected and has been used for the validation of the Holtec International criticality safety methodology. The similarity between the chosen experiments and the actual systems has been based on a set of screening criteria as is stated in the NUREG/CR-6698 [5]. Experiments have been categorized by fuel burnup as fresh UO_2 fuel and spent fuel with HTC and MOX experiments or by unborated and borated water condition and

parameterized by key variables such as lattice pitch / assembly pitch, absorber solution concentration, number of fuel rods, rod outer diameter, fuel density, screen array distance, fuel enrichment and EALF. Benchmark calculations have been performed using the Monte Carlo code MCNP5-1.51. It was determined that HTC experiments and selected experiments are in sufficient agreement that this sets are lumped together as a single set of 532 experiments. The bias and bias uncertainty are presented in section D.3.4. The applicability of validation results is considered in section D.3.5.

The range of key parameters for the design application, benchmarks and validated AOA are summarized in Table D.3-17. A point by point comparison between design application and benchmarks shows that the experimental range covers all the parameters. The soluble boron concentration is extrapolated generously since ^{10}B is a 1/v absorber (as permitted on Table 2.3 of [5]).

As for the fuel density, Table 2.3 of Reference [5] states there is "no requirement" and that "experiments should be as close to the desired concentration as possible". Since the experiment fuel density is 9.2 – 10.4 g/cm^3 and the design application one is around 10.0 – 10.7 g/cm^3, it is considered that the values are very close so the validated AOA covers the design application range.

The fuel enrichment can be up to 5%. The experiments used go up to 5.74 wt% ^{235}U. Therefore, it is considered that the validated AOA covers the design application range.

D.5 References

[D.1] "MCNP - A General Monte Carlo N-Particle Transport Code, Version 5"; Los Alamos National Laboratory, LA-UR-03-1987 (Revised 2/1/2008).

[D.2] J. W. Barnes, "Statistical Analysis for Engineers and Scientists", McGraw-Hill Inc., 1988

Table D.2-1 ZAIDs Used for Each Nuclide

Nuclide	MCNP5.1.51 ZAID	Nuclide	MCNP5.1.51 ZAID	Nuclide	MCNP5.1.51 ZAID
^{1}H	1001.70c	^{48}Ti	22048.70c	^{100}Mo	42100.70c
^{2}H	1002.70c	^{49}Ti	22049.70c	^{107}Ag	47107.70c
^{4}He	2004.70c	^{50}Ti	22050.70c	^{109}Ag	47109.70c
^{10}B	5010.70c	^{50}Cr	24050.70c	^{106}Cd	48106.70c
^{11}B	5011.70c	^{52}Cr	24052.70c	^{108}Cd	48108.70c
C	6000.70c	^{53}Cr	24053.70c	^{110}Cd	48110.70c
^{14}N	7014.70c	^{54}Cr	24054.70c	^{111}Cd	48111.70c
^{16}O	8016.70c	^{55}Mn	25055.70c	^{112}Cd	48112.70c
^{20}Ne	10020.42c	^{54}Fe	26054.70c	^{113}Cd	48113.70c
^{23}Na	11023.70c	^{56}Fe	26056.70c	^{114}Cd	48114.70c
^{24}Mg	12024.70c	^{57}Fe	26057.70c	^{116}Cd	48116.70c
^{25}Mg	12025.70c	^{58}Fe	26058.70c	^{113}In	49113.70c
^{26}Mg	12026.70c	^{59}Co	27059.70c	^{115}In	49115.70c
^{27}Al	13027.70c	^{58}Ni	28058.70c	^{112}Sn	50112.70c
^{28}Si	14028.70c	^{60}Ni	28060.70c	^{114}Sn	50114.70c
^{29}Si	14029.70c	^{61}Ni	28061.70c	^{115}Sn	50115.70c
^{30}Si	14030.70c	^{62}Ni	28062.70c	^{116}Sn	50116.70c
^{31}P	15031.70c	^{64}Ni	28064.70c	^{117}Sn	50117.70c
^{32}S	16032.70c	^{63}Cu	29063.70c	^{118}Sn	50118.70c
^{36}Ar	18036.70c	^{65}Cu	29065.70c	^{119}Sn	50119.70c
^{38}Ar	18038.70c	Zn	30000.70c	^{120}Sn	50120.70c
^{40}Ar	18040.70c	^{90}Zr	40090.70c	^{122}Sn	50122.70c
^{39}K	19039.70c	^{91}Zr	40091.70c	^{124}Sn	50124.70c
^{40}K	19040.70c	^{92}Zr	40092.70c	^{144}Sm	62144.70c
^{41}K	19041.70c	^{94}Zr	40094.70c	^{147}Sm	62147.70c
^{40}Ca	20040.70c	^{96}Zr	40096.70c	^{148}Sm	62148.70c
^{42}Ca	20042.70c	^{93}Nb	41093.70c	^{149}Sm	62149.70c
^{43}Ca	20043.70c	^{92}Mo	42092.70c	^{150}Sm	62150.70c
^{44}Ca	20044.70c	^{94}Mo	42094.70c	^{152}Sm	62152.70c
^{46}Ca	20046.70c	^{95}Mo	42095.70c	^{154}Sm	62154.70c
^{48}Ca	20048.70c	^{96}Mo	42096.70c	^{152}Gd	64152.70c
^{46}Ti	22046.70c	^{97}Mo	42097.70c	^{154}Gd	64154.70c
^{47}Ti	22047.70c	^{98}Mo	42098.70c	^{155}Gd	64155.70c

Nuclide	MCNP5.1.51 ZAID	Nuclide	MCNP5.1.51 ZAID	Nuclide	MCNP5.1.51 ZAID
^{156}Gd	64156.70c	^{179}Hf	72179.70c	^{236}U	92236.70c
^{157}Gd	64157.70c	^{180}Hf	72180.70c	^{238}U	92238.70c
^{158}Gd	64158.70c	^{204}Pb	82204.70c	^{238}Pu	94238.70c
^{160}Gd	64160.70c	^{206}Pb	82206.70c	^{239}Pu	94239.70c
^{174}Hf	72174.70c	^{207}Pb	82207.70c	^{240}Pu	94240.70c
^{176}Hf	72176.70c	^{208}Pb	82208.70c	^{241}Pu	94241.70c
^{177}Hf	72177.70c	^{234}U	92234.70c	^{242}Pu	94242.70c
^{178}Hf	72178.70c	^{235}U	92235.70c	^{241}Am	95241.70c

Table D.3-1 The MCNP5-1.51 Calculational Results and Measurements Uncertainties for Phase 1 Critical Experiments: Water-Moderated and Reflected Arrays

Case	Evaluation Identification	File-name	k_{eff-i}	$\pm \sigma_{calc-i}$	$\pm \sigma_{exp}$	$\pm \sigma_i$	EALF (eV)
1	MIX-COMP-THERM-HTC-001	[redacted]	[redacted]	[redacted]	[redacted]	[redacted]	[redacted]
2	MIX-COMP-THERM-HTC-002	[redacted]	[redacted]	[redacted]	[redacted]	[redacted]	[redacted]
3	MIX-COMP-THERM-HTC-003	[redacted]	[redacted]	[redacted]	[redacted]	[redacted]	[redacted]
4	MIX-COMP-THERM-HTC-004	[redacted]	[redacted]	[redacted]	[redacted]	[redacted]	[redacted]
5	MIX-COMP-THERM-HTC-005	[redacted]	[redacted]	[redacted]	[redacted]	[redacted]	[redacted]
6	MIX-COMP-THERM-HTC-006	[redacted]	[redacted]	[redacted]	[redacted]	[redacted]	[redacted]
7	MIX-COMP-THERM-HTC-007	[redacted]	[redacted]	[redacted]	[redacted]	[redacted]	[redacted]
8	MIX-COMP-THERM-HTC-008	[redacted]	[redacted]	[redacted]	[redacted]	[redacted]	[redacted]
9	MIX-COMP-THERM-HTC-009	[redacted]	[redacted]	[redacted]	[redacted]	[redacted]	[redacted]
10	MIX-COMP-THERM-HTC-010	[redacted]	[redacted]	[redacted]	[redacted]	[redacted]	[redacted]
11	MIX-COMP-THERM-HTC-011	[redacted]	[redacted]	[redacted]	[redacted]	[redacted]	[redacted]
12	MIX-COMP-THERM-HTC-012	[redacted]	[redacted]	[redacted]	[redacted]	[redacted]	[redacted]
13	MIX-COMP-THERM-HTC-013	[redacted]	[redacted]	[redacted]	[redacted]	[redacted]	[redacted]
14	MIX-COMP-THERM-HTC-014	[redacted]	[redacted]	[redacted]	[redacted]	[redacted]	[redacted]
15	MIX-COMP-THERM-HTC-015	[redacted]	[redacted]	[redacted]	[redacted]	[redacted]	[redacted]
16	MIX-COMP-THERM-HTC-016	[redacted]	[redacted]	[redacted]	[redacted]	[redacted]	[redacted]
17	MIX-COMP-THERM-HTC-017	[redacted]	[redacted]	[redacted]	[redacted]	[redacted]	[redacted]
18	MIX-COMP-THERM-HTC-018	[redacted]	[redacted]	[redacted]	[redacted]	[redacted]	[redacted]

Table D.3-2 The MCNP5-1.51 Calculational Results and Measurements Uncertainties for Phase 2 Critical Experiments: Reflected Simple Arrays Moderated by Poisoned Water with Gadolinium or Boron

Case	Evaluation Identification	File-name	k_{eff-i}	$\pm \sigma_{calc-i}$	$\pm \sigma_{exp}$	$\pm \sigma_i$	EALF (eV)
19	MIX-COMP-THERM-HTC-019	[redacted]	[redacted]	[redacted]	[redacted]	[redacted]	[redacted]
20	MIX-COMP-THERM-HTC-020	[redacted]	[redacted]	[redacted]	[redacted]	[redacted]	[redacted]
21	MIX-COMP-THERM-HTC-021	[redacted]	[redacted]	[redacted]	[redacted]	[redacted]	[redacted]
22	MIX-COMP-THERM-HTC-022	[redacted]	[redacted]	[redacted]	[redacted]	[redacted]	[redacted]
23	MIX-COMP-THERM-HTC-023	[redacted]	[redacted]	[redacted]	[redacted]	[redacted]	[redacted]
24	MIX-COMP-THERM-HTC-024	[redacted]	[redacted]	[redacted]	[redacted]	[redacted]	[redacted]
25	MIX-COMP-THERM-HTC-025	[redacted]	[redacted]	[redacted]	[redacted]	[redacted]	[redacted]
26	MIX-COMP-THERM-HTC-026	[redacted]	[redacted]	[redacted]	[redacted]	[redacted]	[redacted]
27	MIX-COMP-THERM-HTC-027	[redacted]	[redacted]	[redacted]	[redacted]	[redacted]	[redacted]
28	MIX-COMP-THERM-HTC-028	[redacted]	[redacted]	[redacted]	[redacted]	[redacted]	[redacted]
29	MIX-COMP-THERM-HTC-029	[redacted]	[redacted]	[redacted]	[redacted]	[redacted]	[redacted]
30	MIX-COMP-THERM-HTC-030	[redacted]	[redacted]	[redacted]	[redacted]	[redacted]	[redacted]
31	MIX-COMP-THERM-HTC-031	[redacted]	[redacted]	[redacted]	[redacted]	[redacted]	[redacted]
32	MIX-COMP-THERM-HTC-032	[redacted]	[redacted]	[redacted]	[redacted]	[redacted]	[redacted]
33	MIX-COMP-THERM-HTC-033	[redacted]	[redacted]	[redacted]	[redacted]	[redacted]	[redacted]
34	MIX-COMP-THERM-HTC-034	[redacted]	[redacted]	[redacted]	[redacted]	[redacted]	[redacted]
35	MIX-COMP-THERM-HTC-035	[redacted]	[redacted]	[redacted]	[redacted]	[redacted]	[redacted]
36	MIX-COMP-THERM-HTC-036	[redacted]	[redacted]	[redacted]	[redacted]	[redacted]	[redacted]
37	MIX-COMP-THERM-HTC-037	[redacted]	[redacted]	[redacted]	[redacted]	[redacted]	[redacted]
38	MIX-COMP-THERM-HTC-038	[redacted]	[redacted]	[redacted]	[redacted]	[redacted]	[redacted]
39	MIX-COMP-THERM-HTC-039	[redacted]	[redacted]	[redacted]	[redacted]	[redacted]	[redacted]
40	MIX-COMP-THERM-HTC-040	[redacted]	[redacted]	[redacted]	[redacted]	[redacted]	[redacted]
41	MIX-COMP-THERM-HTC-041	[redacted]	[redacted]	[redacted]	[redacted]	[redacted]	[redacted]
42	MIX-COMP-THERM-HTC-042	[redacted]	[redacted]	[redacted]	[redacted]	[redacted]	[redacted]
43	MIX-COMP-THERM-HTC-043	[redacted]	[redacted]	[redacted]	[redacted]	[redacted]	[redacted]
44	MIX-COMP-THERM-HTC-044	[redacted]	[redacted]	[redacted]	[redacted]	[redacted]	[redacted]
45	MIX-COMP-THERM-HTC-045	[redacted]	[redacted]	[redacted]	[redacted]	[redacted]	[redacted]
46	MIX-COMP-THERM-HTC-046	[redacted]	[redacted]	[redacted]	[redacted]	[redacted]	[redacted]
47	MIX-COMP-THERM-HTC-047	[redacted]	[redacted]	[redacted]	[redacted]	[redacted]	[redacted]
48	MIX-COMP-THERM-HTC-048	[redacted]	[redacted]	[redacted]	[redacted]	[redacted]	[redacted]
49	MIX-COMP-THERM-HTC-049	[redacted]	[redacted]	[redacted]	[redacted]	[redacted]	[redacted]
50	MIX-COMP-THERM-HTC-050	[redacted]	[redacted]	[redacted]	[redacted]	[redacted]	[redacted]
51	MIX-COMP-THERM-HTC-051	[redacted]	[redacted]	[redacted]	[redacted]	[redacted]	[redacted]
52	MIX-COMP-THERM-HTC-052	[redacted]	[redacted]	[redacted]	[redacted]	[redacted]	[redacted]
53	MIX-COMP-THERM-HTC-053	[redacted]	[redacted]	[redacted]	[redacted]	[redacted]	[redacted]
54	MIX-COMP-THERM-HTC-054	[redacted]	[redacted]	[redacted]	[redacted]	[redacted]	[redacted]
55	MIX-COMP-THERM-HTC-055	[redacted]	[redacted]	[redacted]	[redacted]	[redacted]	[redacted]

Case	Evaluation Identification	File-name	k_{eff-i}	$\pm \sigma_{calc-i}$	$\pm \sigma_{exp}$	$\pm \sigma_i$	EALF (eV)
56	MIX-COMP-THERM-HTC-056	[redacted]	[redacted]	[redacted]	[redacted]	[redacted]	[redacted]
57	MIX-COMP-THERM-HTC-057	[redacted]	[redacted]	[redacted]	[redacted]	[redacted]	[redacted]
58	MIX-COMP-THERM-HTC-058	[redacted]	[redacted]	[redacted]	[redacted]	[redacted]	[redacted]
59	MIX-COMP-THERM-HTC-059	[redacted]	[redacted]	[redacted]	[redacted]	[redacted]	[redacted]

Table D.3-3 The MCNP5-1.51 Calculational Results and Measurements Uncertainties for Phase 3 Critical Experiments: Pool Storage

Case	Evaluation Identification	File-name	k_{eff-i}	$\pm \sigma_{calc-i}$	$\pm \sigma_{exp}$	$\pm \sigma_i$	EALF (eV)
60	MIX-COMP-THERM-HTC-060	[redacted]	[redacted]	[redacted]	[redacted]	[redacted]	[redacted]
61	MIX-COMP-THERM-HTC-061	[redacted]	[redacted]	[redacted]	[redacted]	[redacted]	[redacted]
62	MIX-COMP-THERM-HTC-062	[redacted]	[redacted]	[redacted]	[redacted]	[redacted]	[redacted]
63	MIX-COMP-THERM-HTC-063	[redacted]	[redacted]	[redacted]	[redacted]	[redacted]	[redacted]
64	MIX-COMP-THERM-HTC-064	[redacted]	[redacted]	[redacted]	[redacted]	[redacted]	[redacted]
65	MIX-COMP-THERM-HTC-065	[redacted]	[redacted]	[redacted]	[redacted]	[redacted]	[redacted]
66	MIX-COMP-THERM-HTC-066	[redacted]	[redacted]	[redacted]	[redacted]	[redacted]	[redacted]
67	MIX-COMP-THERM-HTC-067	[redacted]	[redacted]	[redacted]	[redacted]	[redacted]	[redacted]
68	MIX-COMP-THERM-HTC-068	[redacted]	[redacted]	[redacted]	[redacted]	[redacted]	[redacted]
69	MIX-COMP-THERM-HTC-069	[redacted]	[redacted]	[redacted]	[redacted]	[redacted]	[redacted]
70	MIX-COMP-THERM-HTC-070	[redacted]	[redacted]	[redacted]	[redacted]	[redacted]	[redacted]
71	MIX-COMP-THERM-HTC-071	[redacted]	[redacted]	[redacted]	[redacted]	[redacted]	[redacted]
72	MIX-COMP-THERM-HTC-072	[redacted]	[redacted]	[redacted]	[redacted]	[redacted]	[redacted]
73	MIX-COMP-THERM-HTC-073	[redacted]	[redacted]	[redacted]	[redacted]	[redacted]	[redacted]
74	MIX-COMP-THERM-HTC-074	[redacted]	[redacted]	[redacted]	[redacted]	[redacted]	[redacted]
75	MIX-COMP-THERM-HTC-075	[redacted]	[redacted]	[redacted]	[redacted]	[redacted]	[redacted]
76	MIX-COMP-THERM-HTC-076	[redacted]	[redacted]	[redacted]	[redacted]	[redacted]	[redacted]
77	MIX-COMP-THERM-HTC-077	[redacted]	[redacted]	[redacted]	[redacted]	[redacted]	[redacted]
78	MIX-COMP-THERM-HTC-078	[redacted]	[redacted]	[redacted]	[redacted]	[redacted]	[redacted]
79	MIX-COMP-THERM-HTC-079	[redacted]	[redacted]	[redacted]	[redacted]	[redacted]	[redacted]
80	MIX-COMP-THERM-HTC-080	[redacted]	[redacted]	[redacted]	[redacted]	[redacted]	[redacted]
81	MIX-COMP-THERM-HTC-081	[redacted]	[redacted]	[redacted]	[redacted]	[redacted]	[redacted]
82	MIX-COMP-THERM-HTC-082	[redacted]	[redacted]	[redacted]	[redacted]	[redacted]	[redacted]
83	MIX-COMP-THERM-HTC-083	[redacted]	[redacted]	[redacted]	[redacted]	[redacted]	[redacted]
84	MIX-COMP-THERM-HTC-084	[redacted]	[redacted]	[redacted]	[redacted]	[redacted]	[redacted]
85	MIX-COMP-THERM-HTC-085	[redacted]	[redacted]	[redacted]	[redacted]	[redacted]	[redacted]

Table D.3-4 The MCNP5-1.51 Calculational Results and Measurements Uncertainties for Phase 4 Critical Experiments: Shipping Cask

Case	Evaluation Identification	File-name	k_{eff-i}	$\pm \sigma_{calc-i}$	$\pm \sigma_{exp}$	$\pm \sigma_i$	EALF (eV)
86	MIX-COMP-THERM-HTC-086	[redacted]	[redacted]	[redacted]	[redacted]	[redacted]	[redacted]
87	MIX-COMP-THERM-HTC-087	[redacted]	[redacted]	[redacted]	[redacted]	[redacted]	[redacted]
88	MIX-COMP-THERM-HTC-088	[redacted]	[redacted]	[redacted]	[redacted]	[redacted]	[redacted]
89	MIX-COMP-THERM-HTC-089	[redacted]	[redacted]	[redacted]	[redacted]	[redacted]	[redacted]
90	MIX-COMP-THERM-HTC-090	[redacted]	[redacted]	[redacted]	[redacted]	[redacted]	[redacted]
91	MIX-COMP-THERM-HTC-091	[redacted]	[redacted]	[redacted]	[redacted]	[redacted]	[redacted]
92	MIX-COMP-THERM-HTC-092	[redacted]	[redacted]	[redacted]	[redacted]	[redacted]	[redacted]
93	MIX-COMP-THERM-HTC-093	[redacted]	[redacted]	[redacted]	[redacted]	[redacted]	[redacted]
94	MIX-COMP-THERM-HTC-094	[redacted]	[redacted]	[redacted]	[redacted]	[redacted]	[redacted]
95	MIX-COMP-THERM-HTC-095	[redacted]	[redacted]	[redacted]	[redacted]	[redacted]	[redacted]
96	MIX-COMP-THERM-HTC-096	[redacted]	[redacted]	[redacted]	[redacted]	[redacted]	[redacted]
97	MIX-COMP-THERM-HTC-097	[redacted]	[redacted]	[redacted]	[redacted]	[redacted]	[redacted]
98	MIX-COMP-THERM-HTC-098	[redacted]	[redacted]	[redacted]	[redacted]	[redacted]	[redacted]
99	MIX-COMP-THERM-HTC-099	[redacted]	[redacted]	[redacted]	[redacted]	[redacted]	[redacted]
100	MIX-COMP-THERM-HTC-100	[redacted]	[redacted]	[redacted]	[redacted]	[redacted]	[redacted]
101	MIX-COMP-THERM-HTC-101	[redacted]	[redacted]	[redacted]	[redacted]	[redacted]	[redacted]
102	MIX-COMP-THERM-HTC-102	[redacted]	[redacted]	[redacted]	[redacted]	[redacted]	[redacted]
103	MIX-COMP-THERM-HTC-103	[redacted]	[redacted]	[redacted]	[redacted]	[redacted]	[redacted]
104	MIX-COMP-THERM-HTC-104	[redacted]	[redacted]	[redacted]	[redacted]	[redacted]	[redacted]
105	MIX-COMP-THERM-HTC-105	[redacted]	[redacted]	[redacted]	[redacted]	[redacted]	[redacted]
106	MIX-COMP-THERM-HTC-106	[redacted]	[redacted]	[redacted]	[redacted]	[redacted]	[redacted]
107	MIX-COMP-THERM-HTC-107	[redacted]	[redacted]	[redacted]	[redacted]	[redacted]	[redacted]
108	MIX-COMP-THERM-HTC-108	[redacted]	[redacted]	[redacted]	[redacted]	[redacted]	[redacted]
109	MIX-COMP-THERM-HTC-109	[redacted]	[redacted]	[redacted]	[redacted]	[redacted]	[redacted]
110	MIX-COMP-THERM-HTC-110	[redacted]	[redacted]	[redacted]	[redacted]	[redacted]	[redacted]
111	MIX-COMP-THERM-HTC-111	[redacted]	[redacted]	[redacted]	[redacted]	[redacted]	[redacted]
112	MIX-COMP-THERM-HTC-112	[redacted]	[redacted]	[redacted]	[redacted]	[redacted]	[redacted]
113	MIX-COMP-THERM-HTC-113	[redacted]	[redacted]	[redacted]	[redacted]	[redacted]	[redacted]
114	MIX-COMP-THERM-HTC-114	[redacted]	[redacted]	[redacted]	[redacted]	[redacted]	[redacted]
115	MIX-COMP-THERM-HTC-115	[redacted]	[redacted]	[redacted]	[redacted]	[redacted]	[redacted]
116	MIX-COMP-THERM-HTC-116	[redacted]	[redacted]	[redacted]	[redacted]	[redacted]	[redacted]
117	MIX-COMP-THERM-HTC-117	[redacted]	[redacted]	[redacted]	[redacted]	[redacted]	[redacted]
118	MIX-COMP-THERM-HTC-118	[redacted]	[redacted]	[redacted]	[redacted]	[redacted]	[redacted]
119	MIX-COMP-THERM-HTC-119	[redacted]	[redacted]	[redacted]	[redacted]	[redacted]	[redacted]
120	MIX-COMP-THERM-HTC-120	[redacted]	[redacted]	[redacted]	[redacted]	[redacted]	[redacted]
121	MIX-COMP-THERM-HTC-121	[redacted]	[redacted]	[redacted]	[redacted]	[redacted]	[redacted]
122	MIX-COMP-THERM-HTC-122	[redacted]	[redacted]	[redacted]	[redacted]	[redacted]	[redacted]
123	MIX-COMP-THERM-HTC-123	[redacted]	[redacted]	[redacted]	[redacted]	[redacted]	[redacted]

Case	Evaluation Identification	File-name	k_{eff-i}	$\pm \sigma_{calc-i}$	$\pm \sigma_{exp}$	$\pm \sigma_i$	EALF (eV)
124	MIX-COMP-THERM-HTC-124	[redacted]	[redacted]	[redacted]	[redacted]	[redacted]	[redacted]
125	MIX-COMP-THERM-HTC-125	[redacted]	[redacted]	[redacted]	[redacted]	[redacted]	[redacted]
126	MIX-COMP-THERM-HTC-126	[redacted]	[redacted]	[redacted]	[redacted]	[redacted]	[redacted]
127	MIX-COMP-THERM-HTC-127	[redacted]	[redacted]	[redacted]	[redacted]	[redacted]	[redacted]
128	MIX-COMP-THERM-HTC-128	[redacted]	[redacted]	[redacted]	[redacted]	[redacted]	[redacted]
129	MIX-COMP-THERM-HTC-129	[redacted]	[redacted]	[redacted]	[redacted]	[redacted]	[redacted]
130	MIX-COMP-THERM-HTC-130	[redacted]	[redacted]	[redacted]	[redacted]	[redacted]	[redacted]
131	MIX-COMP-THERM-HTC-131	[redacted]	[redacted]	[redacted]	[redacted]	[redacted]	[redacted]
132	MIX-COMP-THERM-HTC-132	[redacted]	[redacted]	[redacted]	[redacted]	[redacted]	[redacted]
133	MIX-COMP-THERM-HTC-133	[redacted]	[redacted]	[redacted]	[redacted]	[redacted]	[redacted]
134	MIX-COMP-THERM-HTC-134	[redacted]	[redacted]	[redacted]	[redacted]	[redacted]	[redacted]
135	MIX-COMP-THERM-HTC-135	[redacted]	[redacted]	[redacted]	[redacted]	[redacted]	[redacted]
136	MIX-COMP-THERM-HTC-136	[redacted]	[redacted]	[redacted]	[redacted]	[redacted]	[redacted]
137	MIX-COMP-THERM-HTC-137	[redacted]	[redacted]	[redacted]	[redacted]	[redacted]	[redacted]
138	MIX-COMP-THERM-HTC-138	[redacted]	[redacted]	[redacted]	[redacted]	[redacted]	[redacted]
139	MIX-COMP-THERM-HTC-139	[redacted]	[redacted]	[redacted]	[redacted]	[redacted]	[redacted]
140	MIX-COMP-THERM-HTC-140	[redacted]	[redacted]	[redacted]	[redacted]	[redacted]	[redacted]
141	MIX-COMP-THERM-HTC-141	[redacted]	[redacted]	[redacted]	[redacted]	[redacted]	[redacted]
142	MIX-COMP-THERM-HTC-142	[redacted]	[redacted]	[redacted]	[redacted]	[redacted]	[redacted]
143	MIX-COMP-THERM-HTC-143	[redacted]	[redacted]	[redacted]	[redacted]	[redacted]	[redacted]
144	MIX-COMP-THERM-HTC-144	[redacted]	[redacted]	[redacted]	[redacted]	[redacted]	[redacted]
145	MIX-COMP-THERM-HTC-145	[redacted]	[redacted]	[redacted]	[redacted]	[redacted]	[redacted]
146	MIX-COMP-THERM-HTC-146	[redacted]	[redacted]	[redacted]	[redacted]	[redacted]	[redacted]
147	MIX-COMP-THERM-HTC-147	[redacted]	[redacted]	[redacted]	[redacted]	[redacted]	[redacted]
148	MIX-COMP-THERM-HTC-148	[redacted]	[redacted]	[redacted]	[redacted]	[redacted]	[redacted]
149	MIX-COMP-THERM-HTC-149	[redacted]	[redacted]	[redacted]	[redacted]	[redacted]	[redacted]
150	MIX-COMP-THERM-HTC-150	[redacted]	[redacted]	[redacted]	[redacted]	[redacted]	[redacted]
151	MIX-COMP-THERM-HTC-151	[redacted]	[redacted]	[redacted]	[redacted]	[redacted]	[redacted]
152	MIX-COMP-THERM-HTC-152	[redacted]	[redacted]	[redacted]	[redacted]	[redacted]	[redacted]
153	MIX-COMP-THERM-HTC-153	[redacted]	[redacted]	[redacted]	[redacted]	[redacted]	[redacted]
154	MIX-COMP-THERM-HTC-154	[redacted]	[redacted]	[redacted]	[redacted]	[redacted]	[redacted]
155	MIX-COMP-THERM-HTC-155	[redacted]	[redacted]	[redacted]	[redacted]	[redacted]	[redacted]
156	MIX-COMP-THERM-HTC-156	[redacted]	[redacted]	[redacted]	[redacted]	[redacted]	[redacted]

Table D.3-5 The MCNP5-1.51 Calculational Results and Measurements Uncertainties for Selected Critical Experiments

Case	Evaluation Identification	File-name	k_{eff-i}	$\pm \sigma_{calc-i}$	$\pm \sigma_{exp}$	$\pm \sigma_i$	EALF (eV)
157	Core I	[redacted]	[redacted]	[redacted]	[redacted]	[redacted]	[redacted]
158	Core II	[redacted]	[redacted]	[redacted]	[redacted]	[redacted]	[redacted]
159	Core III	[redacted]	[redacted]	[redacted]	[redacted]	[redacted]	[redacted]
160	Core IX	[redacted]	[redacted]	[redacted]	[redacted]	[redacted]	[redacted]
161	Core X	[redacted]	[redacted]	[redacted]	[redacted]	[redacted]	[redacted]
162	Core XI	[redacted]	[redacted]	[redacted]	[redacted]	[redacted]	[redacted]
163	Core XII	[redacted]	[redacted]	[redacted]	[redacted]	[redacted]	[redacted]
164	Core XIII	[redacted]	[redacted]	[redacted]	[redacted]	[redacted]	[redacted]
165	Core XIV	[redacted]	[redacted]	[redacted]	[redacted]	[redacted]	[redacted]
166	Core XV	[redacted]	[redacted]	[redacted]	[redacted]	[redacted]	[redacted]
167	Core XVI	[redacted]	[redacted]	[redacted]	[redacted]	[redacted]	[redacted]
168	Core XVII	[redacted]	[redacted]	[redacted]	[redacted]	[redacted]	[redacted]
169	Core XVIII	[redacted]	[redacted]	[redacted]	[redacted]	[redacted]	[redacted]
170	Core XIX	[redacted]	[redacted]	[redacted]	[redacted]	[redacted]	[redacted]
171	Core XX	[redacted]	[redacted]	[redacted]	[redacted]	[redacted]	[redacted]
172	Core XXI	[redacted]	[redacted]	[redacted]	[redacted]	[redacted]	[redacted]
173	S-type Fuel, w/886 ppm B	[redacted]	[redacted]	[redacted]	[redacted]	[redacted]	[redacted]
174	S-type Fuel, w/746 ppm B	[redacted]	[redacted]	[redacted]	[redacted]	[redacted]	[redacted]
175	SO-type Fuel, w/1156 ppm B	[redacted]	[redacted]	[redacted]	[redacted]	[redacted]	[redacted]
176	Case 1 1337 ppm B	[redacted]	[redacted]	[redacted]	[redacted]	[redacted]	[redacted]
177	Case 12 1899 ppm B	[redacted]	[redacted]	[redacted]	[redacted]	[redacted]	[redacted]
178	Water Moderator 0 gap	[redacted]	[redacted]	[redacted]	[redacted]	[redacted]	[redacted]
179	Water Moderator 2.5 cm gap	[redacted]	[redacted]	[redacted]	[redacted]	[redacted]	[redacted]
180	Water Moderator 5 cm gap	[redacted]	[redacted]	[redacted]	[redacted]	[redacted]	[redacted]
181	Water Moderator 10 cm gap	[redacted]	[redacted]	[redacted]	[redacted]	[redacted]	[redacted]
182	Steel Reflector, 1.321 cm separation	[redacted]	[redacted]	[redacted]	[redacted]	[redacted]	[redacted]
183	Steel Reflector, 2.616 cm separation	[redacted]	[redacted]	[redacted]	[redacted]	[redacted]	[redacted]
184	Steel Reflector, 3.912 cm separation	[redacted]	[redacted]	[redacted]	[redacted]	[redacted]	[redacted]
185	Steel Reflector, Infinite separation	[redacted]	[redacted]	[redacted]	[redacted]	[redacted]	[redacted]
186	Steel Reflector, 1.321 cm separation	[redacted]	[redacted]	[redacted]	[redacted]	[redacted]	[redacted]
187	Steel Reflector, 2.616 cm separation	[redacted]	[redacted]	[redacted]	[redacted]	[redacted]	[redacted]
188	Steel Reflector, 5.405 cm separation	[redacted]	[redacted]	[redacted]	[redacted]	[redacted]	[redacted]
189	Steel Reflector, Infinite separation	[redacted]	[redacted]	[redacted]	[redacted]	[redacted]	[redacted]
190	Steel Reflector, with Boral Sheets	[redacted]	[redacted]	[redacted]	[redacted]	[redacted]	[redacted]
191	Lead Reflector, 0.55 cm sepn.	[redacted]	[redacted]	[redacted]	[redacted]	[redacted]	[redacted]
192	Lead Reflector, 1.956 cm sepn.	[redacted]	[redacted]	[redacted]	[redacted]	[redacted]	[redacted]
193	Lead Reflector, 5.405 cm sepn.	[redacted]	[redacted]	[redacted]	[redacted]	[redacted]	[redacted]
194	Experiment 004/032 – no absorber	[redacted]	[redacted]	[redacted]	[redacted]	[redacted]	[redacted]

Case	Evaluation Identification	File-name	k_{eff-i}	$\pm \sigma_{calc-i}$	$\pm \sigma_{exp}$	$\pm \sigma_i$	EALF (eV)
195	Exp. 009 1.05% Boron Steel plates						
196	Exp. 009 1.62% Boron Steel plates						
197	Exp. 031 – Boral plates						
198	Experiment 214R – with flux traps						
199	Experiment 214V3 –with flux trap						
200	Case 173 – 0 ppm B						
201	Case 177 – 2550 ppm B						
202	MOX Fuel – Type 3.2 Exp. 21						
203	MOX Fuel – Type 3.2 Exp. 43						
204	MOX Fuel – Type 3.2 Exp. 13						
205	MOX Fuel – Type 3.2 Exp. 32						
206	Saxton Case 52 PuO2 0.52” pitch						
207	Saxton Case 52 U 0.52” pitch						
208	Saxton Case 56 PuO2 0.56” pitch						
209	Saxton Case 56 borated PuO2						
210	Saxton Case 56 U 0.56” pitch						
211	Saxton Case 79 PuO2 0.79” pitch						
212	Saxton Case 79 U 0.79” pitch						
213	0.700-in. pitch 0 ppm B						
214	0.700-in. pitch 688 ppm B						
215	0.870-in. pitch 0 ppm B						
216	0.870-in. pitch 1090 ppm B						
217	0.990-in. pitch 0 ppm B						
218	0.990-in. pitch 767 ppm B						
219	Saxton Case PuO2 0.735” pitch						
220	Saxton Case PuO2 1.04” pitch						
221	8 wt% 240Pu 0.80” pitch						
222	8 wt% 240Pu 0.93” pitch						
223	8 wt% 240Pu 1.05” pitch						
224	8 wt% 240Pu 1.143” pitch						
225	8 wt% 240Pu 1.32” pitch						
226	8 wt% 240Pu 1.386” pitch						
227	16 wt% 240Pu 0.93” pitch						
228	16 wt% 240Pu 1.05” pitch						
229	16 wt% 240Pu 1.143” pitch						
230	16 wt% 240Pu 1.32” pitch						
231	24 wt% 240Pu 0.80” pitch						
232	24 wt% 240Pu 0.93” pitch						
233	24 wt% 240Pu 1.05” pitch						
234	24 wt% 240Pu 1.143” pitch						

Case	Evaluation Identification	File-name	k_{eff-i}	$\pm \sigma_{calc-i}$	$\pm \sigma_{exp}$	$\pm \sigma_i$	EALF (eV)
235	24 wt% 240Pu 1.32” pitch						
236	24 wt% 240Pu 1.386” pitch						
237	18 wt% 240Pu 0.85” pitch						
238	18 wt% 240Pu 0.93” pitch						
239	18 wt% 240Pu 1.05” pitch						
240	18 wt% 240Pu 1.143” pitch						
241	18 wt% 240Pu 1.386” pitch						
242	18 wt% 240Pu 1.60” pitch						
243	18 wt% 240Pu 1.70” pitch						
244	1 Cluster						
245	3 Clusters, Separation 11.92 cm						
246	3 Clusters, Separation 8.41 cm						
247	3 Clusters, Separation 10.05 cm						
248	3 Clusters, Separation 6.39 cm						
249	3 Clusters, Separation 9.01 cm						
250	3 Clusters, Separation 4.46						
251	1 Cluster, 10x11.51						
252	1 Cluster, 9x13.35						
253	1 Cluster, 8x16.37						
254	3 Clusters, Separation 7.11 cm						
255	1 Cluster, 614.4 Rods, Gd water impurity						
256	1 Cluster, 529.3 Rods						
257	1 Cluster, 523.9 Rods						
258	1 Cluster, 525.3 Rods						
259	1 Cluster, 595.4 Rods						
260	1 Cluster, 485.8 Rods						
261	1 Cluster, 523.8 Rods						
262	1 Cluster, 505.4 Rods						
263	4 Clusters, Separation 2.59 cm						
264	2 Clusters, Separation 1.68 cm						
265	4 Clusters, Separation 4.27 cm						
266	4 Clusters, Separation 5.95 cm						
267	4 Clusters, Separation 5.11 cm						
268	4 Clusters, Separation 6.66 cm						
269	4 Clusters, Separation 7.53 cm						
270	4 Clusters, Separation 9.00 cm						
271	4 Clusters, Separation 9.97 cm						
272	4 Clusters, Separation 11.45 cm						
273	4 Clusters, Separation 13.87 cm						

Case	Evaluation Identification	File-name	k_{eff-i}	$\pm \sigma_{calc-i}$	$\pm \sigma_{exp}$	$\pm \sigma_i$	EALF (eV)
274	3 Clusters, Separation 9.88 cm						
275	3 Clusters, Separation 6.78 cm						
276	3 Clusters, Separation 6.176 cm						
277	1 Cluster, 225.8 Rods, Gd water impurity						
278	1 Cluster, 216.2 Rods						
279	1 Cluster, 216.6 Rods						
280	1 Cluster, 218.6 Rods						
281	1 Cluster, 167.85 Rods						
282	1 Cluster, 203 Rods						
283	1 Cluster, 173.5 Rods						
284	2 Clusters, Separation 2.83 cm						
285	3 Clusters, Separation 12.27 cm						
286	3 Clusters, Separation 12.493 cm						
287	4 Clusters, Separation 4.72 cm						
288	4 Clusters, Separation 8.38 cm						
289	4 Clusters, Separation 10.86 cm						
290	4 Clusters, Separation 11.29 cm						
291	4 Clusters, Separation 12.02 cm						
292	4 Clusters, Separation 13.64 cm						
293	4 Clusters, Separation 14.98 cm						
294	4 Clusters, Separation 19.81 cm						
295	4 Clusters, Separation 8.50 cm						
296	19x19, Rod Pitch - 1.849 cm						
297	20x20, Rod Pitch - 1.849 cm						
298	21x21, Rod Pitch - 1.849 cm						
299	17x17, Rod Pitch - 1.956 cm						
300	18x18, Rod Pitch - 1.956 cm						
301	19x19, Rod Pitch - 1.956 cm						
302	20x20, Rod Pitch - 1.956 cm						
303	21x21, Rod Pitch - 1.956 cm						
304	16x16, Rod Pitch - 2.15 cm						
305	17x17, Rod Pitch - 2.15 cm						
306	18x18, Rod Pitch - 2.15 cm						
307	19x19, Rod Pitch - 2.15 cm						
308	20x20, Rod Pitch - 2.15 cm						
309	15x15, Rod Pitch - 2.293 cm						
310	16x16, Rod Pitch - 2.293 cm						
311	17x17, Rod Pitch - 2.293 cm						
312	18x18, Rod Pitch - 2.293 cm						

Case	Evaluation Identification	File-name	k_{eff-i}	$\pm \sigma_{calc-i}$	$\pm \sigma_{exp}$	$\pm \sigma_i$	EALF (eV)
313	19x19, Rod Pitch - 2.293 cm						
314	Core XI, 1511 ppm						
315	Core XI, 1335.5 ppm						
316	Core XI, 1335.5 ppm						
317	Core XI, 1182 ppm, 36 Pyrex Rods						
318	Core XI, 1182 ppm, 36 Pyrex Rods						
319	Core XI, 1032.5 ppm, 72 Pyrex Rods						
320	Core XI, 1032.5 ppm, 72 Pyrex Rods						
321	Core XI, 794 ppm, 144 Pyrex Rods						
322	Core XI, 779 ppm, 144 Pyrex Rods						
323	Core XI, 1245 ppm, 72 Vicor Rods						
324	Core XI, 1384 ppm, 144 Al_2O_3 Rods						
325	Core XI, 1348 ppm, 36 Al2O3 Rods						
326	Core XI, 1348 ppm, 36 Al2O3 Rods						
327	Core XI, 1363 ppm, 72 Al2O3 Rods						
328	Core XI, 1362 ppm, 72 Al2O3 Rods						
329	Core XI, 1158 ppm						
330	Core XI, 921 ppm						
331	0% Boron Steel plates, dist. 0.245 cm						
332	0% Boron Steel plates, dist. 3.277 cm						
333	0% Boron Steel plates, dist. 0.428 cm						
334	0% Boron Steel plates, dist. 3.277 cm						
335	1.05% Boron Steel plates, dist. 3.277 cm						
336	1.62% Boron Steel plates, dist. 3.277 cm						
337	Al plates, dist. 0.105 cm						
338	Al plates, dist. 3.277 cm						
339	Zircaloy-4 plates, dist. 0.078 cm						
340	Zircaloy-4 plates, dist. 3.277 cm						
341	Lead Reflector, 0 cm separation						
342	Lead Reflector, 0.660 cm separation						
343	Lead Reflector, 1.321 cm separation						
344	Lead Reflector, 5.405 cm separation						
345	Steel Reflector, 0 cm separation						
346	Steel Reflector, 0.660 cm separation						
347	Steel Reflector, 1.321 cm separation						
348	Steel Reflector, 2.616 cm separation						
349	Steel Reflector, 5.405 cm separation						
350	Steel Reflector, 0 cm separation						

Case	Evaluation Identification	File-name	k_{eff-i}	$\pm \sigma_{calc-i}$	$\pm \sigma_{exp}$	$\pm \sigma_i$	EALF (eV)
351	Steel Reflector, 0.660 cm separation						
352	Steel Reflector, 1.956 cm separation						
353	Lead Reflector, 0 cm separation						
354	Core IIIA						
355	Core IIIC						
356	Core IIID						
357	Core IIIE						
358	Core IIIF						
359	Core IIIG						
360	Core IV						
361	Core V						
362	Core VI						
363	Core VII						
364	Core VIII						
365	0% Boron Steel plate, Gd water impurity						
366	1.1% Boron Steel plate						
367	1.6% Boron Steel plate						
368	Boral B plate						
369	Boral C plate						
370	Boroflex, 1.84 cm separation						
371	Boroflex, 1.73 cm separation						
372	Steel Reflector, 0% Boron Steel plate						
373	Steel Reflector, 1.1% Boron Steel plate						
374	Steel Reflector, Boroflex, 8.37 cm separation						
375	Borated Water, 490 ppm						
376	Unborated Water						
377	Borated Water, 1030 ppm						
378	0% Boron Steel plates, dist. 0.645 cm						
379	0% Boron Steel plates, dist. 2.732 cm						
380	0% Boron Steel plates, dist. 4.042 cm						
381	0% Boron Steel plates, dist. 0.645 cm						
382	0% Boron Steel plates, dist. 4.042 cm						
383	0% Boron Steel plates, dist. 0.645 cm						
384	0% Boron Steel plates, dist. 4.042 cm						
385	1.05% Boron Steel plates, dist. 0.645 cm						
386	1.05% Boron Steel plates, dist. 4.042 cm						

Case	Evaluation Identification	File-name	k_{eff-i}	$\pm \sigma_{calc-i}$	$\pm \sigma_{exp}$	$\pm \sigma_i$	EALF (eV)
387	1.62% Boron Steel plates, dist. 0.645 cm	[redacted]	[redacted]	[redacted]	[redacted]	[redacted]	[redacted]
388	1.62% Boron Steel plates, dist. 4.042 cm	[redacted]	[redacted]	[redacted]	[redacted]	[redacted]	[redacted]
389	Boral plates, dist. 0.645 cm	[redacted]	[redacted]	[redacted]	[redacted]	[redacted]	[redacted]
390	Boral plates, dist. 4.442 cm	[redacted]	[redacted]	[redacted]	[redacted]	[redacted]	[redacted]
391	Boral plates, dist. 0.645 cm	[redacted]	[redacted]	[redacted]	[redacted]	[redacted]	[redacted]
392	Al plates, dist. 0.645 cm	[redacted]	[redacted]	[redacted]	[redacted]	[redacted]	[redacted]
393	Al plates, dist. 4.042 cm	[redacted]	[redacted]	[redacted]	[redacted]	[redacted]	[redacted]
394	Al plates, dist. 4.442 cm	[redacted]	[redacted]	[redacted]	[redacted]	[redacted]	[redacted]
395	Zircaloy-4 plates, dist. 0.645 cm	[redacted]	[redacted]	[redacted]	[redacted]	[redacted]	[redacted]
396	Zircaloy-4 plates, dist. 4.042 cm	[redacted]	[redacted]	[redacted]	[redacted]	[redacted]	[redacted]
397	Hex, 621 Rods, Temperature 20.1C	[redacted]	[redacted]	[redacted]	[redacted]	[redacted]	[redacted]
398	Hex, 889 Rods, Temperature 231.4C	[redacted]	[redacted]	[redacted]	[redacted]	[redacted]	[redacted]
399	Hex, 1951 Rods, Temperature 19.3C	[redacted]	[redacted]	[redacted]	[redacted]	[redacted]	[redacted]
400	Hex, 2791 Rods, Temperature 206.0C	[redacted]	[redacted]	[redacted]	[redacted]	[redacted]	[redacted]
401	Hex, 325/680 Rods, Temperature 20.8C	[redacted]	[redacted]	[redacted]	[redacted]	[redacted]	[redacted]
402	Hex, 325/912 Rods, Temperature 212.1C	[redacted]	[redacted]	[redacted]	[redacted]	[redacted]	[redacted]
403	Core XIA	[redacted]	[redacted]	[redacted]	[redacted]	[redacted]	[redacted]
404	Core XIC	[redacted]	[redacted]	[redacted]	[redacted]	[redacted]	[redacted]
405	Core XID	[redacted]	[redacted]	[redacted]	[redacted]	[redacted]	[redacted]
406	Core XIE	[redacted]	[redacted]	[redacted]	[redacted]	[redacted]	[redacted]
407	Core XIF	[redacted]	[redacted]	[redacted]	[redacted]	[redacted]	[redacted]
408	Core XIG	[redacted]	[redacted]	[redacted]	[redacted]	[redacted]	[redacted]
409	Core XIIIA	[redacted]	[redacted]	[redacted]	[redacted]	[redacted]	[redacted]
410	No Boron Steel plates	[redacted]	[redacted]	[redacted]	[redacted]	[redacted]	[redacted]
411	0% Boron Steel plates, 3 mm, dist. 0	[redacted]	[redacted]	[redacted]	[redacted]	[redacted]	[redacted]
412	0% Boron Steel plates, 6 mm, dist. 0	[redacted]	[redacted]	[redacted]	[redacted]	[redacted]	[redacted]
413	0% Boron Steel plates, 6 mm, dist. 0.5	[redacted]	[redacted]	[redacted]	[redacted]	[redacted]	[redacted]
414	0% Boron Steel plates, 6 mm, dist. 1	[redacted]	[redacted]	[redacted]	[redacted]	[redacted]	[redacted]
415	0.67% Boron Steel plates, 3 mm, dist. 0	[redacted]	[redacted]	[redacted]	[redacted]	[redacted]	[redacted]
416	0.67% Boron Steel plates, 6 mm, dist. 0	[redacted]	[redacted]	[redacted]	[redacted]	[redacted]	[redacted]
417	0.67% Boron Steel plates, 3 mm, dist. 0.5	[redacted]	[redacted]	[redacted]	[redacted]	[redacted]	[redacted]
418	0.67% Boron Steel plates, 6 mm, dist. 0.5	[redacted]	[redacted]	[redacted]	[redacted]	[redacted]	[redacted]
419	0.67% Boron Steel plates, 3 mm, dist. 1	[redacted]	[redacted]	[redacted]	[redacted]	[redacted]	[redacted]
420	0.67% Boron Steel plates, 6 mm, dist.	[redacted]	[redacted]	[redacted]	[redacted]	[redacted]	[redacted]

Case	Evaluation Identification	File-name	k_{eff-i}	$\pm \sigma_{calc-i}$	$\pm \sigma_{exp}$	$\pm \sigma_i$	EALF (eV)
	1						
421	0.98% Boron Steel plates, 3 mm, dist. 0	[redacted]	[redacted]	[redacted]	[redacted]	[redacted]	[redacted]
422	0.98% Boron Steel plates, 6 mm, dist. 0	[redacted]	[redacted]	[redacted]	[redacted]	[redacted]	[redacted]
423	0.98% Boron Steel plates, 6 mm, dist. 0.5	[redacted]	[redacted]	[redacted]	[redacted]	[redacted]	[redacted]
424	0.98% Boron Steel plates, 6 mm, dist. 1	[redacted]	[redacted]	[redacted]	[redacted]	[redacted]	[redacted]
425	No Boron Steel plates	[redacted]	[redacted]	[redacted]	[redacted]	[redacted]	[redacted]
426	0% Boron Steel plates, dist. 0	[redacted]	[redacted]	[redacted]	[redacted]	[redacted]	[redacted]
427	0.67% Boron Steel plates, dist. 0	[redacted]	[redacted]	[redacted]	[redacted]	[redacted]	[redacted]
428	0.98% Boron Steel plates, dist. 0	[redacted]	[redacted]	[redacted]	[redacted]	[redacted]	[redacted]
429	No Boron Steel plates	[redacted]	[redacted]	[redacted]	[redacted]	[redacted]	[redacted]
430	0% Boron Steel plates, dist. 0	[redacted]	[redacted]	[redacted]	[redacted]	[redacted]	[redacted]
431	0% Boron Steel plates, dist. 0.5	[redacted]	[redacted]	[redacted]	[redacted]	[redacted]	[redacted]
432	0% Boron Steel plates, dist. 0	[redacted]	[redacted]	[redacted]	[redacted]	[redacted]	[redacted]
433	0% Boron Steel plates, dist. 0.5	[redacted]	[redacted]	[redacted]	[redacted]	[redacted]	[redacted]
434	0.67% Boron Steel plates, dist. 0	[redacted]	[redacted]	[redacted]	[redacted]	[redacted]	[redacted]
435	0.67% Boron Steel plates, dist. 0.5	[redacted]	[redacted]	[redacted]	[redacted]	[redacted]	[redacted]
436	0.67% Boron Steel plates, dist. 0	[redacted]	[redacted]	[redacted]	[redacted]	[redacted]	[redacted]
437	0.67% Boron Steel plates, dist. 0.5	[redacted]	[redacted]	[redacted]	[redacted]	[redacted]	[redacted]
438	0.98% Boron Steel plates, dist. 0	[redacted]	[redacted]	[redacted]	[redacted]	[redacted]	[redacted]
439	0.98% Boron Steel plates, dist. 0.5	[redacted]	[redacted]	[redacted]	[redacted]	[redacted]	[redacted]
440	0.98% Boron Steel plates, dist. 0	[redacted]	[redacted]	[redacted]	[redacted]	[redacted]	[redacted]
441	0.98% Boron Steel plates, dist. 0.5	[redacted]	[redacted]	[redacted]	[redacted]	[redacted]	[redacted]
442	Otto Hahn, ZrB_2 and B_4C rods	[redacted]	[redacted]	[redacted]	[redacted]	[redacted]	[redacted]
443	IPEN/MB-01 (580 pins)	[redacted]	[redacted]	[redacted]	[redacted]	[redacted]	[redacted]
444	IPEN/MB-01 (560 pins)	[redacted]	[redacted]	[redacted]	[redacted]	[redacted]	[redacted]
445	670 pins, Al_2O_3-B_4C rods	[redacted]	[redacted]	[redacted]	[redacted]	[redacted]	[redacted]
446	672 pins, Al_2O_3-B_4C rods	[redacted]	[redacted]	[redacted]	[redacted]	[redacted]	[redacted]
447	668 pins, Al_2O_3-B_4C rods	[redacted]	[redacted]	[redacted]	[redacted]	[redacted]	[redacted]
448	668 pins, Al_2O_3-B_4C rods	[redacted]	[redacted]	[redacted]	[redacted]	[redacted]	[redacted]
449	664 pins, 16 steel rods	[redacted]	[redacted]	[redacted]	[redacted]	[redacted]	[redacted]
450	662 pins, 18 steel rods	[redacted]	[redacted]	[redacted]	[redacted]	[redacted]	[redacted]
451	658 pins, 14 steel rods	[redacted]	[redacted]	[redacted]	[redacted]	[redacted]	[redacted]
452	660 pins, 12 steel rods	[redacted]	[redacted]	[redacted]	[redacted]	[redacted]	[redacted]
453	660 pins, 12 steel rods	[redacted]	[redacted]	[redacted]	[redacted]	[redacted]	[redacted]
454	661 pins, 17 steel rods	[redacted]	[redacted]	[redacted]	[redacted]	[redacted]	[redacted]
455	662 pins, 16 steel rods	[redacted]	[redacted]	[redacted]	[redacted]	[redacted]	[redacted]
456	634 pins, 12 steel rods	[redacted]	[redacted]	[redacted]	[redacted]	[redacted]	[redacted]

Case	Evaluation Identification	File-name	k_{eff-i}	$\pm \sigma_{calc-i}$	$\pm \sigma_{exp}$	$\pm \sigma_i$	EALF (eV)
457	620 pins, 26 steel rods						
458	668 pins, 0 steel rods, 4 Gd_2O_3 rods						
459	648 pins, 0 steel rods, 8 Gd_2O_3 rods						
460	672 pins, 0 steel rods, 4 Gd_2O_3 rods						
461	646 pins, 4 steel rods, 4 Gd_2O_3 rods						
462	656 pins, 4 steel rods, 4 Gd_2O_3 rods						
463	664 pins, 4 steel rods, 2 Gd_2O_3 rods						
464	670 pins, 2 steel rods, 2 Gd_2O_3 rods						
465	664 pins, 2 steel rods, 2 Gd_2O_3 rods						
466	656 pins, 0 steel rods, 2 Gd_2O_3 rods						
467	23x23, 1.825 cm pitch						
468	23x23, 1.825 cm pitch						
469	23x23, 1.825 cm pitch						
470	21x21, 1.956 cm pitch						
471	21x21, 1.956 cm pitch						
472	21x21, 1.956 cm pitch						
473	20x20, 2.225 cm pitch						
474	20x20, 2.225 cm pitch						
475	20x20, 2.225 cm pitch						
476	21x21, 2.474 cm pitch						
477	21x21, 2.474 cm pitch						
478	8 wt% 240Pu 1.05” pitch, Al Rods						
479	8 wt% 240Pu 1.05” pitch, B4 Rods						
480	8 wt% 240Pu 1.05” pitch, B3 Rods						
481	8 wt% 240Pu 1.05” pitch, B2 Rods						
482	8 wt% 240Pu 1.05” pitch, B1 Rods						
483	8 wt% 240Pu 1.05” pitch, Al+Cd Rods						
484	8 wt% 240Pu 1.05” pitch, B4+Cd Rods						
485	8 wt% 240Pu 1.05” pitch, B3+Cd Rods						
486	8 wt% 240Pu 1.05” pitch, B2+Cd Rods						
487	8 wt% 240Pu 1.05” pitch, B1+Cd Rods						
488	8 wt% 240Pu 1.05” pitch, Air+Cd Rods						
489	8 wt% 240Pu 1.05” pitch, H2O+Cd Rods						
490	8 wt% 240Pu 1.32” pitch, Al Rods						
491	8 wt% 240Pu 1.32” pitch, B4 Rods						

Case	Evaluation Identification	File-name	k_{eff-i}	$\pm \sigma_{calc-i}$	$\pm \sigma_{exp}$	$\pm \sigma_i$	EALF (eV)
492	8 wt% 240Pu 1.32” pitch, B3 Rods						
493	8 wt% 240Pu 1.32” pitch, B2 Rods						
494	8 wt% 240Pu 1.32” pitch, B1 Rods						
495	8 wt% 240Pu 1.32” pitch, Al+Cd Rods						
496	8 wt% 240Pu 1.32” pitch, B4+Cd Rods						
497	8 wt% 240Pu 1.32” pitch, B3+Cd Rods						
498	8 wt% 240Pu 1.32” pitch, B2+Cd Rods						
499	8 wt% 240Pu 1.32” pitch, B1+Cd Rods						
500	8 wt% 240Pu 1.32” pitch, Air+Cd Rods						
501	8 wt% 240Pu 1.32” pitch, H2O+Cd Rods						
502	16 wt% 240Pu 1.386” pitch						
503	16 wt% 240Pu 1.05” pitch, Al Rods						
504	16 wt% 240Pu 1.05” pitch, B4 Rods						
505	16 wt% 240Pu 1.05” pitch, B3 Rods						
506	16 wt% 240Pu 1.05” pitch, B2 Rods						
507	16 wt% 240Pu 1.05” pitch, B1 Rods						
508	16 wt% 240Pu 1.05” pitch, Al+Cd Rods						
509	16 wt% 240Pu 1.05” pitch, B4+Cd Rods						
510	16 wt% 240Pu 1.05” pitch, B3+Cd Rods						
511	16 wt% 240Pu 1.05” pitch, B2+Cd Rods						
512	16 wt% 240Pu 1.05” pitch, B1+Cd Rods						
513	16 wt% 240Pu 1.05” pitch, Air+Cd Rods						
514	16 wt% 240Pu 1.05” pitch, H2O+Cd Rods						
515	24 wt% 240Pu 1.05” pitch, Al Rods						
516	24 wt% 240Pu 1.05” pitch, B4 Rods						
517	24 wt% 240Pu 1.05” pitch, B3 Rods						
518	24 wt% 240Pu 1.05” pitch, B2 Rods						
519	24 wt% 240Pu 1.05” pitch, B1 Rods						
520	24 wt% 240Pu 1.05” pitch, Al+Cd Rods						
521	24 wt% 240Pu 1.05” pitch, B4+Cd						

Case	Evaluation Identification	File-name	k_{eff-i}	$\pm \sigma_{calc-i}$	$\pm \sigma_{exp}$	$\pm \sigma_i$	EALF (eV)
	Rods						
522	24 wt% 240Pu 1.05” pitch, B3+Cd Rods	[redacted]	[redacted]	[redacted]	[redacted]	[redacted]	[redacted]
523	24 wt% 240Pu 1.05” pitch, B2+Cd Rods	[redacted]	[redacted]	[redacted]	[redacted]	[redacted]	[redacted]
524	24 wt% 240Pu 1.05” pitch, B1+Cd Rods	[redacted]	[redacted]	[redacted]	[redacted]	[redacted]	[redacted]
525	24 wt% 240Pu 1.05” pitch, Air+Cd Rods	[redacted]	[redacted]	[redacted]	[redacted]	[redacted]	[redacted]
526	24 wt% 240Pu 1.05” pitch, H2O+Cd Rods	[redacted]	[redacted]	[redacted]	[redacted]	[redacted]	[redacted]
527	8 wt% 240Pu 0.55” pitch	[redacted]	[redacted]	[redacted]	[redacted]	[redacted]	[redacted]
528	8 wt% 240Pu 0.60” pitch	[redacted]	[redacted]	[redacted]	[redacted]	[redacted]	[redacted]
529	8 wt% 240Pu 0.71” pitch	[redacted]	[redacted]	[redacted]	[redacted]	[redacted]	[redacted]
530	8 wt% 240Pu 0.80” pitch	[redacted]	[redacted]	[redacted]	[redacted]	[redacted]	[redacted]
531	8 wt% 240Pu 0.90” pitch	[redacted]	[redacted]	[redacted]	[redacted]	[redacted]	[redacted]
532	8 wt% 240Pu 0.93” pitch	[redacted]	[redacted]	[redacted]	[redacted]	[redacted]	[redacted]

Table D.3-6 Descriptive Statistics of the MCNP5-1.51 Calculational Results

Experiment Description	No. of exp.	k_{eff} range	EALF (eV) range
HTC Experiments	156	[redacted]	[redacted]
Selected Experiments	376	[redacted]	[redacted]
All experiments	532	[redacted]	[redacted]

Table D.3-7 Normality Test Results for the MCNP5-1.51 calculations

Experiment Description	No. of exp.	Shapiro-Wilk		Pearson's chi-square (χ^2)			
		Wtest	W	χ^2	n	$P_d(\chi^2;d)$	Normal
HTC Experiments	156	N/A	N/A	[redacted]	[redacted]	[redacted]	[redacted]
Selected Experiments	376	N/A	N/A	[redacted]	[redacted]	[redacted]	[redacted]
All experiments	532	N/A	N/A	[redacted]	[redacted]	[redacted]	[redacted]

Table D.3-8 Trending Analysis Results for the MCNP5-1.51 calculations

Experiment Description	No. of exp.	Correlated Parameter, *x*	Correlation Coefficient, r^2	Probability, Pd(N;r)	Correlation	Regression Equation, k(*x*)
All experiments	532	EALF	[redacted]	[redacted]	[redacted]	[redacted]
		Pitch	[redacted]	[redacted]	[redacted]	[redacted]
		Rod OD	[redacted]	[redacted]	[redacted]	[redacted]
		Fuel Density	[redacted]	[redacted]	[redacted]	[redacted]

Table D.3-9 Analysis of Neutron Absorbers and Reflector Materials for the MCNP5-1.51 calculations

Experiment Description	No. of exp.	Bias	Bias Uncertainty	Normality χ^2 ($P_d(\chi^2;d)$)	Linear Correlation	Residuals Normality, ($P_d(\chi^2;d)$)
All experiments	532					
All except those with Gadolinium, Cadmium and Lead	365					

Table D.3-10 Bias and Bias Uncertainty as a Function of Independent Parameter

Experiment Description	Independent Parameter, x	Calculated k_{eff}	Bias	Bias Uncertainty
All except those with Gadolinium, Cadmium and Lead	EALF			
	[redacted]	[redacted]	[redacted]	[redacted]
	[redacted]	[redacted]	[redacted]	[redacted]
	[redacted]	[redacted]	[redacted]	[redacted]
	[redacted]	[redacted]	[redacted]	[redacted]
	[redacted]	[redacted]	[redacted]	[redacted]
	[redacted]	[redacted]	[redacted]	[redacted]
	[redacted]	[redacted]	[redacted]	[redacted]
	[redacted]	[redacted]	[redacted]	[redacted]
	[redacted]	[redacted]	[redacted]	[redacted]
	[redacted]	[redacted]	[redacted]	[redacted]
	[redacted]	[redacted]	[redacted]	[redacted]
	[redacted]	[redacted]	[redacted]	[redacted]
	[redacted]	[redacted]	[redacted]	[redacted]
	[redacted]	[redacted]	[redacted]	[redacted]
	[redacted]	[redacted]	[redacted]	[redacted]
	[redacted]	[redacted]	[redacted]	[redacted]
	[redacted]	[redacted]	[redacted]	[redacted]
	[redacted]	[redacted]	[redacted]	[redacted]
	[redacted]	[redacted]	[redacted]	[redacted]
	[redacted]	[redacted]	[redacted]	[redacted]
	[redacted]	[redacted]	[redacted]	[redacted]

Table D.3-11 Analysis of Fuel Burnup for the MCNP5-1.51 calculations

Experiment Description	No. of exp.	Bias	Bias Uncertainty	Normality χ^2 ($P_d(\chi^2;d)$)	Linear Correlation	Residuals Normality, ($P_d(\chi^2;d)$)
All except those with Gadolinium, Cadmium and Lead[†]	365					
Fresh UO_2 Fuel	207					
HTC + MOX Experiments	158					
						

Table D.3-12 Bias and Bias Uncertainty as a Function of Independent Parameter

Experiment Description	Independent Parameter, x	Calculated k_{eff}	Bias	Bias Uncertainty	Independent Parameter, x	Calculated k_{eff}	Bias	Bias Uncertainty
HTC + MOX Experiments	EALF				Pu Enrichment			
	[redacted]							

Table D.3-13 Analysis of the Unborated and Borated Water for the MCNP5-1.51 calculations

Experiment Description	No. of exp.	Bias	Bias Uncertainty	Normality χ^2 ($P_d(\chi^2;d)$)	Linear Correlation	Residuals Normality, ($P_d(\chi^2;d)$)
All except those with Gadolinium, Cadmium and Lead†	365					
All with Fresh Water	287					
						
All with Borated Water	78					
						
						

†Note: Critical experiments with Gadolinium, Cadmium and Lead were excluded from all subsequent subsets.

Table D.3-14 Bias and Bias Uncertainty as a Function of Independent Parameter

Experiment Description	Independent Parameter, x	Calculated k_{eff}	Bias	Bias Uncertainty	Independent Parameter, x	Calculated k_{eff}	Bias	Bias Uncertainty
All with Fresh Water	EALF				U Enrichment			
	[redacted]	[redacted]	[redacted]	[redacted]	[redacted]	[redacted]	[redacted]	[redacted]
	[redacted]	[redacted]	[redacted]	[redacted]	[redacted]	[redacted]	[redacted]	[redacted]
	[redacted]	[redacted]	[redacted]	[redacted]	[redacted]	[redacted]	[redacted]	[redacted]
	[redacted]	[redacted]	[redacted]	[redacted]	[redacted]	[redacted]	[redacted]	[redacted]
	[redacted]	[redacted]	[redacted]	[redacted]	[redacted]	[redacted]	[redacted]	[redacted]
	[redacted]	[redacted]	[redacted]	[redacted]	[redacted]	[redacted]	[redacted]	[redacted]
	[redacted]	[redacted]	[redacted]	[redacted]	[redacted]	[redacted]	[redacted]	[redacted]
	[redacted]	[redacted]	[redacted]	[redacted]	[redacted]	[redacted]	[redacted]	[redacted]
	[redacted]	[redacted]	[redacted]	[redacted]	[redacted]	[redacted]	[redacted]	[redacted]
	[redacted]	[redacted]	[redacted]	[redacted]	[redacted]	[redacted]	[redacted]	[redacted]
	[redacted]	[redacted]	[redacted]	[redacted]	[redacted]	[redacted]	[redacted]	[redacted]
	[redacted]	[redacted]	[redacted]	[redacted]	[redacted]	[redacted]	[redacted]	[redacted]
	[redacted]	[redacted]	[redacted]	[redacted]	[redacted]	[redacted]	[redacted]	[redacted]
	[redacted]	[redacted]	[redacted]	[redacted]	[redacted]	[redacted]	[redacted]	[redacted]
	[redacted]	[redacted]	[redacted]	[redacted]	[redacted]	[redacted]	[redacted]	[redacted]
	[redacted]	[redacted]	[redacted]	[redacted]	[redacted]	[redacted]	[redacted]	[redacted]
	[redacted]	[redacted]	[redacted]	[redacted]	[redacted]	[redacted]	[redacted]	[redacted]
	[redacted]	[redacted]	[redacted]	[redacted]	[redacted]	[redacted]	[redacted]	[redacted]
	[redacted]	[redacted]	[redacted]	[redacted]	[redacted]	[redacted]	[redacted]	[redacted]
	[redacted]	[redacted]	[redacted]	[redacted]	[redacted]	[redacted]	[redacted]	[redacted]
	[redacted]	[redacted]	[redacted]	[redacted]	[redacted]	[redacted]	[redacted]	[redacted]
	[redacted]	[redacted]	[redacted]	[redacted]	[redacted]	[redacted]	[redacted]	[redacted]
All with Borated Water	Density				N/A			
	[redacted]	[redacted]	[redacted]	[redacted]				
	[redacted]	[redacted]	[redacted]	[redacted]				
	[redacted]	[redacted]	[redacted]	[redacted]				
	[redacted]	[redacted]	[redacted]	[redacted]				
	[redacted]	[redacted]	[redacted]	[redacted]				
	[redacted]	[redacted]	[redacted]	[redacted]				
	[redacted]	[redacted]	[redacted]	[redacted]				
	[redacted]	[redacted]	[redacted]	[redacted]				
	[redacted]	[redacted]	[redacted]	[redacted]				
	[redacted]	[redacted]	[redacted]	[redacted]				

Experiment Description	Independent Parameter, x	Calculated k_{eff}	Bias	Bias Uncertainty	Independent Parameter, x	Calculated k_{eff}	Bias	Bias Uncertainty
	[redacted]	[redacted]	[redacted]	[redacted]				
	[redacted]	[redacted]	[redacted]	[redacted]				
	[redacted]	[redacted]	[redacted]	[redacted]				
	[redacted]	[redacted]	[redacted]	[redacted]				
	[redacted]	[redacted]	[redacted]	[redacted]				
	[redacted]	[redacted]	[redacted]	[redacted]				
	[redacted]	[redacted]	[redacted]	[redacted]				
	[redacted]	[redacted]	[redacted]	[redacted]				
	[redacted]	[redacted]	[redacted]	[redacted]				

Table D.3-15 Analysis of the Combinations of Fuel Burnup and Unborated/Borated Water for the MCNP5-1.51 calculations

Experiment Description	No. of exp.	Bias	Bias Uncertainty	Normality χ^2 ($P_d(\chi^2;d)$)	Linear Correlation	Residuals Normality, ($P_d(\chi^2;d)$)
All except those with Gadolinium, Cadmium and Lead†	365					
Fresh UO_2 Fuel with Fresh Water	154					
Fresh UO_2 Fuel with Borated Water	53					
HTC + MOX Fuel with Fresh Water	133				 	 
HTC + MOX Fuel with Borated Water	25				 	 

†Note: Critical experiments with Gadolinium, Cadmium and Lead were excluded from all subsequent subsets.

Table D.3-16 Bias and Bias Uncertainty as a Function of Independent Parameter

Experiment Description	Independent Parameter, x	Calculated k_{eff}	Bias	Bias Uncertainty	Independent Parameter, x	Calculated k_{eff}	Bias	Bias Uncertainty
Fresh UO_2 Fuel with Fresh Water	EALF				N/A			
	[redacted]	[redacted]	[redacted]	[redacted]				
HTC + MOX Fuel with Fresh Water	EALF				Pu Enrichment			
	[redacted]	[redacted]	[redacted]	[redacted]	[redacted]	[redacted]	[redacted]	[redacted]

Experiment Description	Independent Parameter, x	Calculated k_{eff}	Bias	Bias Uncertainty	Independent Parameter, x	Calculated k_{eff}	Bias	Bias Uncertainty
	[redacted]	[redacted]	[redacted]	[redacted]	[redacted]	[redacted]	[redacted]	[redacted]
	[redacted]	[redacted]	[redacted]	[redacted]	[redacted]	[redacted]	[redacted]	[redacted]
	[redacted]	[redacted]	[redacted]	[redacted]	[redacted]	[redacted]	[redacted]	[redacted]
	[redacted]	[redacted]	[redacted]	[redacted]	[redacted]	[redacted]	[redacted]	[redacted]
	[redacted]	[redacted]	[redacted]	[redacted]	[redacted]	[redacted]	[redacted]	[redacted]
	[redacted]	[redacted]	[redacted]	[redacted]	[redacted]	[redacted]	[redacted]	[redacted]
	[redacted]	[redacted]	[redacted]	[redacted]	[redacted]	[redacted]	[redacted]	[redacted]
	[redacted]	[redacted]	[redacted]	[redacted]	[redacted]	[redacted]	[redacted]	[redacted]
	[redacted]	[redacted]	[redacted]	[redacted]	[redacted]	[redacted]	[redacted]	[redacted]
	[redacted]	[redacted]	[redacted]	[redacted]	[redacted]	[redacted]	[redacted]	[redacted]
HTC + MOX Fuel with Borated Water	Rod OD				Density			
	[redacted]	[redacted]	[redacted]	[redacted]	[redacted]	[redacted]	[redacted]	[redacted]
	[redacted]	[redacted]	[redacted]	[redacted]	[redacted]	[redacted]	[redacted]	[redacted]
	[redacted]	[redacted]	[redacted]	[redacted]	[redacted]	[redacted]	[redacted]	[redacted]
	[redacted]	[redacted]	[redacted]	[redacted]	[redacted]	[redacted]	[redacted]	[redacted]
	[redacted]	[redacted]	[redacted]	[redacted]	[redacted]	[redacted]	[redacted]	[redacted]
	[redacted]	[redacted]	[redacted]	[redacted]	[redacted]	[redacted]	[redacted]	[redacted]
	[redacted]	[redacted]	[redacted]	[redacted]	[redacted]	[redacted]	[redacted]	[redacted]
	[redacted]	[redacted]	[redacted]	[redacted]	[redacted]	[redacted]	[redacted]	[redacted]
	[redacted]	[redacted]	[redacted]	[redacted]	[redacted]	[redacted]	[redacted]	[redacted]
	[redacted]	[redacted]	[redacted]	[redacted]	[redacted]	[redacted]	[redacted]	[redacted]
	[redacted]	[redacted]	[redacted]	[redacted]	[redacted]	[redacted]	[redacted]	[redacted]
	[redacted]	[redacted]	[redacted]	[redacted]	[redacted]	[redacted]	[redacted]	[redacted]
	[redacted]	[redacted]	[redacted]	[redacted]	[redacted]	[redacted]	[redacted]	[redacted]
	[redacted]	[redacted]	[redacted]	[redacted]	[redacted]	[redacted]	[redacted]	[redacted]
	[redacted]	[redacted]	[redacted]	[redacted]	[redacted]	[redacted]	[redacted]	[redacted]
	[redacted]	[redacted]	[redacted]	[redacted]	[redacted]	[redacted]	[redacted]	[redacted]
	[redacted]	[redacted]	[redacted]	[redacted]	[redacted]	[redacted]	[redacted]	[redacted]
	[redacted]	[redacted]	[redacted]	[redacted]	[redacted]	[redacted]	[redacted]	[redacted]
	[redacted]	[redacted]	[redacted]	[redacted]	[redacted]	[redacted]	[redacted]	[redacted]
	[redacted]	[redacted]	[redacted]	[redacted]	[redacted]	[redacted]	[redacted]	[redacted]
	[redacted]	[redacted]	[redacted]	[redacted]	[redacted]	[redacted]	[redacted]	[redacted]
	[redacted]	[redacted]	[redacted]	[redacted]	[redacted]	[redacted]	[redacted]	[redacted]
	[redacted]	[redacted]	[redacted]	[redacted]	[redacted]	[redacted]	[redacted]	[redacted]
	[redacted]	[redacted]	[redacted]	[redacted]	[redacted]	[redacted]	[redacted]	[redacted]
	[redacted]	[redacted]	[redacted]	[redacted]	[redacted]	[redacted]	[redacted]	[redacted]
	[redacted]	[redacted]	[redacted]	[redacted]	[redacted]	[redacted]	[redacted]	[redacted]
	[redacted]	[redacted]	[redacted]	[redacted]	[redacted]	[redacted]	[redacted]	[redacted]

Table D.3-17 Comparison of Key Parameters and Definition of Validated AOA

Parameter	Design Application	Benchmarks	Validated
Fissionable Material	^{235}U, ^{239}Pu, ^{241}Pu	^{235}U, ^{239}Pu, ^{241}Pu	^{235}U, ^{239}Pu, ^{241}Pu
Isotopic Composition			
$^{235}U/Ut$	< 5.0wt%	1.57 – 5.74%	< 5wt%
Pu/(U+Pu)	< 20wt%	1.104 - 20 %	< 20wt%
Physical Form	UO_2, MOX	UO_2, MOX	UO_2, MOX
Fuel Density (g/cm^3)	10.0 – 10.7	9.2 – 10.4	9.2 – 10.7
Moderator Material (coolant)	H	H	H
Physical Form	H_20	H_20	H_20
Density (g/cm^3)	around 1.0 g/cm^3	around 1.0 g/cm^3	around 1.0 g/cm^3
Reflector Material	H	H	H
Physical Form	H_20	H_20	H_20
Density (g/cm^3)	around 1.0 g/cm^3	around 1.0 g/cm^3	around 1.0 g/cm^3
Interstitial Reflector Material			
Plate	Steel or Lead	Steel or Lead	Steel or Lead
Absorber Material			
Soluble	None, Boron or Gadolinium	None, Boron (15 - 2550 ppm) or Gadolinium (48 – 197 ppm)	None, Boron (0 - 2550 ppm) or Gadolinium (48 to 197 ppm)
Rods	Boron	Pyrex®, Vicor®, Steel or B-Al	Boron
Separating Material			
Plate	Water, B-SS, Boral or Cadmium	Water, B-SS, Boral, Boroflex, Zircaloy or Cadmium	Water, B-SS, Boral, Boroflex, Zircaloy or Cadmium
Geometry			
Lattice type	Square	Square, Triangle	Square, Triangle
Lattice Pitch (cm)	1.26 – 1.47 (PWR) 1.24 – 1.88 (BWR)	0.968 to 4.318	0.968 to 4.318
Neutron Energy	Thermal spectrum	Thermal spectrum	Thermal spectrum

Figure Proprietary

Figure D.3-1 Frequency Chart for Calculated k_{eff} of the Selected 532 Benchmarks for the MCNP5-1.51 code

Figure Proprietary

Figure D.3-2 Frequency Chart for Calculated EALF (eV) of the Selected 532 Benchmarks for the MCNP5-1.51 code

Figure Proprietary

Figure D.3-3 MCNP5-1.51 Calculated k_{eff} Values for Various Values of the Spectral Index (All Experiments)

Figure Proprietary

Figure D.3-4 MCNP5-1.51 Calculated k_{eff} Values for Various Values of the Spectral Index

Figure Proprietary

Figure D.3-5 MCNP5-1.51 Calculated k_{eff} Values for Various Values of the Spectral Index

Figure Proprietary

Figure D.3-6 MCNP5-1.51 Calculated k_{eff} Values for Various Values of the Pu Enrichment

Figure Proprietary

Figure D.3-7 MCNP5-1.51 Calculated k_{eff} Values for Various Values of the Spectral Index

Figure Proprietary

Figure D.3-8 MCNP5-1.51 Calculated k_{eff} Values for Various Values of the U Enrichment

Figure Proprietary

Figure D.3-9 MCNP5-1.51 Calculated k_{eff} Values for Various Values of the Fuel Density

Figure Proprietary

Figure D.3-10 MCNP5-1.51 Calculated k_{eff} Values for Various Values of the Spectral Index

Figure Proprietary

Figure D.3-11 MCNP5-1.51 Calculated k_{eff} Values for Various Values of the Spectral Index

Figure Proprietary

Figure D.3-12 MCNP5-1.51 Calculated k_{eff} Values for Various Values of the Pu Enrichment

Figure Proprietary

Figure D.3-13 MCNP5-1.51 Calculated k_{eff} Values for Various Values of the Rod OD

Figure Proprietary

Figure D.3-14 MCNP5-1.51 Calculated k_{eff} Values for Various Values of the Fuel Density